NASA CR-159653
GDC-CRAD-80-003

CAPILLARY ACQUISITION DEVICES FOR HIGH-PERFORMANCE VEHICLES — EXECUTIVE SUMMARY

GENERAL DYNAMICS
Convair Division

NASA CR-159658
GDC-CRAD-80-003

CAPILLARY ACQUISITION DEVICES FOR HIGH-PERFORMANCE VEHICLES — EXECUTIVE SUMMARY

February 1980

Prepared by
M.H. Blatt
R.D. Bradshaw
J.A. Risberg

Prepared for
National Aeronautics and Space Administration
LEWIS RESEARCH CENTER
21000 Brookpark Road
Cleveland, Ohio 44135

Prepared Under
Contract NAS3-20092

Prepared by
GENERAL DYNAMICS CONVAIR DIVISION
P.O. Box 80847
San Diego, California 92138

1. Report No. NASA-CR-159658	2. Government Accession No.	3. Recipient's Catalog No.
4. Title and Subtitle Capillary Acquisition Devices for High Performance Vehicles - Executive Summary		5. Report Date February 1980 6. Performing Organization Code
7. Author(s) M. H. Blatt, R. D. Bradshaw and J. A. Risberg		8. Performing Organization Report No. GDC-CRAD-80-003
9. Performing Organization Name and Address General Dynamics Convair Division P.O. Box 80847 San Diego, CA 92138		10. Work Unit No. 11. Contract or Grant No. NAS3-17802, NAS3-19693, and NAS3-20092
12. Sponsoring Agency Name and Address NASA Lewis Research Center Cleveland, OH 44135		13. Type of Report and Period Covered Contractor Report January 1974 to Sept. 1979 14. Sponsoring Agency Code

15. Supplementary Notes
Project Manager, E. P. Symons, NASA Lewis Research Center, Cleveland, OH 44135

16. Abstract

Technology areas critical to the development of cryogenic capillary devices were studied. Passive cooling of capillary devices was investigated with an analytical and experimental study of wicking flow. This investigation revealed that passive thermal conditioning was feasible and provided considerable weight advantage over active systems using throttled vent fluid. Capillary device refilling with settled fluid was studied using an analytical and experimental program that resulted in successful correlation of a versatile computer program with test data. This program was used to predict Centaur D-1S LO_2 and LH_2 start basket refilling. Comparisons were made between the baseline Centaur D-1S propellant feed system and feed system alternatives including systems using capillary devices. The comparisons resulted in the baseline Centaur D-1S system (using pressurization, boost pumps and propellant settling) being selected as the best candidate based on payload weight penalty. However, other comparison criteria and advanced mission conditions were identified where capillary devices, boost pumps fed thermally subcooled propellants and pressure fed systems would be selected as attractive alternatives. In a follow-on effort to this system comparison, the preferred concepts from the Centaur D-1S study were examined for APOTV and POTV vehicles for delivery and round-trip transfer of payloads between LEO and GEO. Mission profiles were determined to provide propellant usage timelines and the payload partials were defined. Of the three system concepts studied propellant settling with pressure fed boost pumps had the lowest payload penalty, the concept with propellant settling and a thermal subcooler to provide NPSP had the lowest hardware weight, while capillary devices (start baskets) with thermal subcoolers were heaviest in both respects. The LO_2 fluid residuals with thermal subcoolers were a major weight penalty. All OTV concepts considered used tank-mounted boost pumps to satisfy turbopump NPSP requirements. The preferred system, the D-1S system, chosen in the earlier study was also settled for APOTV and POTV vehicles.

17. Key Words (Suggested by Author(s))	18. Distribution Statement		
Acquisition, Capillary Flow, Expulsion, Fluid Flow, Heat Exchangers, Heat Transfer, Mixing, Screens, Venting, Wicks.	Unclassified - Unlimited STAR Category 20		
19. Security Classif. (of this report) Unclassified	20. Security Classif. (of this page) Unclassified	21. No. of Pages 105	22. Price*

*For sale by the National Technical Information Service Springfield Virginia 22151

FOREWORD

This report documents the cumulative results of Contract NAS3-17802, "Centaur Propellant Acquisition System Study," Contract NAS3-19693, "Centaur Propellant Thermal Conditioning Study," and NAS3-20092," A Study of Liquid and Vapor Flow Into a Centaur Capillary Device." These contracts were conducted over a period from January 1974 to September 1979. The NASA/LeRC Program Managers were W. J. Masica and J. C. Aydelott for NAS3-17802, J. C. Aydelott for NAS3-19693, and E. P. Symons and J. C. Aydelott for NAS3-20092. The General Dynamics Convair Program Managers were M. H. Blatt for NAS3-17802 and NAS3-19693 and M. H. Blatt and R. D. Bradshaw for NAS3-20092.

Three reports documenting the results of each individual contract have been published. These reports are NASA CR-134811, "Centaur Propellant Acquisition System Study," June 1975; NASA CR-135032, "Centaur Propellant Thermal Conditioning Study," and NASA CR-159657, "Liquid and Vapor Flow Into a Centaur Capillary Acquisition Device," September 1979.

A follow-on effort to NAS3-20092 is reported on in Section 2.4 of this report to extend the study results to Orbital Transfer Vehicles. Unlike the above three contracts which are summarized in this document, this effort has not been reported elsewhere. Concepts and procedures developed in the prior studies were employed to define the mission variables and to make the systems comparisons for these vehicles.

In addition to the program managers many General Dynamics Convair personnel contributed to the studies. The key individuals and their contributions are listed below.

M. D. Walter	Acquisition System Design
R. L. Pleasant	Turbopump Thermal Subcooler Analysis
R. C. Erickson	Vent/Mixer Analysis
H. Brittain	Wicking Test Conductor
D. Uhlken	Liquid and Vapor Flow Test Conductor
J. A. Risberg	Liquid and Vapor Flow Test Correlation
M. E. Hill	Settling Analysis

All data are presented with the International System of Units as the primary system and English units as secondary. The English system was used for the basic calculations.

TABLE OF CONTENTS

			Page
FOREWORD			iv
SUMMARY			v
1	INTRODUCTION		1-1
	1.1	GROUND RULES	1-3
2	STUDY RESULTS AND DISCUSSION		
	2.1	RESULTS OF NAS3-17802, "CENTAUR PROPELLANT ACQUISITION SYSTEM STUDY"	2-1
	2.1.1	FLUID ANALYSIS	2-5
	2.1.2	THERMAL ANALYSIS	2-8
	2.1.3	SYSTEM DESIGN	2-10
	2.1.4	SYSTEM COMPARISON	2-11
	2.2	RESULTS OF NAS3-19693, "CENTAUR PROPELLANT THERMAL CONDITIONING STUDY"	2-14
	2.2.1	PASSIVE THERMAL CONDITIONING	2-14
	2.2.2	THERMAL SUBCOOLING	2-25
	2.2.3	THERMODYNAMIC VENT MIXER ANALYSES	2-27
	2.3	RESULTS OF NAS3-20092, "A STUDY OF LIQUID AND VAPOR FLOW INTO A CENTAUR CAPILLARY DEVICE"	2-29
	2.3.1	REFILLING ANALYSIS	2-29
	2.3.2	REFILLING TESTS	2-30
	2.3.3	VAPOR INFLOW ANALYSIS	2-32
	2.3.4	VAPOR INFLOW TESTING	2-33
	2.3.5	PROPELLANT FEED SYSTEM COMPARISONS	2-34
	2.4	PROPELLANT ACQUISITION FOR ORBITAL TRANSFER VEHICLES	2-41
	2.4.1	VEHICLE AND MISSION DEFINITION	2-41
	2.4.2	PROPELLANT ACQUISITION WITH CAPILLARY DEVICES	2-51
	2.4.3	PROPELLANT ACQUISITION WITH SETTLING	2-69
	2.4.4	FEED SYSTEM COMPARISONS	2-79
3	REFERENCES		3-1
4	DISTRIBUTION LIST - NAS3-20092		4-1

LIST OF FIGURES

Figure		Page
1-1	Capillary Acquisition Subsystem Interfaces	1-2
1-2	Evolution of the Existing Centaur D-1T to a Centaur Compatible With Space Shuttle	1-3
2-1	Centaur Propellant Acquisition Decision-Making Process (Decision Tree)	2-4
2-2	LO_2 Start Basket Refilling	2-8
2-3	Schematic of Thermal Subcooling	2-9
2-4	Cooling Fluid Thermodynamic States	2-9
2-5	LO2 Tank Thermal Subcooler	2-9
2-6	LO_2 Start Basket and Subcooler	2-12
2-7	LH_2 Start Basket and Subcooler	2-12
2-8	LO_2 Start Tank	2-13
2-9	LH_2 Start Tank	2-13
2-10	Experiment Apparatus	2-22
2-11	Increased Wicking Capability for the Plate/Screen-Screen/Plate and Screen/Plate Configuration	2-24
2-12	Compact Heat Exchanger Vent System Schematic	2-27
2-13	Test Apparatus Schematic	2-30
2-14	REFILL Computer Program Simulation of Test Run No. 15	2-32
2-15	Typical Characteristics of Personnel Orbital Transfer Vehicle (POTV)	2-42
2-16	Typical Characteristics of All Propulsive Orbital Transfer Vehicle (APOTV)	2-43
2-17	Mission Profile LEO to GEO and Return for Single Stage OTV	2-44
2-18	Mission Profile LEO to GEO and Return for Dual Stage OTV	2-44
2-19	Capillary Device Schematic	2-53
2-20	LO_2 Subcooler Sizing for APOTV and POTV Vehicles	2-59
2-21	LH_2 Subcooler Sizing for APOTV and POTV Vehicles	2-60

LIST OF FIGURES, Contd.

Figure		Page
2-22	Liquid Oxygen Capillary Acquisition Device for POTV	2-65
2-23	Liquid Oxygen Capillary Acquisition Device for APOTV	2-66
2-24	Liquid Hydrogen Capillary Acquisition Device for POTV	2-67
2-25	Liquid Hydrogen Capillary Acquisition Device for APOTV	2-68
2-26	Relation of Settling Times to Tank Stations	2-72
2-27	Propellant Mass Required to Settle Liquid Hydrogen for Various Thrust Levels	2-76

LIST OF TABLES

Table		Page
1-1	Planetary Mission Profile	1-4
1-2	Synchronous Equatorial Mission Profile	1-4
1-3	Low Earth Orbit Mission Profile	1-5
2-1	Recommended Acquisition Subsystem Candidates	2-2
2-2	Recommended Capillary Device Fabrication Candidates	2-2
2-3	LO_2 Start Basket Refilling Time	2-8
2-4	LH_2 Start Basket Refilling Time	2-8
2-5	Start Basket Volumetric Requirements	2-11
2-6	Passive Cooling Requirements	2-16
2-7	Candidate Wicking Configuration	2-17
2-8	Manufacturing of Configurations	2-20
2-9	Selected Specimen Geometries	2-21
2-10	Wicking Correction Factors	2-25
2-11	Feed System Candidates	2-36
2-12	Payload Weight Penalties for System Comparisons, kg_m (lb_m), Five Burn Mission, RL10A-3-3 Engine	2-38
2-13	Relative Reliability of Propellant Feed System Concepts	2-39
2-14	Propellant and Dry Weights Used for all Stages	2-45
2-15	Mission Profile Velocity Requirements for Synchronous Missions	2-45
2-16	Mission Profile and Propellant Usage for APOTV (Delivery Only) Single Stage	2-46
2-17	Mission Profile and Propellant Usage for APOTV (Round Trip) Dual Stage	2-47
2-18	Mission Profile and Propellant Usage for POTV (Delivery Only) Single Stage	2-48
2-19	Mission Profile and Propellant Usage for POTV (Round Trip) Dual Stage	2-49
2-20	Payload Sensitivity Factors for Geosynchronous Orbits	2-50

LIST OF TABLES, CONTD

Table		Page
2-21	Capillary Device Characteristics	2-54
2-22	Start Basket Refilling Times	2-55
2-23	Subcooler Related Weight Penalties, kg_m (lb_m) at Two Potential Tank Operating Pressures	2-57
2-24	Vehicle Fill Level, Mass, and Acceleration for Various Mission-MES	2-71
2-25	Settling Burn Times in Seconds Determined by Two Calculation Methods	2-73
2-26	Collection Times in Seconds From Weighted Average of the Times Contained in Table 2-25	2-75
2-27	Helium Expended for Pressurization, kg_m (lb_m), Single Stage APOTV - Delivery Only	2-77
2-28	Helium Expended for Pressurization, kg_m (lb_m), Dual Stage APOTV - Round Trip	2-77
2-29	Helium Expended for Pressurization, kg_m (lb_m), Single Stage Stage POTV - Delivery Only	2-78
2-30	Helium Expended for Pressurization, kg_m (ib_m), Dual Stage POTV - Round Trip	2-78
2-31	Hardware Weight Penalties for Systems Comparison, kg_m (lb_m), APOTV Single Stage	2-80
2-32	Hardware Weight Penalties for Systems Comparison, kg_m (lb_m), APOTV Dual Stage	2-80
2-33	Hardware Weight Penalties for Systems Comparison, kg_m (lb_m), POTV Single Stage	2-81
2-34	Hardware Weight Penalties for Systems Comparison, kg_m (lb_m), POTV Dual Stage	2-81
2-35	Payload Weight Penalties for System Comparison, kg_m (lb_m), APOTV Single Stage	2-83
2-36	Payload Weight Penalties for System Comparison, kg_m (lb_m), APOTV Dual Stage	2-83
2-37	Payload Weight Penalties for System Comparison, kg_m (lb_m), POTV Single Stage	2-84

LIST OF TABLES, CONTD

Table		Page
2-38	Payload Weight Penalties for System Comparison, kg_m (lb_m), POTV Dual Stage	2-84
2-39	Comparison of Relative Reliability for Three Concepts Under Comparison	2-85

SUMMARY

This report represents a summary of a continuing effort, spanning more than five years and three separate contracts, to evaluate and investigate alternative cryogenic propellant management systems for a Shuttle-based upper stage vehicle. The vehicle used for the comparisons was the Centaur D-1S. This was the best defined Shuttle-based upper stage vehicle at the initiation of the study.

The initial study was a comparison of alternative propellant management systems that included start tanks, start baskets and settling thrusters. The comparison showed that passively cooled start baskets with heat exchangers to subcool fluid flowing to the boost pumps were a promising candidate for multiburn missions.

Passive cooling, thermal subcooling, and fluid mixing were examined in detail. An analytical and experimental study of wicking using candidate screen configurations successfully demonstrated the feasibility of capillary device passive cooling. Thermal subcooler sizing analysis was performed for providing Centaur D-1S turbopump NPSP (net positive suction pressure) for three engine candidates. Existing experimental mixing studies to destroy thermal stratification were compared to obtain the best mixing correlation. This correlation was used to size thermodynamic vent systems for Centaur D-1S and other advanced Shuttle-based Centaur derivatives.

Capillary device refilling using settled fluid and vapor inflow across wetted screens were studied analytically and experimentally. A computer program developed to predict capillary device performance was successfully correlated with experimental data and used to analyze Centaur D-1S LO_2 and LH_2 capillary device refilling. Vapor inflow analysis resulted in development of a semi-empirical model for vapor flow across a wetted screen window that was only partially correlated with test data due to difficulties in obtaining repeatable test results.

A propellant management system comparison was conducted for the Centaur D-1S to compare capillary devices versus settling; pressure fed pumps, boost pump fed pumps and pumps using thermally subcooled propellants; cooled and uncooled ducts; and dumping any coolant overboard versus pumping it back into the tank. The comparisons showed that the baseline Centaur D-1S system (using pressurization, boost pumps and propellant settling) was the best candidate (for missions having five burns or less) based on payload weight penalty. Other comparison criteria and advanced mission conditions were identified where pressure fed system, boost pumps using thermally subcooled propellants and capillary devices would be selected as attractive alternatives.

In a follow-on effort to the system comparison described in the above paragraph, the preferred concepts from that study were examined for APOTV and POTV vehicles for delivery and round-trip transfer of payloads between LEO and GEO. Mission profiles were determined to provide propellant usage timelines and the payload partials were defined. Three system concepts were studied: the concept with propellant settling and pressurization had the lowest payload penalty, the concept with propellant settling and a thermal subcooler to provide NPSP had the lowest hardware weight, while the capillary start basket with a thermal subcooler was heaviest in both respects. The LO_2 fluid residuals with thermal subcoolers are a major weight penalty. All concepts considered used tank-mounted boost pumps to minimize NPSP requirements. The preferred system for APOTV and POTV vehicles was also selected in the earlier study and is the Centaur D-1S system.

1

INTRODUCTION

During low-gravity coast, vehicle drag and disturbing acceleration may position propellant away from the tank outlet. Engine start under these conditions will cause vapor to enter the pumps, producing cavitation, poor engine operation, and possible feed system failure. To eliminate these undesirable occurrences, means must be provided to position liquid in the sump and over the tank outlet. The method currently used on Centaur is to settle the propellants by using small thrusters to apply a linear acceleration to the vehicle. This method, while well proven, imposes mission constraints in waiting for propellant to be settled and weight penalties which are a function of the number of engine burns. The use of a capillary or surface tension device to trap propellants over the outlet in low gravity is a more advanced but less proven technique. The weight penalty for the surface tension device is less sensitive to number of engine burns and provides added mission flexibility in allowing quick engine startup.

Capillary acquisition systems fall into two main classes, partial acquisition devices, such as start baskets or start tanks that rely upon fluid settling for refill, and "total" acquisition concepts, such as liners or channels that cover a substantial portion of tank area and maintain continuous contact with the main liquid pool. A partial acquisition concept operates by maintaining liquid over the outlet in sufficient quantity to allow the main liquid pool to be settled. The settled liquid refills the acquisition device. During engine firing, vapor enters the acquisition device volume. Capillary device geometry must be designed so that the entering vapor does not create adverse liquid spilling from the basket away from the engine outlet or cause difficulties in refilling the device with liquid. Total control devices are either maintained full of liquid during main engine burns or refilled between burns by capillary pumping, venting, or mechanical pumping.

Start baskets perform the function of retaining propellants over the tank outlet for boost pump and engine startup. This study examined both the requirements of cryogenic start basket acquisition systems in performing this function and the interaction of the acquisition system with related vehicle systems.

Systems interacting with the acquisition system are shown in Figure 1-1: the pressurization, vent, and propellant gaging systems, main engines; boost pumps and propellant ducts.

Thermal conditioning of the capillary device is a major design consideration. To maintain liquid over the tank outlet, propellant vaporization and bulk boiling within the acquisition device must be prevented. Vaporization can be caused by incident

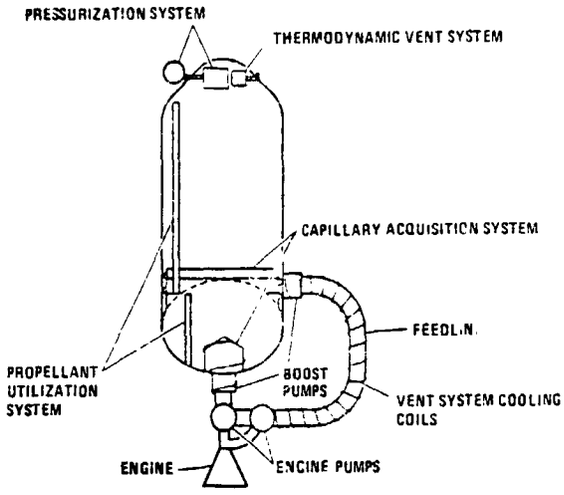

Figure 1-1. Capillary Acquisition Sub-System Interfaces

heating through the tank walls, heating from the engines, boost pumps, and feedlines, and by pressure fluctuations in the tank due to venting or pressurant cooling.

The pressurization system has a major interaction with the acquisition device. Since pressurization will be accomplished when the liquid is unsettled, the use of warm pressurant will cause rapid ullage pressure decay when the cold liquid is "settled" through the pressurant. Cold pressurant should be used in lieu of warm pressurant to alleviate this problem.

The vent system influences the acquisition system design by causing forced convection heat transfer to occur at the basket surface and by causing tank pressure reductions that could drop the saturation temperature of the tank below the acquisition device surface temperature. Both factors cause increased requirements for thermal conditioning liquid to prevent screen dryout. (Both active and passive thermal conditioning systems were designed for preventing screen dryout. Active thermal conditioning was initially considered in the most detail).

Propellant utilization systems such as the capacitance gaging technique used on the Centaur D-1S cannot sense any liquid trapped in the capillary device above the settled liquid. Means must be provided for either separately sensing this trapped liquid or empirically verifying analytical predictions of the trapped liquid quantity.

A primary consideration of the study was the interaction of the boost pump and propellant ducts with the capillary device. The method of thermal conditioning the boost pumps and ducts directly affects feed system chilldown and capillary device volumetric requirements. Methods of supplying boost pump NPSH were a major concern in studying pressurization system alternatives. Feed system startup and shutdown transients may influence acquisition system retention requirements.

Engine soakback heating contributes to feed system chilldown requirements. Engine vibrations may induce capillary device vibrations that cause loss of retention capability.

The initial major effort in the study compared capillary acquisition systems to the baseline Centaur D-1S propellant acquisition system using settling thrusters, pressure-fed boost pumps and uncooled propellant ducts. Since the acquisition system interacts with many other systems in the vehicle, comparison of acquisition devices considered all changes to the vehicle caused by the particular acquisition system being implemented. Acquisition systems that appeared promising were studied in more detail.

The analysis to be described in Section 2, Study Results and Discussion, indicated that passively cooled start baskets fabricated from fine mesh screen materials, together with thermal subcoolers (for replacing the main tank pressurization system) were promising for multiple burn missions. As a result of this analysis, studies were undertaken to define critical processes in passively cooled capillary device operation. Passive cooling of cryogenic capillary device screen surfaces was identified as the only low weight and high reliability thermal conditioning option available. Heat exchangers for subcooling liquid to provide pump NPSP are a necessary subsystem when capillary devices are employed because of the high weight requirement of the cold pressurant system otherwise required. Capillary device refilling with settled fluid is a critical process in the operation of a start basket. Screen wetting when subjected to vapor flow is a critical process in start basket passive cooling.

Thermodynamic vent system development was identified in Reference 1 as a critical technology item in the evolution of the current Centaur D-1T to a Shuttle-based Centaur.

1.3 GROUND RULES

The baseline vehicle configuration was the Centaur D-1S as defined in Contract NAS3-16786 and reported in NASA CR-134488 (Reference 1). This vehicle represented a minimum change D-1T configuration (Centaur currently used with Titan) modified to be compatible with the Space Shuttle interface, operations and safety requirements. Since the time of Contract NAS3-16786 there have been a number of changes in this configuration as a result of later studies. However, the data in this report represents results using the original configuration when the initial capillary acquisition device study (Contract NAS3-17802, Reference 2) was conducted. Approximately 95 percent of the existing D-1T components remain unchanged for the D-1S. Figure 1-2 illustrates the modifications made to the existing D-1T to evolve to a D-1S that affected acquisition subsystem design and tradeoffs.

Mission profiles for the study were the planetary, synchronous equatorial and low earth mission profiles of NAS3-16786 (Reference 1), as given in Tables 1-1, 1-2 and 1-3.

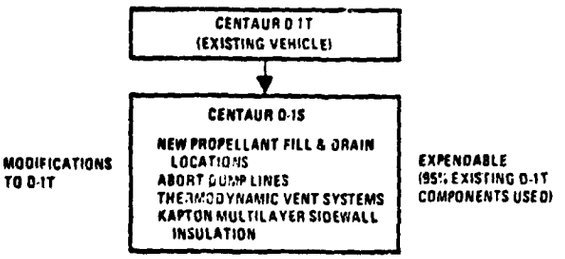

Figure 1-2. Evolution of the Existing Centaur D-1T to a Centaur Compatible With Space Shuttle

Heating rates, nominal tank pressure levels, and other mission conditions were also obtained from Reference 1. Parameters not specified were generated using analytical or empirical techniques consistent with the design of the Centaur D-1T and D-1S. The systems designed in the study did not impose constraints on the operation of the Shuttle or affect the Centaur/Shuttle abort capability.

Only for the task of determining worst case thermodynamic vent/mixer requirements

Table 1-1. Planetary Mission Profile

Event/ Time (min.)		Initial Mass, kg_m (lb_m)	Burn Time, sec	Propellant Burned, kg_m (lb_m)	Final Mass, kg_m (lb_m)	Initial Percent Full*	Initial Acceleration, g
Loading (T = 0)	LO_2	11,554 (25,450)					
	LH_2	2,397 (5,279)					
MES1 (T = 67)	Vehicle	22,434 (49,413)			8,888 (19,578)		
	LO_2	11,488 (25,304)	441.4	11,302 (24,894)	186 (410)	96	0.61
	LH_2	2,344 (5,164)		2,243 (4,941)	101 (223)	95	

*Assumes 11,946 kg_m (26,313 lb_m), LO_2 2,478 kg_m (5,459 lb_m), LH_2 for full tank.

Main engine thrust = 13,620 kg_f (30,000 lb_f)
Maximum ACS thrust = 10.9 kg_f (24 lb_f)
Maximum ACS acceleration before last burn = 4.86×10^{-4} g's
Main engine flow rates, LO_2 = 25.6 kg/sec (56.4 lb/sec)
LH_2 = 5.1 kg/sec (11.2 lb/sec)

ISP = 443.82 sec
Payload = 6,567 kg_m (14,465 lb_m)
Dry weight = 2,015 kg_m (4,439 lb_m)
Burnout acceleration = 1.53 g's

Table 1-2. Synchronous Equatorial Mission Profile

Event/ Time (min.)		Initial Mass, kg_m (lb_m)	Burn Time, sec	Propellant Burned, kg_m (lb_m)	Final Mass, kg_m (lb_m)	Initial Percent Full*	Initial Acceleration, g
Loading (T = 0)	LO_2	11,554 (25,450)					
	LH_2	2,397 (5,279)					
MES1 (T = 67)	Vehicle	21,541 (47,447)			12,100 (26,653)		
	LO_2	11,488 (25,304)	305.4	7,854 (17,299)	3,634 (8,005)	96	.3
	LH_2	2,344 (5,164)		1,525 (3,360)	819 (1,804)	95	
MES2 (T = 384)	Vehicle	12,162 (26,788)			7,956 (17,525)		
	LO_2	3,621 (7,975)	132.3	3,403 (7,496)	190 (419)	30.3	1.12
	LH_2	782 (1,723)		665 (1,465)	117 (258)	31.6	

*Assumes 11,946 kg_m (26,313 lb_m), LO_2 2,478 kg_m (5,459 lb_m), LH_2 for full tank.

Main engine thrust = 13,620 kg_f (30,000 lb_f)
Maximum ACS thrust = 10.9 kg_f (24 lb_f)
Max. ACS acceleration before last burn = 8.96×10^{-4} g's
Mixture ratio = 5.0
Main engine flow rates, LO_2 = 25.7 kg/sec (56.65 lb/sec)
LH_2 = 5.01 kg/sec (11.03 lb/sec)

ISP = 443.35 sec
Payload = 5,538 kg_m (12,199 lb_m)
Dry weight = 2,090 kg_m (4,604 lb_m)
Burnout acceleration = 1.71 g's

Table 1-3. Low Earth Orbit Mission Profile

Event/ Time (min.)		Initial Mass, kg_m (lb_m)	Burn Time, sec	Propellant Burned, kg_m (lb_m)	Final Mass kg_m (lb_m)	Initial Percent Full*	Initial Acceleration, g
Loading (T = 0)	LO_2	11,554 (25,450)					
	LH_2	2,397 (5,279)					
MES1 (T = 67)	Vehicle	19,090 (42,048)			16,363 (36,042)		
	LO_2	11,488 (25,304)	88.6	2,294 (5,052)	9,194 (20,252)	96	0.71
	LH_2	2,344 (5,164)		434 (955)	1,911 (4,209)	95	
MES2 (T = 118)	Vehicle	16,264 (35,824)			10,373 (22,849)		
	LO_2	9,155 (20,165)	131.32	4,955 (10,915)	4,200 (9,250)	77	0.84
	LH_2	1,885 (4,153)		935 (2,060)	950 (2,093)	76	
MES3 (T = 408)	Vehicle	10,246 (22,568)			6,536 (14,397)		
	LO_2	4,162 (9,167)	120.51	3,121 (6,875)	1,038 (2,286)	35	1.33
	LH_2	913 (2,010)		587 (1,294)	325 (716)	37	
MES4 (T = 459)	Vehicle	6,443 (14,192)			5,861 (12,910)		
	LO_2	998 (2,198)	18.90	489 (1,078)	509 (1,121)	8.4	2.11
	LH_2	295 (650)		93 (204)	207 (456)	11.9	
MES5 (T = 553)	Vehicle	5,765 (12,698)			5,433 (11,967)		
	LO_2	468 (1,031)	10.8	279 (614)	189 (417)	3.9	2.36
	LH_2	178 (393)		53 (116)	126 (277)	7.2	

*Assumes 11,946 kg_m (26,313 lb_m), LO_2, 2,478 kg_m (5,459 lb_m), LH_2 for full tank.

Main engine thrust = 13,620 kg_f (30,000 lb_f)
Maximum ACS thrust = 10.9 kg_f (24 lb_f)
Max. ACS acceleration before 5th burn = 1.89×10^{-3} g's
Mixture ratio = 5.298
Main engine flow rates, LO_2 = 25.9 kg/sec (57.05 lb/sec)
LH_2 = 4.89 kg/sec (10.77 lb/sec)

ISP = 443.8 sec
Payload = 2,842 kg_m (6,260 lb_m)
Dry weight = 2,225 kg_m (4,901 lb_m)
Burnout acceleration = 2.51 g's

were vehicle candidates expanded beyond that of the Centaur D-1S. For that task all versions (current in 1975) of Shuttle-based Centaur were considered. Three tank sizes were investigated for each expendable and reusable version of the Centaur Interim Upper Stage vehicle. The expendable versions were similar to the Centaur D-1S relative to thermal protection, fill and drain and propulsion. The reusable versions had Superfloc multilayer insulation. Vehicle conditions affecting thermodynamic vent system sizing were determined based on information developed in F04701-75-C-0035, "Centaur Interim Upper Stage Systems Study," Reference 3. Thermodynamic vent system design conditions were also evaluated for the Space Tug configuration defined in Reference 4.

2

STUDY RESULTS AND DISCUSSION

2.1 RESULTS OF NAS3-17802, "CENTAUR PROPELLANT ACQUISITION SYSTEM STUDY"

The initial objective of the study was to screen candidate systems to identify possible methods of accomplishing capillary propellant acquisition for the Centaur D-1S and to evaluate these systems based upon weight, feasibility and operational advantages to determine which candidates compare favorably to the baseline Centaur hydrogen peroxide system.

In determining candidate acquisition subsystem concepts for capillary device fluid containment, pressurization, thermal conditioning, structure and assembly, and feedline thermal conditioning were considered separately. Initially, all possible means of satisfying mission and vehicle requirements were identified for each concept category. Each fluid acquisition system candidate was conceptually designed to meet Centaur D-1S mission requirements and was then evaluated based upon approximate weight and operational advantages compared to the existing hydrogen peroxide system. Candidates were screened only to the point at which they could be logically rejected. For example, if a device could not be conceptually designed to meet Centaur D-1S requirements, it was eliminated without determining system weight. Further, if the weight exceeded existing system weight by more than 20%, the concept was rejected. If the concept still remained a candidate, then operational advantages or disadvantages compared to the existing system and to other candidate acquisition systems were assessed.

Thermal conditioning and pressurization candidates were compared based on relative advantages and disadvantages, complexity, and weight. Promising fabrication alternatives were determined for screen-to-backup material joining, backup material selection, barrier material selection, load support and cooling tube attachment. Recommended candidates are shown in Tables 2-1 and 2-2.

Eighteen capillary fluid acquisition candidates, seven capillary device thermal conditioning candidates, and four pressurization system candidates were considered. Since pressurization will be accomplished when the propellant is unsettled (Reference 2), the use of warm pressurant will result in rapid ullage pressure decay when the cold liquid "settles" through the pressurant. Cold pressurant used to alleviate the problem imposes a severe weight penalty on the capillary acquisition subsystem. Thermal subcooling was identified as a promising candidate for providing boost pump NPSP. This concept uses throttled vent fluid to subcool the main engine inflow in a compact heat exchanger before it enters the boost pump.

Table 2-1. Recommended Acquisition Subsystem Candidates

Fluid Conditioning Candidates	Capillary Device Thermal Conditioning Candidates	Boost Pump Thermal Conditioning Candidates	Propellant Ducting Thermal Conditioning Candidates
1. Start Basket – Screen device over outlet & sump provides liquid for thermal conditioning requirements between burns from a liner or channel sized to remain full during entire mission. Propellant duct cooling and/or chilldown as well as capillary device cooling requirements are supplied from this liner. The basket is sized to provide liquid outflow to main engines during fluid settling, collection & capillary device refill. Screened compartments are required in LH_2 tank start basket to maintain liner flow between burns & liquid over outlet. Lightest weight & least complex fluid containment concept. If main tank pressurization is required, however, cold gas pressurant requirements severely penalize this concept. 2 Start Tank – Bypass Feed Device – Separate tank of approximately the same volume as the start basket is located near sump of main tank. Outflow requirements, inner screened compartments, liner & channels are similar to those of start basket. Valves are used to control outflow & refilling. Only start tank must be pressurized for main engine start. 3. Channel Refilled by Pumping – This concept does not rely upon fluid settling for refill. Uses channels that are wetted after a main engine burn by capillary action. When channels are completely wetted, a pump connected between tank contents & a channel manifold begins pumping. Channels maintain contact with liquid pool in tank so that liquid circulates through channels as fluid in the channels is pumped back into tank. Surface tension retention capability of wetted channel keeps vapor from flowing into channels during pumping. Subsystem operation produces full channels just before burn. During main engine burn, most of the liquid spills from the channel toward the outlet because retention capability is exceeded. Acquisition device weight is greater than the other two recommended candidates. Requires unique flow analysis compared to the other two candidates (settling & spilling, wicking, wetting & internal vapor flow).	1 Acquisition Device Cooling – Uses active cooling coils wrapped around device. Cooling coils are fed throttled vent fluid from compartments inside acquisition device. Primary cooling mode is continuous flow, although intermittent-flow designs will be considered. Coils contained fluid sufficiently to prevent vaporization. 2 Thermal Subcooling – Uses active cooling coils similar to Concept 1 but coils contained fluid only enough to provide boost pump NPSH. This concept could eliminate main tank pressurization subsystem, potentially reducing subsystem weight by 540 lb. Useful for start basket & channels refilled by pumping concepts. 3. Pressure Conditioning – Uses cold helium to suppress vaporization in contained liquid. Because of large pressurization subsystem weight penalties, this concept is applicable only to start tank. Since Subsystem 1 is lighter, pressure subcooling will be used as a backup should Subsystem 1 prove too complex or difficult to apply.	1 Wrap Drive Shaft Area Near Pump With Cooling Coils – Heat is taken out near contained fluid. Heat can be removed readily from drive shaft housing but heat removal from drive shaft & impeller between burns is an extremely difficult problem. 2 Purge Turbine With Cold Helium – This system requires a cold helium purge. Drive shaft cooling is difficult. No pump modifications are required & thus is least complex. Removes some heat directly. 3 Purge Turbine With Cold Helium & Use Cooling Coils to Intercept Incident Heating – More uniform cooling & design flexibility in removing heat by two methods. Pump cooling from sources other than turbine is handled by cooling coils. Note: If Candidates 1 to 3 are not satisfactory in eliminating vaporization in contained boost pump fluid between burns, the more complex candidates employing gearbox purging or drive shaft purging will be required. Modifications required to implement these cooling schemes are of sufficient complexity to severely jeopardize their adoption.	1 Wrap Duct Length With Cooling Coils – Throttle vent fluid & wrap cooling coils around duct. (Consider use of hydrogen to cool LO_2 duct.) May require large quantities of cooling fluid compared to flushing & chilling down the lines before each burn. This could cause a significant increase in acquisition subsystem volumetric requirements. Advantages are elimination of line chilldown and time in start sequence required for engine chilldown & propellant bleed lines. Also might be easier to cool the boost pump if duct is cool, simplifying the engine start sequence. Adds to system complexity because of cooling coils wrapped around duct. 2 Flush Propellant Lines at Either a Low Continuous Rate or at a High Rate for a Specified Period Just Before MES – This eliminates the complexity of wrapping cooling coils around the line. Flushing may require running boost pumps. Lower cooling quantities used than in Concept 1. May not be completely compatible with cooled boost pump option. (A portion of line just downstream of boost pump may be required to keep boost pump cooled efficiently.)

Table 2-2. Recommended Capillary Device Fabrication Candidates

Component or Process	Fabrication Alternatives
Screen Material	1. Aluminum screen where available 2. CRES screen for low micron ratings where aluminum is not available
Screen Mesh	1. Dutch twill screen for wicking applications 2. Square-weave screen where refilling is of overriding importance
Screen Pleating	1. Nonpleated screens are baseline approach 2. Pleated screens where fabrication is not a problem & surface area requirements are high
Screen Backup	1. Perforated aluminum plate is baseline approach 2. Coarse screen should be used if extra stiffness is important 3. Open isogrid offers increased strength
Screen Attachment	1. Resistance welding is baseline method 2. Bolting should be used where screen must be removable
Cooling Tube Attachment	1. Dip brazing for small devices 2. Resistance welding of extruded webbed tubes for large devices

Sixteen potential methods were considered for cooling the boost pump. Effective cooling methods were found to be too complex to be adopted. Boost pump cooling was thus considered unfeasible. The nine propellant duct thermal conditioning methods considered were eliminated since a wet line requires a wet boost pump.

To use program resources most efficiently, the recommended subsystems in Table 2-1 were analyzed to determine which combinations were most desirable. These combinations were then focused upon for the remainder of the study.

The process of discriminating between these subsystems was formulated into a decision tree, as shown in Figure 2-1. Decisions were structured so that answering a question affirmatively allowed adoption of a less complex, lighter, and less costly system (shown on the left); while answering negatively forced adoption of the more complex, heavier, and more costly system (on the right). The main design drivers, considering the Centaur D-1S and other advanced versions of Centaur, were cost, complexity, and weight.

The first decision to be made was whether settling can be used to refill the capillary device successfully. If the answer was positive, a start basket or start tank system could be used. If settling could not refill the capillary devices, channels refilled by pumping should be studied. An approach using channels refilled by pumping is heavier than the start basket and start tank and is more complex because it has a lower state of development, requires rotating machinery, and will probably require an orbital test to prove out its operation.

Looking at the left side of the tree, the next decision to be made was whether thermal subcooling could be used to provide NPSP for the contained fluid and thus eliminate the need for main tank pressurization. If this was answered affirmatively, the lighter-weight, lower-cost, passive start basket would be used. If thermal subcooling could not successfully provide NPSP requirements, the start tank would be chosen to minimize main tank pressurization system requirements.

Going down the tree, the subsequent decisions affect feed system complexity. It is desirable to make no changes to the existing boost pumps and propellant ducts. As shown on the tree, the next question in the left-most branch is whether a start sequence can be developed without cooling the boost pump. If boost pump cooling is required, then the need for feedline cooling should be assessed.

On the right half of the tree, the concept using channels refilled by pumping was evaluated. The first question was whether the system will successfully clear vapor from the channels between burns. If this could not be accomplished, none of the recommended capillary systems would be satisfactory and the existing hydrogen peroxide system would win by default. If the system would clear vapor, the next question would be whether thermal subcooling can be achieved. If this could not be done, the need for thermal conditioning would then be determined. Since the channels could be pumped full just before the start

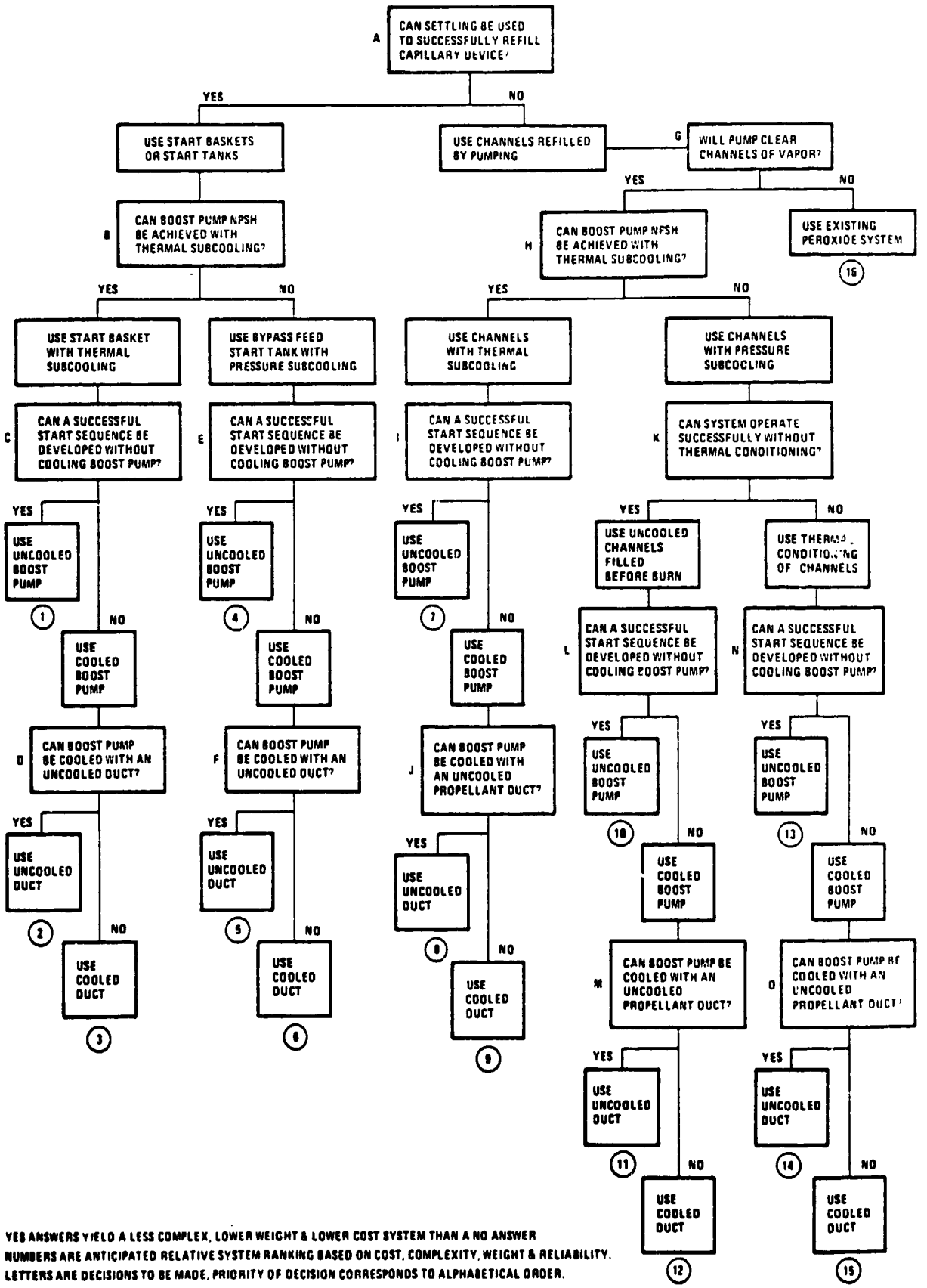

Figure 2-1. Centaur Propellant Acquisition Decision-Making Process (Decision Tree)

sequence, it was possible that active thermal conditioning (other than the channel pumping) would not be required. Other decisions were similar to those discussed in the left branch of the tree.

Each of the small circles at the end of each branch denotes a system; numbers represent the preliminary ranking in terms of desirability. The most desirable system, for example, is No. 1, the start basket using thermal subcooling and no boost pump or propellant duct cooling. This approach appeared to be several hundred pounds lighter than the baseline settling system. It was similar in complexity to the baseline system because addition of the acquisition subsystem will be offset by elimination of the main tank pressurization subsystem. System 2 also would be potentially several hundred pounds lighter than the baseline system, but would be more complex since cooling coils and purging would probably be required to cool the boost pump. System 3 is more complex due to cooling coils required for the duct. Systems 4, 5 and 6 are heavier than No. 1, 2 and 3 due to pressurization requirements. In terms of complexity, the start tank of System 4 has an extra tank, three or four valves, and a start tank pressurization system compared to the boost pump and feedline cooling of No. 3. System 4 is thus at least as complex as No. 3 and is heavier. Similar arguments can be made for the other relative rankings given.

Priority was given to answering the critical questions represented in the decision tree: (1) Can settling be used to successfully refill the capillary device? (2) Can boost pump NPSP be achieved with thermal subcooling? and (3) Can a successful start sequence be developed without cooling the boost pump? These questions were answered affirmatively and System 1 using a start basket with thermal subcooling and an uncooled boost pump was selected as one of the devices to be designed. To have two distinctly different subsystems for design and comparison, a bypass feed start tank using an uncooled boost pump was also selected.

2.1.1 FLUID ANALYSIS. Start tank and start basket fluid analyses were performed to determine capillary acquisition volumetric requirements and performance. Initially, the critical questions in Figure 2-1 were addressed: Can a successful start sequence be achieved without cooling the boost pump? Can settling be used successfully to refill the capillary device? A successful start sequence was developed and a conservative analysis affirming successful refilling with settled fluid was performed. Fluid analysis then was continued by determining the effect of start transients and vibrations on capillary device liquid retention. Start basket and start tank sizing was then performed based upon start sequence, thermal conditioning, residual and channel volume requirements. Wicking to provide flow for maintaining wet start basket screens was analyzed. Problems of filling on the ground and possible abort of Centaur while in the Shuttle cargo bay were addressed. The interaction of the propellant utilization subsystem with the start basket was also considered.

2.1.1.1 Start Sequence. A start sequence was selected that avoided costly engine requalification and resembled the existing Centaur start sequence as closely as

possible. The recommended start sequence using start baskets and initially dry propellant ducts is:

1. Open fuel and oxidizer shutoff valves to fill and chill the sump and boost pump.

2. Close the shutoff valves (optional).

3. Start the boost pump and chilldown the lines through the recirculation system.

4. When the boost pump is up to speed, open the shutoff valves, and use a normal chilldown sequence for the engine.

The main difference between this start sequence and the existing start sequence lies in the fact that the existing start sequence settles the propellant before start and, therefore, has the boost pump full. The capillary devices have dry boost pumps upon start sequence initiation. The engine shutoff valves are opened to provide the driving pressure for flow. Start sequence flow rate, thrust levels, and chilldown quantities were developed for Shuttle cargo bay and orbital heating conditions.

2.1.1.2 Settling and Refilling. Examination was made of existing methods of predicting settling time to determine their applicability to Centaur D-1S. For the existing hydrogen peroxide settling system, the settling process occurs at 0.11 kN (24 lb_f) of thrust. For the capillary acquisition system, settling occurs during the start sequence with thrust buildup to a maximum level of 133 kN (30,000 lb_f) during the final stages of settling. Existing correlations proved inadequate either because they are applicable only to low Weber number flow regions, depend upon semiempirical coefficients that cannot be readily evaluated, or require the use of a complicated computer model that, while applicable to the high Bond number and Weber number regimes where geysering and recirculation are dominant, has limited predesign value due to its running time and complexity.

Another method of computing settling time is an approximation sometimes used for predesign calculations. This method merely multiplies the free-fall time (the time between initiation of thrust and liquid impingement on the aft bulkhead) by a constant to account for liquid geysering and energy dissipation after liquid impingement on the aft bulkhead. The justification for using an approximation of this type is that the constant can be chosen to yield a conservative settling time value and that no better simple method is available at this time. Settling calculations were performed using this method and the start sequence thrust profile.

Thrust barrel refilling calculations were performed. The thrust barrel for the baseline Centaur D-1S consists of a cylindrical shell of 0.63 m (24.73 in) radius and 0.41 m (16 in) high placed symmetrically over the LO_2 tank outlet to distribute the load from the thrust structure. On the top surface of the thrust barrel are 0.04 m (1.5 in) and 0.10 m (4 in) diameter holes with a total area of 0.11 m^2 (1.18 ft^2). On the side of

the thrust barrel near the bottom are nineteen 0.06 m (2.4 in) diameter holes and sixty-six 0.013 m (0.5 in) diameter holes with a total flow area of 0.064 m^2 (0.69 ft^2).

An analysis was performed for both stable (Bo < 0.84) and unstable (Bo > 0.84) holes on the top of the thrust barrel. For stable holes, surface tension will resist the passage of vapor out of the thrust barrel and retard the refilling process.

The analysis assumed that liquid covers the thrust barrel completely before refilling commences. The hydrostatic head must, therefore, drive the liquid into the basket while permitting an equal volume of vapor to be ejected. Thrust barrel refilling times were found to be three to six seconds using main engine thrust. This additional outflow time resulted in approximately a 75 percent increase in capillary device volume. This was unacceptable because of the small quantity of propellant remaining in the tank and the resultant difficulty in submerging the capillary device for refill. To alleviate this problem, thrust barrel refilling time was decreased by increasing side hole area to 0.383 m^2 (4.12 ft^2) and top hole area to 0.323 m^2 (3.48 ft^2). This reduced thrust barrel refilling time to about one second at main engine thrust conditions.

Settling and thrust barrel refilling calculations were used to compute available refilling time. The fourth burn on the five-burn mission was found to have minimum refilling time for both LO_2 and LH_2 start baskets. For the LO2 tank, refilling time available was 15.66 seconds (18.90 seconds of burn time minus 1.54 seconds for thrust barrel refilling, and 1.70 seconds for settling). For the LH_2 tank, refilling time available was 15.07 seconds (18.90 seconds of burn time minus 3.83 seconds for settling).

Refilling calculations performed for the start basket assumed only hydrostatic pressure as the driving pressure with no dynamic refilling. Refilling was considered not to start until settling was complete. Screen wetting was assumed to exist during the entire refilling period. The screen retention pressure thus inhibited refilling during the entire period. Capillary device refilling was computed based on pressure differences between the inside and outside of the capillary device.

Start tank refilling was successfully accomplished by venting the start tanks to 34.45 kN/m^2 (5 psia) below the main tank pressures. This pressure difference was maintained by venting during refilling.

For the LO_2 start basket, refilling calculations were carried out incrementally. As shown in Figure 2-2, the LO_2 basket was broken down into three regions: a sump, a cylinder, and a cone. Equations were formulated and solved for each region as a function of screen open area, as presented in Table 2-3.

System design calculations indicated that screen open area will be 32 percent; thus, capillary device refilling will take place within the allowable 15.66 seconds. The LO_2 basket screen is 50 × 250 mesh.

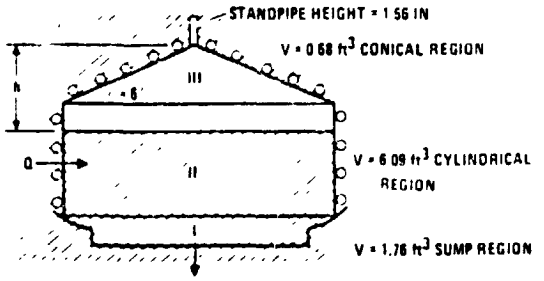

Figure 2-2. LO_2 Start Basket Refilling

Table 2-3. LO_2 Start Basket Refilling Time

Screen Open Area (%)	Refilling Time (sec)			
	Sump	Cylinder	Cone	Total
12.5	0 61	3 86	9.0	13 47
25	0.30	1 93	4.5	6 71
50	0.15	0.96	2.25	3 36
100	0.08	0 48	1.13	1 69

For the LH_2 start basket, a similar analysis was used with a single-step procedure to compute refilling time as a function of screen open area. Results appear in Table 2-4. A standpipe height of 0.14 m (5.58 in) was used to minimize trapped vapor volume. Screen open area is anticipated to be 29 percent; thus refilling will take place within the allowable 15.07 seconds. The LH_2 basket is divided into two compartments: the top is 40 × 200 mesh screen; the lower is 50 × 250 mesh. The compartments are separated by 14 mesh screen.

2.1.2 THERMAL ANALYSIS. Thermal analysis was performed in the areas of thermal subcooling, start basket and start tank thermal conditioning, tank pressure control, and boost pump thermal conditioning. Major emphasis was placed upon the critical areas of thermal subcooling to provide boost pump NPSP and start basket thermal conditioning to prevent screen dryout.

2.1.2.1 Thermal Subcooling. To provide satisfactory boost pump operation, adequate subcooling must be supplied to prevent cavitation. The subcooling must be sufficient to intercept heat input to the fluid entering the boost pump as well as to provide boost pump NPSP. These requirements are 4.22 kw (4 Btu/sec) and 0.83 kN/m^2 (0.12 psi) for the LH_2 boost pump, and 4.22 kw (4 Btu/sec) and 4.96 kN/m^2 (0.72 psi) for the LO_2 boost pump. In the existing Centaur, pressurant is used to subcool the liquid flowing to the pumps and suppress boiling. For the start basket application, throttled vent fluid is used to remove heat from this fluid to achieve subcooling. Heat exchangers were analyzed for supplying boost pump NPSP by cooling the liquid flowing to the boost pump. This thermal subcooling concept eliminates main tank pressurization and requires pressurization only for auxiliary systems such as attitude control. The heat exchanger concept, shown schematically in Figure 2-3, uses throttled vent fluid, as shown thermodynamically in Figure 2-4, to cool any hot-side fluid flowing to the boost pumps.

Table 2-4. LH_2 Start Basket Refilling Time

Screen Open Area (%)	Refilling Time (sec)
12.5	10.9
25	5.45
50	2.72
100	1.36

Sufficient heat must be transferred in the subcooler to remove heating to the hot-side fluid from the warm boost pump and bearings, provide boost pump NPSP, and counteract any pressure drop caused by the thermal subcooler itself.

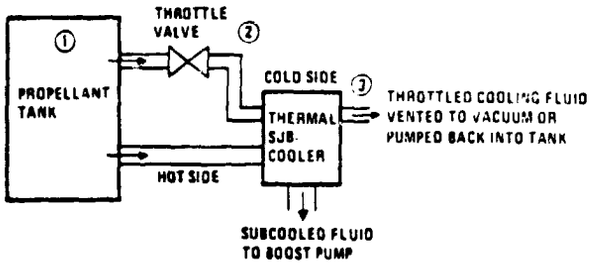

Figure 2-3. Schematic of Thermal Subcooling

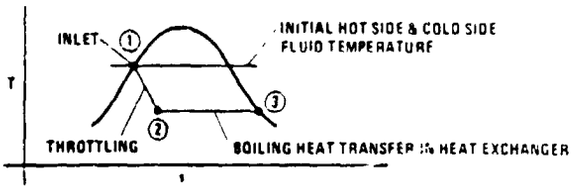

Figure 2-4. Cooling Fluid Thermodynamic States

Screened channels of 325 × 2300 mesh provide liquid flow to the hot side of the exchanger. The cold side fluid is also extracted from the screened channels and throttled to a lower pressure and temperature before entering the subcooler. Multipass, parallel-flow heat exchangers were used. Several configurations were examined for both the LO_2 and LH_2 subcoolers. The objective in designing the heat exchanger surface was to provide high heat exchanger effectiveness coupled with a low pressure drop.

The subcooler designed for the LO_2 tank is shown in Figure 2-5.

2.1.2.2 Start Basket Thermal Conditioning. The objectives of start basket thermal conditioning were to prevent dryout of the start basket outer screens and to prevent vapor formation in the screened channels feeding the subcoolers. Screen dryout must be prevented because capillary devices for wetting fluids operate by keeping vapor out

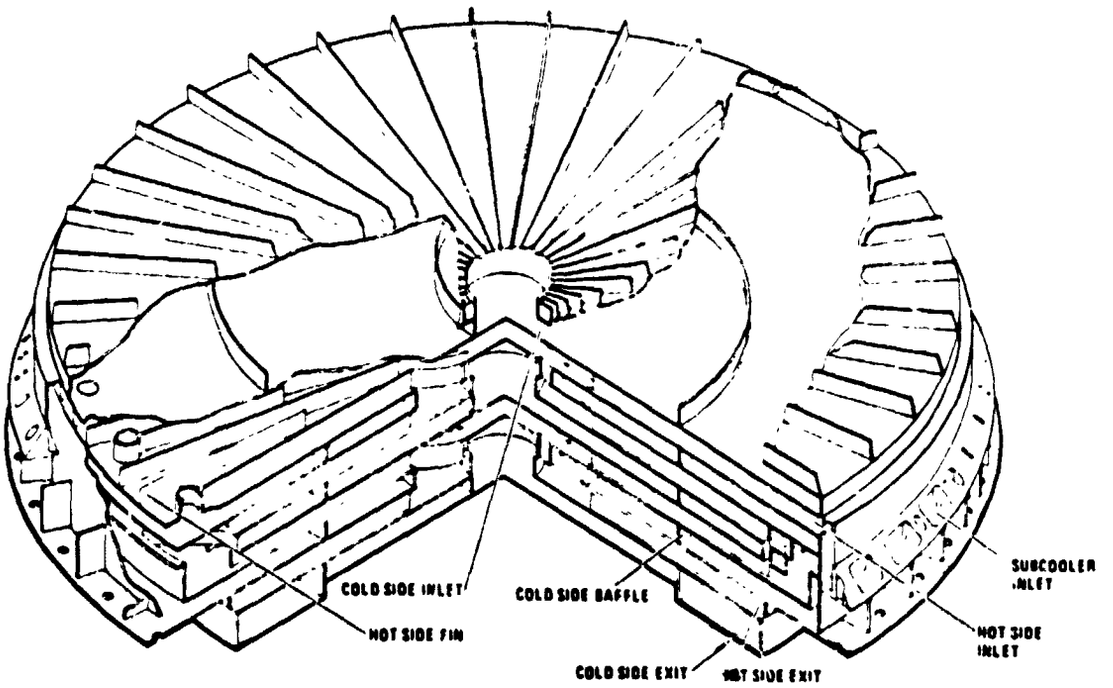

Figure 2-5. LO_2 Tank Thermal Subcooler

of the contained liquid space. If screens dry out, vapor can enter freely, allowing the wetting fluid to migrate from the screened enclosure. Vapor formation in the start basket will occur due to pressure changes, or incident heating or fluid removal. Screened channels within the start basket prevent vapor from entering the subcooler and capillary device thermal conditioning system. To obtain satisfactory subcooler and capillary device thermal conditioning, the channels must be kept full at all times. To prevent heat input to the channels from causing vaporization in the channels, the capillary device cooling system is designed to maintain the basket surfaces slightly below saturation temperature.

The primary approach to start basket thermal conditioning was to use throttled vent fluid in cooling coils attached to the outer screened surface. This concept was studied in detail with design drawings developed showing cooling subsystem hardware, and cooling coil attachment and routine. This system had a high vent fluid penalty and cooling coil weight penalty because of the high condensation heat loads. Condensation, by itself, will not cause screen drying. However, if cooling tubes are designed to intercept heat input that could cause screen drying (forced convection, free convection, or conduction from superheated vapor) then all the cooling capacity of the throttled vent fluid will be used up in a short length of tubing if condensation occurs. No cooling capacity will then be available for the remainder of the cooling loop and incident heat transfer could cause screen drying. Thus, an active thermal conditioning subsystem must be designed for condensation heat transfer.

Several options were briefly analyzed for reducing cooling system weight penalty. One option used a pumping system consisting of a surge tank and vacuum pump to return the throttled cooling fluid to the main propellant tank. This approach can also be used to return subcooler coolant to the main propellant tanks. Passive cooling was analyzed, using wicking fluid provided by wicking channels, parallel plates, or parallel screens. Cooling system alternatives were evaluated as separate options in comparing the baseline system with start baskets and start tanks.

2.1.3 SYSTEM DESIGN. Preliminary designs were made of both a start tank and start basket for both the LO_2 tank and the LH_2 tank.

The start baskets for both fluids are basically similar in that they have an outer screen cooled by liquid from screened capillary channels inside the start basket. Also, each has an internal subcooler fed from the same capillary channels.

The start tanks are not cooled but are insulated to prevent excessive heat input and pressure rise. Pleated screen channels at the tank outlet prevent vapor outflow and reduce residuals.

In the start basket configurations, all fluid for the engines passes through the basket and subcooler throughout engine operation; in the start tank, bypass valves are necessary so that only the initial starting fluid is provided by the start tank.

2.1.3.1 Capillary Device Volumetric Requirements. Start basket volumetric requirements were determined based on a conservative case for start sequence usage, trapped vapor, outflow, thermal conditioning, and thermal subcooling requirements. Results are shown in Table 2-5. Isometric sketches of the LO_2 and LH_2 start baskets and thermal subcooler are shown in Figures 2-6 and 2-7.

Start tank volumetric requirements were determined based upon the sum of start requirements, main tank settling, screen channel volume, liquid volume required to prevent vapor ingestion, and ullage volume requirements based upon anticipated pressure rise rates. Nonvented start tanks were used to simplify thermal conditioning requirements. Start tank volumes were found to be 0.24 m^3 (8.45 ft^3) for LO_2 and 1.04 m^3 (36.84 ft^3) for LH_2. Start tank isometric sketches are shown in Figures 2-8 and 2-9.

2.1.4 SYSTEM COMPARISON. Comparisons were made between the capillary acquisition systems designed and the existing hydrogen peroxide settling and warm helium pressurization systems. In addition to the actively cooled start baskets, passively cooled start baskets using capillary pumping to replace the cooling coils were considered. The options compared were:

1. Baseline pressurization subsystem plus settling system.

2. Start baskets using passive capillary device cooling (wicking) and subcoolers for providing boost pump NPSP with subcooler coolant flow dumped overboard.

3. Start baskets using passive cooling and subcoolers for NPSP with subcooler coolant flow pumped back into the tank.

4. Start baskets using cooling coils for capillary device cooling and subcoolers for NPSP with all coolant flow dumped overboard.

5. Start baskets using cooling coils for capillary device cooling and subcoolers for NPSP with all coolant flow pumped back into the tank.

Table 2-5. Start Basket Volumetric Requirements

Requirement	LH_2, m^3 (ft^3)	LO_2, m^3 (ft^3)
START SEQUENCE		
Sump and Pump Chill and Vent	0.046 (1.64)	0.006 (0.02)
Sump and Pump Fill	0.062 (2.18)	0.043 (1.53)
Boost Pump Startup	0.158 (5.60)	0.044 (1.57)
Engine Chilldown	0.314 (11.11)	0.023 (0.83)
Settling (Main Engine)	0.27 (9.54)	0.04 (1.41)
Thrust Barrel Filling (Main Engine)		0.036 (1.28)
Total	0.85 (30.07)	0.19 (6.64)
THERMAL CONDITIONING		
Subcooling Flow	0.043 (1.53)	0.0084 (0.30)
Conditioning Flow (Active Cooling)	0.384 (13.6)	0.037 (1.29)
CHANNEL VOLUME	0.061 (2.17)	0.0051 (0.18)
RESIDUAL VOLUME	0.027 (0.97)	0.0034 (0.12)
TRAPPED VAPOR (BOTTOM COMPARTMENT)	0.008 (0.28)	
Total	1.37 (48.62)	0.24 (8.53)

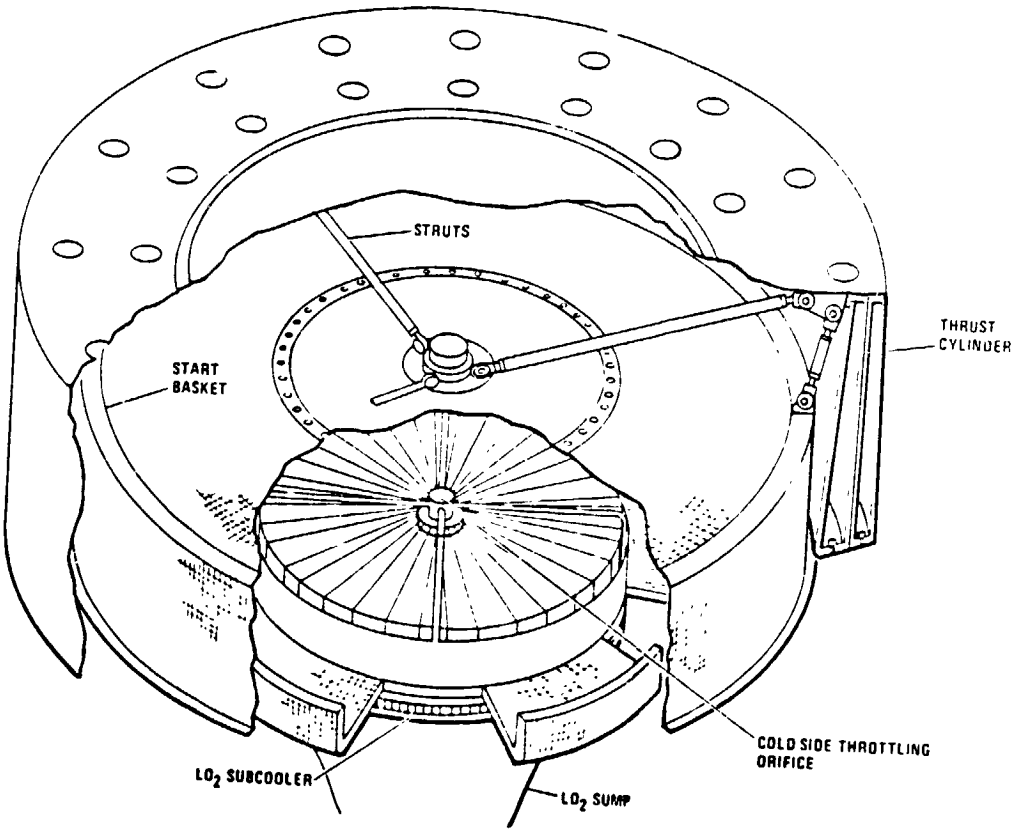

Figure 2-6. LO_2 Start Basket and Subcooler

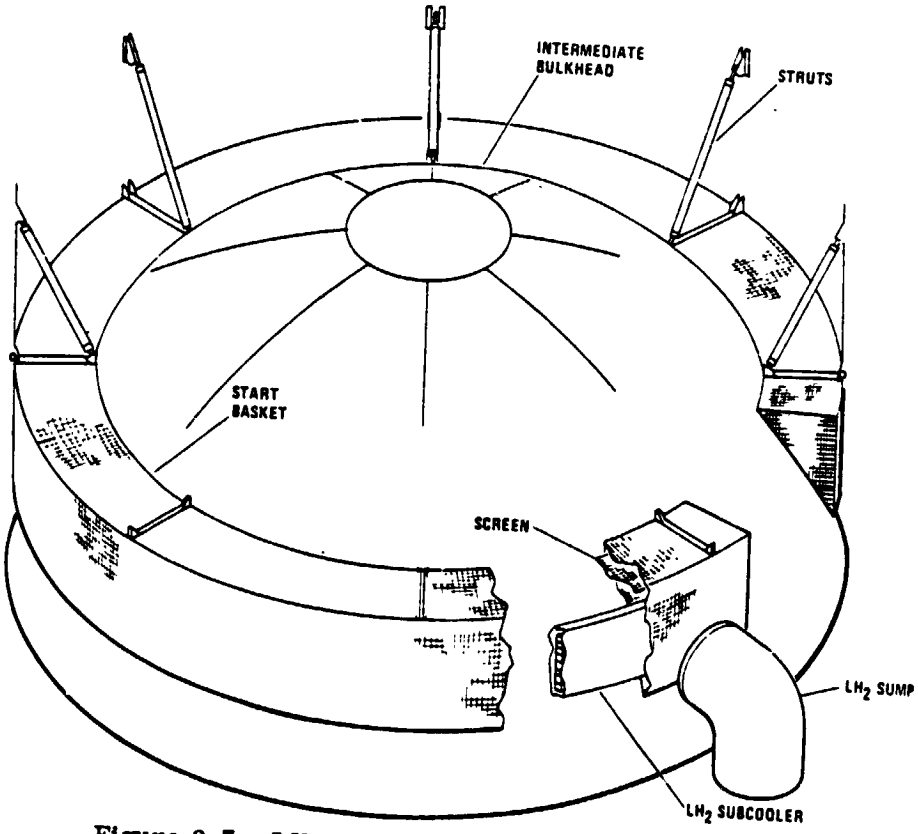

Figure 2-7. LH_2 Start Basket and Subcooler

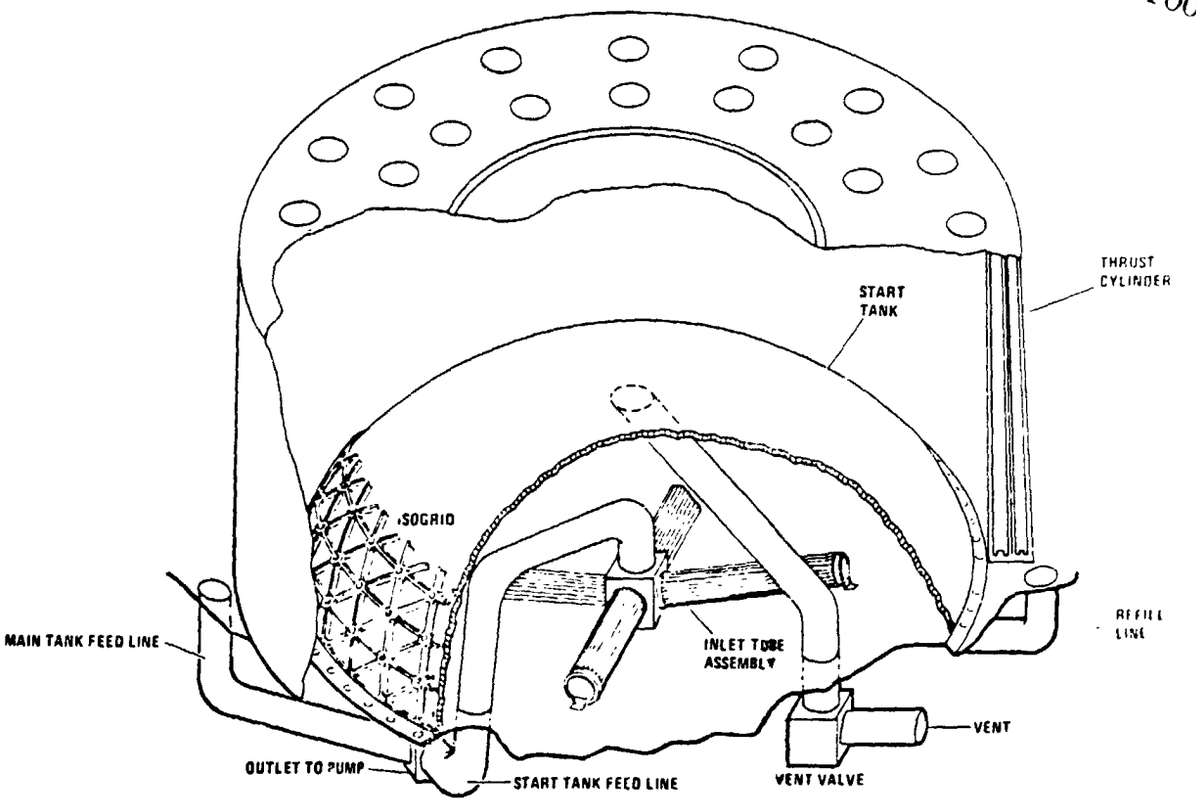

Figure 2-8. LO_2 Start Tank

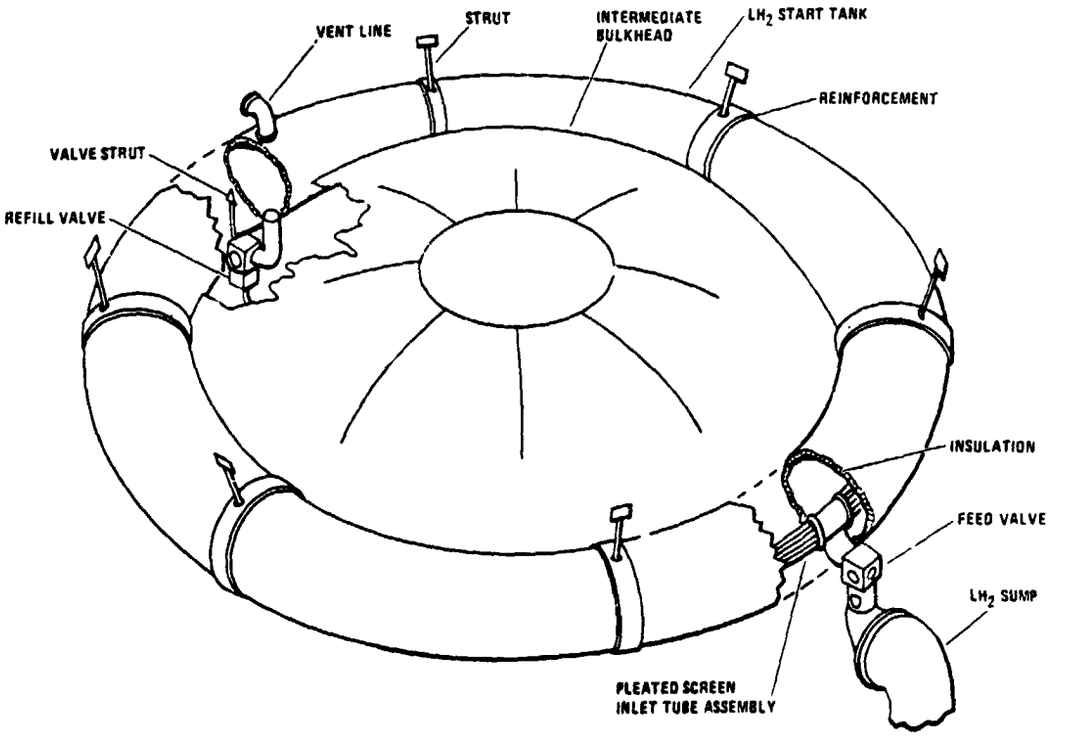

Figure 2-9. LH_2 Start Tank

6. Start baskets using cooling coils for capillary device cooling and subcoolers for NPSP with cooling coil flow dumped overboard and subcooler flow pumped back into the tank.

7. Start baskets using cooling coils for capillary device cooling and subcoolers for NPSP with cooling coil flow pumped back into the tank and subcooler flow dumped overboard.

8. Bypass feed start tanks with cold helium pressurization.

Comparisons were made on the basis of relative reliability, hardware weight, payload penalty, recurring costs, power requirements, and flight profile flexibility for the eight options for each of the three reference missions. These comparisons indicated that for multiburn missions, particularly missions with five burns or greater, passively cooled capillary devices with subcooler fluid returned to the tank offers the greatest payload weight advantage. This option (Option 3) is relatively insensitive to the number of burns. Based on the comparisons, discussed in more detail in Reference 2, passive cooling for capillary device thermal conditioning and thermal subcooling to provide pump NPSP were identified as promising concepts requiring more detailed study. A development plan was prepared for evolving from current passively cooled start basket technology to the point where a non-interference flight test could be performed on a future Centaur vehicle.

2.2 RESULTS OF NAS3-19693, "CENTAUR PROPELLANT THERMAL CONDITIONING STUDY

Based on the results of NAS3-17802, passive thermal conditioning of capillary devices, thermal subcooling for providing turbopump NPSP and design of vent/mixers for cryogenic pressure control in zero gravity were selected as areas requiring additional investigation.

2.2.1 PASSIVE THERMAL CONDITIONING. Capillary acquisition device passive thermal conditioning offers reduced complexity, hardware weight and vented fluid weight compared to an actively cooled system for preventing screen dryout (maintaining wet screens) between burns. Work was performed to analytically and experimentally examine wicking configurations that could enhance the heat interception capability of a screen alone. Wicking configurations for passive thermal conditioning were evaluated by establishing the ground rules of the study, determining the method of analysis, and selecting the most promising configurations for satisfying heat flux interception requirements. Fabricability of each wick configuration was assessed for LO_2 and LH_2 Centaur D-1S start basket cooling requirements. Wick configurations were selected for testing and test results obtained with ethanol were compared to analytical predictions of wicking versus time.

Heat transfer conditions that could cause screen drying were examined for all start basket screened surfaces for Centaur D-1S mission conditions. Local heat transfer coefficients as well as average heat transfer coefficients were established for forced convection, free convection, and conduction with vapor adjacent to the start basket screened surfaces. Total fluid vaporized, assuming interception of heat by wicking, was determined for each portion of the mission for both the oxygen and hydrogen capillary device. Only mission conditions were considered where there was a possibility that the entire basket could be surrounded by vapor. Vapor volumes generated were translated into wicking distances for each basket surface, assuming worst-case vapor location in the start baskets.

Table 2-6 represents the matrix of possible worst-case wicking rate requirements and was used to determine wicking geometry for each specimen of interest.

2.2.1.1 Analysis. Flow analysis of capillary pumping for providing capillary device passive thermal conditioning was initiated. A literature review was performed to assess the available information on wicking flow. The pressure differentials of interest are those dependent upon surface tension (ΔP_σ), gravity (ΔP_g) and viscosity (ΔP_f) (laminar frictional pressure loss). Momentum losses can normally be neglected for the low flow rates that occur during wicking. The pressure differentials are related by

$$\Delta P_\sigma = \Delta P_g + \Delta P_f \tag{2-1}$$

Expressions were derived for the surface tension pressure differential

$$\Delta P_\sigma = -\sigma\,(1/R_1 + 1/R_2) \approx F/A_F \tag{2-2}$$

where

R_1 & R_2 = principal radii of curvature of the liquid wicking front

σ = liquid surface tension

F = surface force

A_F = cross-sectional area of the wicking front

The surface force $F = \sigma$ (WP), where WP is the wetted perimeter of the wicking front.

Surface tension pressure differentials were derived for each configuration of interest (Table 2-7), using Equation 2-2. For open channels, the results of Bressler and Wyatt (Reference 5) were also used to compute the surface tension pressure. They found that an expression

Table 2-6. Passive Cooling Requirements

Basket	Location*	Maximum Average Heat Flux		Maximum Local Heat Flux		Time Period	Maximum Wicking Distance from Pool To Heat Source		Acceleration Level
		Watts/m^2	(Btu/hr-ft^2)	Watts/m^2	(Btu/hr-ft^2)		m	(ft)	g's
LO_2	Bottom	35.3	(11.2)	35.3	(11.2)	Shuttle ACS	0.09	(0.31)	0.0085
		9.8	(3.1)	9.8	(3.1)	Centaur ACS - Low Earth Orbit	0.09	(0.31)	0.00189
		9.8	(3.1)	9.8	(3.1)	Centaur ACS - Synchronous Eq.	0.09	(0.31)	0.0009
	Top	1.9	(0.6)	4.4	(1.4)	Shuttle ACS	0.04	(0.14)	0.0085
		1.9	(0.6)	4.4	(1.4)	Centaur ACS - Low Earth Orbit	0.15	(0.48)	0.00189
		1.9	(0.6)	4.4	(1.4)	Centaur ACS - Synchronous Eq.	0.19	(0.63)	0.0009
	Side	1.8	(0.5)	4.4	(1.4)	Shuttle ACS	0.11	(0.36)	0.0085
		1.6	(0.5)	4.4	(1.4)	Centaur ACS - Low Earth Orbit	0.14	(0.45)	0.00189
		1.6	(0.5)	4.4	(1.4)	Centaur ACS - Synchronous Eq.	0.14	(0.47)	0.0009
LH_2	Bottom	30.3	(9.6)	30.3	(9.6)	Shuttle ACS	0.16	(0.51)	0.0085
		30.3	(9.6)	30.3	(9.6)	Centaur ACS - Low Earth Orbit	0.32	(1.05)	0.00189
		30.3	(9.6)	30.3	(9.6)	Centaur ACS - Synchronous Eq.	0.31	(1.11)	0.0009
	Sidewall	31.5	(10)	31.5	(10)	Shuttle ACS - Insulation Outgassing - t = 480 sec	0	(0)	0.0085
		5.7	(1.8)	5.7	(1.8)	OMS ACS - Avg. Heat Trans.	0.43	(1.4)	0.0085
		2.5	(0.8)	2.5	(0.8)	OMS ACS - Before Deployment	0.56	(1.85)	0.0085
		2.5	(0.8)	2.5	(0.8)	Centaur ACS - Low Earth Orbit	0.63	(2.06)	0.00189
		2.5	(0.8)	2.5	(0.8)	Centaur ACS - Synchronous Eq.	0.66	(2.13)	0.0009
	Top	2.5	(0.8)	2.5	(0.8)	Shuttle ACS	0.38	(1.25)	0.0085
		2.5	(0.8)	2.5	(0.8)	Centaur ACS - Low Earth Orbit	0.41	(1.33)	0.00189
		2.5	(0.8)	2.5	(0.8)	Centaur ACS - Synchronous Eq.	0.41	(1.35)	0.0009
	Side Panel	0.9	(0.3)	2.2	(0.7)	Shuttle ACS	0.73	(2.41)	0.0085
		0.9	(0.3)	2.2	(0.7)	Centaur ACS - Low Earth Orbit	0.73	(2.41)	0.00189
		0.9	(0.3)	2.2	(0.7)	Centaur ACS - Synchronous Eq.	0.73	(2.41)	0.0009

$$\Delta P_\sigma = 2\sigma \cos \phi / R_E$$

successfully correlated their data, where

R_E = effective capillary radius = $2A_F$/(WP Width)

ϕ = contact angle, which is equal to zero for LH_2 and LO_2

The frictional pressure drop was computed using

$$\Delta P_f = \frac{2fL\,\rho V^2}{D_H\,g_c}$$

where

f = Fanning friction factor (Blasius friction factor = 4 × Fanning friction factor)

L = distance between liquid pool and wicking front

D_H = hydraulic diameter of wicking cross-section

Table 2-7. Candidate Wicking Configuration

Config.	Sketch	ΔP_f	ΔP_σ	W_T / W
Circle		$\frac{8 \dot{m} \mu L}{\rho \pi R^4 g_c}$	$\frac{2\sigma}{R}$	$\frac{\rho \lambda \pi R^3 g_c}{8 \mu L}\left[\frac{2\sigma}{R} - \frac{\rho g}{g_c} L \sin\theta\right]$
Closed Semicircle		$\frac{16 \dot{m} \mu L (\pi-2)^2}{\rho \pi^3 R^4 g_c}$	$\frac{2(\pi-2)\sigma}{\pi R}$	$\frac{\rho \lambda R^3 g_c \pi^3}{32 \mu L (\pi-2)^2}\left[\frac{2(\pi-2)\sigma}{\pi R} - \frac{\rho g}{g_c} L \sin\theta\right]$
Open Semicircle		$\frac{16 \dot{m} \mu L}{\rho \pi R^4 g_c}$	$\frac{2\sigma}{R}$	$\frac{\rho \lambda R^3 g_c}{32 \mu L}\left[\frac{2\sigma}{R} - \frac{\rho g}{g_c} L \sin\theta\right]$ $\frac{\rho \lambda R^3 g_c}{32 \mu L}\left[\frac{2(\pi-2)\sigma}{\pi R} - \frac{\rho g}{g_c} L \sin\theta\right]$
Parallel Plates	Plate Screen-Screen Plate 	$\frac{12 \dot{m} \mu L}{\rho a b^3 g_c}$	$\frac{2\sigma}{b}$	$\frac{\rho \lambda b^3 g_c}{12 \mu L}\left[\frac{2\sigma}{b} - \frac{\rho g}{g_c} L \sin\theta\right]$
Parallel Plates	Screen Plate-Plate n = no. of holes  50% Open Area (r = 0.064 cm(0.025 in.)	$\frac{3 \dot{m} \mu L (3a-9ne)^2}{4\rho(b-e)^3 a^3 g_c}$	$\frac{(3a-9ne)\sigma}{2(b-e)a}$	$\frac{4\rho\lambda(b-e)^3 a^2 g_c}{3\mu L(3a-9ne)^2}\left[\frac{\sigma(3a-9ne)}{2(b-e)(a)} - \frac{\rho g}{g_c} L \sin\theta\right]$
Parallel Plates	Plate/Screen-Plate 	$\frac{6 \dot{m} \mu L (3a-4ne)^2}{\rho(2b-e)^3 a^3 g_c}$	$\frac{(3a-4ne)\sigma}{(2b-e)a}$	$\frac{\rho\lambda(2b-e)^3 a^2 g_c}{6\mu L(3a-4ne)^2}\left[\frac{(3a-4ne)\sigma}{(2b-e)a} - \frac{\rho g}{g_c} L \sin\theta\right]$
Parallel Plates	Plate/Screen-Plate/Screen	$\frac{96 \dot{m} \mu L (a-nc)^2}{\rho a^3 (2b-e)^3 g_c}$	$\frac{4(a-nc)\sigma}{a(2b-e)}$	$\frac{\rho\lambda(2b-e)^3 a^2 g_c}{96\mu L(a-nc)^2}\left[\frac{2\sigma(2a-2nc)}{a(2b-e)} - \frac{\rho g}{g_c} L \sin\theta\right]$
Parallel Plates	Screen/Plate-Plate Screen  50% Open Area	$\frac{12 (a-2ne)^2 \dot{m} \mu L}{(b-e)^3 a^3 \rho g_c}$	$\frac{2(a-2ne)\sigma}{(b-e)a}$	$\frac{2\lambda g_c}{12\mu L}\frac{(b-e)^3 a^2}{(a-2ne)^2}\left[\frac{2\sigma(a-2ne)}{(b-e)a} - \frac{\rho g}{g_c} L \sin\theta\right]$
Annuli		$\frac{C \dot{m} \mu L}{2\rho\pi(r_o-r_i)^4 g_c}$	$\frac{2\sigma}{r_o-r_i}$	$\frac{\rho\lambda g_c b^3}{12\mu L}\left[\frac{2\sigma}{b} - \frac{\rho g}{g_c} L \sin\theta\right]$, $b = r_o-r_i$
Rectangular Channels Closed		$\frac{2C \dot{m} \mu L (a-b)^2}{\rho 4(ab)^3 g_c}$	$\frac{2(a-b)}{ab}\sigma$	Square a = b, C = 14.23 $\frac{\rho\lambda g_c a^3}{28.6\mu L}\left[\frac{4\sigma}{a} - \frac{\rho g}{g_c} L \sin\theta\right]$
Rectangular Channels Open		$\frac{3 \dot{m} \mu L (2b+a)^2}{\rho (ab)^3 g_c}$	$\frac{(2b+a)}{ab}\sigma$	$\frac{2\lambda a^2 b^3 g_c}{3\mu L (2b-a)^2}\left[\frac{(2b-a)\sigma}{ab} - \frac{\rho g}{g_c} L \sin\theta\right]$
V Grooves Isosceles Closed		$\frac{96 \dot{m} \mu L \tan\frac{\alpha}{2}\left[\tan\frac{\alpha}{2} \sec\frac{\alpha}{2}\right]^2}{\rho A^4 g_c}$	$\left[4\sigma(\tan\frac{\alpha}{2} - \sec\frac{\alpha}{2})\right]/A$	60° (Equilateral Triangle), C = 13.33 $\frac{\rho\lambda g_c A^3\left[\frac{4\sigma}{A}\left(\tan\frac{\alpha}{2} \sec\frac{\alpha}{2}\right) - \frac{\rho g}{g_c} L \sin\theta\right]}{106.64 \mu L \tan\frac{\alpha}{2}\left(\tan\frac{\alpha}{2} \cdot \sec\frac{\alpha}{2}\right)^2}$
V Grooves Isosceles Open		$\frac{112 \dot{m} \mu L \sin\frac{\alpha}{2}}{\rho A^4 (\cos\frac{\alpha}{2})^2 g_c}$	$\frac{\left[\frac{4}{A}\sec\frac{\alpha}{2}\right]\sigma}{A}$	$\frac{\rho\lambda A^3 (\cos^2\frac{\alpha}{2}) g_c}{112 \mu L (\sin\frac{\alpha}{2})}\left[\frac{4(\sec\frac{\alpha}{2})\sigma}{A} - \frac{\rho g}{g_c} L \sin\theta\right]$
Pleated Screens Open	 p = pitch t = depth of pleat	$\frac{C \dot{m} \mu L (w+\pi r)^2}{16 r^3 \rho (w+2r)^4 g_c}$	$\frac{(\pi r+w)\sigma}{r(w+2r)}$	$\frac{4r^2(w+2r)^3}{C(w+\pi r)^2}\frac{\rho\lambda g_c}{\mu L}\left[\frac{(\pi r+w)\sigma}{r(w+2r)} - \frac{\rho g}{g_c} L \sin\theta\right]$
Pleated Screens Closed		$\frac{C \dot{m} \mu L (w+(\pi-2)r)^2}{16 r^3 \rho (w+2r)^3 g_c}$	$\frac{[w+(\pi-2)r]\sigma}{r(w+2r)}$	$\frac{4r^2(w+2r)^3}{C[w+(\pi-2)r]^2}\frac{\rho\lambda g_c}{\mu L}\left[\frac{[w+(\pi-2)r]\sigma}{r(w+2r)} - \frac{\rho g}{g_c} L \sin\theta\right]$
Screen	 Perforated Plate Backup	$\frac{V_W A_F \mu L}{K_1 A_T g_c}$ A_F = flow area A_T = total cross sectional area K_1 = permeability B = an empirical constant	$\frac{8\sigma}{D_s}$	$\frac{\rho\lambda g_c}{\mu L} B \pi t\left[\sigma - \frac{\rho g}{g_c}\frac{D_s}{8} L \sin\theta\right]$

ρ = fluid density

V = liquid wicking velocity

g_c = a dimensional constant

The friction factor is normally expressed as a function of Reynolds number

$$f = C/Re$$

where

C = constant depending upon the cross-section shape

Re = Reynolds number defined as $(\rho V D_H)/\mu$

where

μ = liquid viscosity

Thus

$$\Delta P_f = \frac{2C\dot{m}\mu L}{D_h^2 A_F g_c \rho} \tag{2-3}$$

where $\dot{m}$ is the wicking mass flow rate.

The hydrostatic pressure differential

$$\Delta P_g = \rho g/g_c \, L \sin\theta \tag{2-4}$$

where

g = ambient acceleration level

θ = angle of wicking direction with horizontal

Equations 2-1 and 2-3 were combined and manipulated to yield the heat rate interception capability, $\dot{Q}_c$, of a wicking barrier for a single capillary.

$$\dot{Q}_c = \frac{\rho \lambda g_c D_h^2 A_F}{2 C \mu L} \left[\Delta P_\sigma - \Delta P_g\right] \tag{2-5}$$

where

$\dot{Q}_c = \dot{m}_c \lambda$

λ = heat of vaporization

For thermal conditioning purposes, it is clearer to express the wicking capability in terms of heat rate per unit width, $\dot{Q}/W$. For a heat source acting along a line at distance L from the liquid pool this is

$$\frac{\dot{Q}}{W} = \frac{\dot{Q}_c}{w} = \frac{\rho \lambda g_c D_h^2 A_F}{2 C \mu L w} \left[\Delta P_\sigma - \Delta P_g\right] \tag{2-6}$$

where

w = width of a single capillary

W = width of the capillary device surface

Equation 2-5, the heat rate interception capability for a single capillary, is transformed into Equation 2-6, the heat rate interception capability for a capillary device surface by multiplying Equation 2-5 by the number of capillaries (W/w) in that surface.

For a distributed heat source, $\dot{Q}/A = \dot{Q}/(WL)$, which is equivalent to evaluating Equation 2-6 for $\dot{Q}/W$ at a distance L from the liquid pool. All heat interception can thus be expressed in terms of $\dot{Q}/W$. Equations for computing the $\dot{Q}/W$ capability of each candidate wicking configuration are given in Table 2-7 with Equation 2-2 and 2-4 substituted into Equation 2-6.

Heat flux interception capability determined from the equations given in Table 2-7 was compared to the requirements given in Table 2-6. This evaluation produced optimum, minimum, and maximum spacings or wick dimensions that could intercept all heat flux conditions for each wick for both LO_2 and LH_2. Details of this procedure are discussed thoroughly in Reference 6.

The manufacturing feasibility of each of these configurations was assessed as shown in Table 2-8. Flow optimization of the triangular and equilateral triangular wick geometry was restricted to square and equilateral triangle dimensions since they would be easiest to manufacture. The screens and parallel plates are the most isotropic in terms of capillary pumping capability. Other configurations show a decided directional preference and would require two orthogonal layers of wick to satisfy all heat flux interception conditions.

Based on Table 2-8 results, four configurations were selected for experimental evaluation. Fine mesh screen spot welded to perforated plate was used to create wicking configurations that were selected for their ease of fabrication. These configurations were: plate/screen-screen/plate, plate/screen-plate/screen, screen/plate-plate/screen and pleated screen. Pleated screen was selected because it offers design

Table 2-8. Manufacturing of Configurations

Configuration	Ll_2 cm (inches)						LO_2 cm (inches)								
	Geometric Variable	Minimum		Optimum		Maximum		Manufacturability	Minimum		Optimum		Maximum		Manufacturability
Plate/Screen-Screen	b	0.03	(0.012)	0.058	(0.023)	0.096	(0.034)	Yes	0.0048	(0.0019)	0.152	(0.06)	0.23	(0.089)	Yes
Plate/Screen-Plate/Screen	b	-		0.028	(0.011)	0.056	(0.022)	Yes	-		0.124	(0.049)	0.20	(0.080)	Yes
Screen/Plate-Plate/Screen	b	-		0.015	(0.0061)	0.028	(0.011)	Yes	-		0.099	(0.039)	0.18	(0.071)	Yes
Plate/Screen-Plate	b	-		0.013	(0.00528)	0.032	(0.132),	Yes	-		0.068	(0.0348)	0.15	(0.058)	Yes
Screen/Plate-Plate	b	-		-		0.0070	(0.0028)	No	-		0.061	(0.024)	0.12	(0.048)	Yes
Closed Semicircles	R	0.022	(0.0089)	0.094	(0.0372)	0.14	(0.0552)	No	0.034	(0.013)	0.25	(0.0972)	0.37	(0.144)	No
Open Semicircles	R	0.025	(0.01)	0.058	(0.0228)	0.086	(0.034)	No	0.0025	(0.00098)	0.15	(0.059)	0.22	(0.0888)	No
Open Semicircles**	R	-		-		-		No	0.043	(0.017)	0.056	(0.022)	0.08	(0.032)	No
Closed Squares	a	0.028	(0.011)	0.11	(0.045)	0.17	(0.067)	No	0.0048	(0.0018)	0.30	(0.119)	0.43	(0.168)	No
Open Squares**	a	0.061	(0.024,	-		0.086	(0.034)	No	0.01	(0.0041)	0.15	(0.060)	0.22	(0.089)	No
Open Squares	a	0.048	(0.019)	0.086	(0.034)	0.13	(0.050)	No	0.081	(0.032)	0.23	(0.090)	0.34	(0.132)	No
Closed Equilateral Triangles	A	0.056	(0.022)	0.23	(0.09)	0.34	(0.132)	No	0.010	(0.004)	0.61	(0.24)	0.89	(0.35)	Yes
Open Equilateral Triangles	A	0.046	(0.018)	0.16	(0.064)	0.198	(0.078)	No	0.0076	(0.003)	0.36	(0.14)	0.53	(0.21)	No
Open Equilateral Triangles**	A	0.064	(0.025)	0.086	(0.026)	0.096	(0.038)	No	0.011	(0.0044)	0.18	(0.069)	0.254	(0.10)	No
Pleated Screen	N = 2	t=0.05	(0.02)	t=0.094	(0.037)	t=0.13	(0.051)	Yes	t=0.01	(0.004)	t=0.025	(0.097)	t=0.35	(0.138)	Yes
		p=0.05	(0.02)	p=0.132	(0.052)	p=0.183	(0.072)		p=0.0147	(0.0058)	p=0.35	(0.136)	p=0.49	(0.192	

** Using surface tension pressure defined by Bressler, R.G. and Wyatt, P.W., "Surface Wetting Through Capillary Grooves," Transactions of the ASME, Journal of Heat Transfer, February 1970.

flexibility in permitting increased screen area (and thus low pressure drop transverse to the capillary barrier) as the ratio of screen flow area to projected area is increased. Optimum wicking configurations were determined for ethanol wicking in normal gravity, using the equations given in Table 2-7 for three specimen angles. As discussed in Reference 6, the upper limit on spacing was controlled by wicking height and the lower limit was controlled by minimum manufacturing tolerances. Wick geometries selected are summarized in Table 2-9. Perforated plate used was 0.0225 inch thick with 3/8-inch holes on 0.50-inch centers (51 percent open area).

Test specimens were three inches wide and 18 inches long. With the exception of one wicking configuration employing 200 × 1400 mesh, all screens used were 50 × 250 mesh.

2.2.1.2 Wicking Apparatus. Test specimens were mounted on an aluminum baseplate, which was enclosed in a transparent box, as shown in Figure 2-10. A glass plate was used for the top cover of the box for viewing and photographically recording data. Glass was used because it is clearer than plastic and less susceptible to scratching or crazing. The sides of the enclosure, the fluid reservoir, reservoir refill, and leveling devices were Lexan polycarbonate. This material was chosen over glass because of its machinability. Joints were cemented leak-tight and reinforced with screws as required. The transparent glass cover was not cemented to the test enclosure. The cover could thus be removed without disturbing the test specimens, baseplate, or test enclosure. Baseplate orientation was controlled by adjusting three point screws.

Fixtures were fabricated for clamping and holding the reference screen specimens during testing. Three coplanar knife edges supported the more rigid sandwich configurations and pleated screen. For some tests, the reservoir edge replaced the knife edge nearest the reservoir to minimize dripping from the specimens.

Table 2-9. Selected Specimen Geometries

Plate/Screen-Screen/Plate, Specimen No. 1	b = 0.089 cm, (0.035 in) e = 0.057 cm (0.0225 in)
Plate/Screen-Screen/Plate, Specimen No. 2	b = 0.111 cm (0.004 in), e = 0.057 cm (0.0225 in)
Plate/Screen-Screen/Plate, Specimen No. 3	b = 0.14 cm (0.056 in) e = 0.057 cm (0.0225 in)
Screen/Plate-Plate/Screen Specimen No. 1	b = 0.05 cm (0.020 in) e = 0.057 cm (0.0225 in)
Screen/Plate-Plate/Screen Specimen No. 2	b = 0.06 cm (0.025 in) e = 0.057 cm (0.0225 in)
Screen/Plate-Plate/Screen Specimen No. 3	b = 0.10 cm (0.038 in) e = 0.057 cm (0.0225 in)
Pleated Screen, Specimen No. 1*	p = 0.22 cm (0.087 in) t = 0.38 cm (0.150 in) N = 4
Plate/Screen-Plate/Screen, Specimen No. 1	b = 0.0635 cm (0.025 in) e = 0.057 cm (0.0225 in)
Plate/Screen-Plate/Screen, Specimen No. 2	b = 0.11 cm (0.044 in) e = 0.057 cm (0.0225 in)

where b is the distance between inner barriers
e is the perforated plate thickness
p is the pleat pitch (distance between corresponding points on adjacent pleats)
t is the pleat depth
N is the screen surface area divided by the projected area

* Minimum pleat pitch and depth for 46 cm (18 in) long pleat.

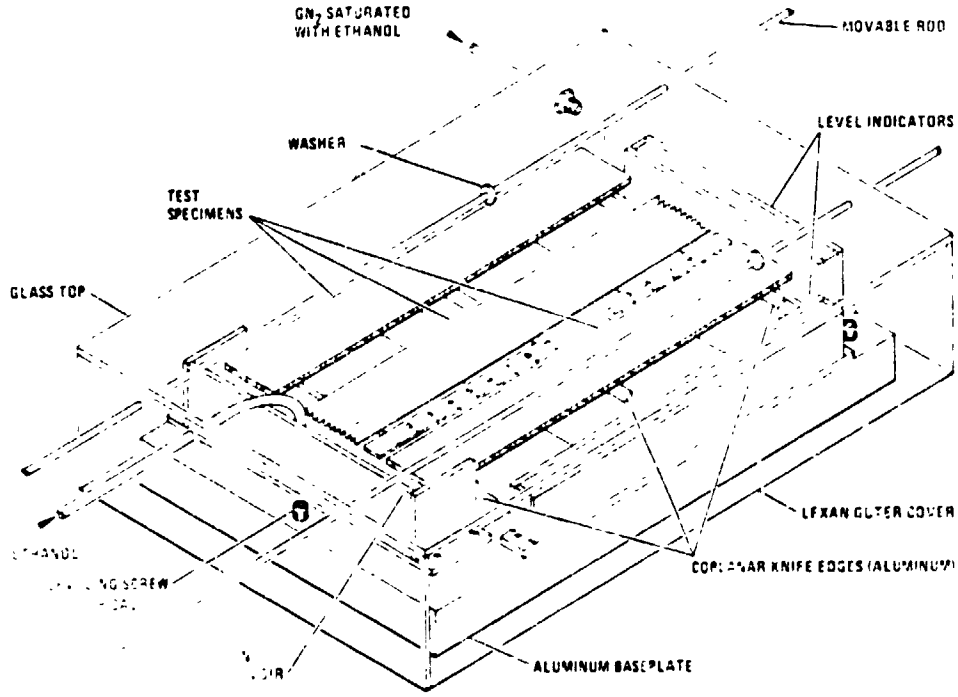

Figure 2-10. Experiment Apparatus

Two levelers, consisting of plastic troughs filled with test fluid, were mounted at right angles to each other on the base plate. These were used in conjunction with a tooling transit to control specimen orientation. With this arrangement, the end of the specimen, approximately 17 inches from the source, could be positioned vertically within 0.00254 cm (0.001 in).

To supply liquid (ethanol) to the test specimen, the upstream side of the specimen was bent down below the edge of the reservoir. The reservoir was kept full to the top of the wick by adjusting a needle valve on the reservoir refill. A fast drain was also provided for initially filling the reservoir or draining the reservoir refill.

Evaporation of the liquid within the test enclosure was minimized by maintaining GN_2 saturated with ethanol in the experiment enclosure. This was accomplished with a pressurized humidifier, containing a 25-watt aquarium heater, partially filled with test fluid through which gaseous nitrogen (boiled off from liquid nitrogen) was bubbled. An aquarium air stone was used to disperse the GN_2 bubbles and the heater was used to replace the heat lost in vaporizing the test fluid. The humidifier was kept several degrees below the test enclosure temperature to prevent liquid condensation on the enclosure surfaces and possible degradation in viewing the wicking. A qualitative humidity indicator made of screen was wetted before each run and examined periodically to note any drying due to ethanol evaporation.

The test enclosure was vented out of the environmentally controlled room to reduce fire potential and to protect test personnel from respiratory hazards. A timer, mounted in the field of view of the camera, was used to measure wicking time. Rulers aligned on the side of wicking specimens measured the distance traveled by the wicking fluid. Thermocouples on the apparatus and reference test specimen, measured the absolute temperature of the enclosure and specimens and the differential between the humidifier and the enclosure. Checkout of the apparatus with the reference specimens showed that temperature differences along the wicking front were negligible. Consequently, thermocouples were not attached to the other wicking test specimens. The humidifier heater was controlled according to the temperature differential between the humidifier and enclosure.

Originally, it was thought that screen wetting would be instantaneous and the wicking front could be recorded by photographing the wetting of the top screen. This proved to be an inaccurate method of recording the position of the wicking from inside the specimen since, in many cases, the top screen wicked ahead of the liquid inside the wick. An indirect method was therefore used to photograph the wicking front. The washers, shown in Figure 2-10, were aligned with the wicking front by sliding a metal rod along as the fluid wicking progressed. With this observation method, only the two end specimens could be recorded simultaneously unless the middle specimen was the pleated screen. The pleated screen wicking was directly photographed.

Testing was conducted using 200-proof reagent grade ethanol with specimens at 0 (0.0), 0.005 (0.25), or 0.007 (0.4) radians (degrees) to the horizontal. A total of 36 runs were made.

2.2.1.3 Data Correlation. Wicking distance versus time was determined by careful inspection of the film results. Linear regression analysis of several runs indicated that the effect of evaporation on test results was negligible. Figure 2-11 shows the improvement in horizontal wicking obtained using plate/screen-screen/plate wicks compared to screen/plate and to screen alone, because spotwelding the screen to the plate was done on only a few dozen lands on the perforated plate. This leaves a path between the screen and plate where they are not in intimate contact.

A correction factor was made to account for screen filling and data was fitted to several possible correlating equations. The equation that best fit the results of the horizontal wicking tests was one one of the form

$$\Delta P_\sigma = \Delta P_f + \Delta P_x \qquad (2\text{-}7)$$

where

ΔP_σ = surface tension driving pressure

ΔP_f = frictional pressure loss

ΔP_x = correction term

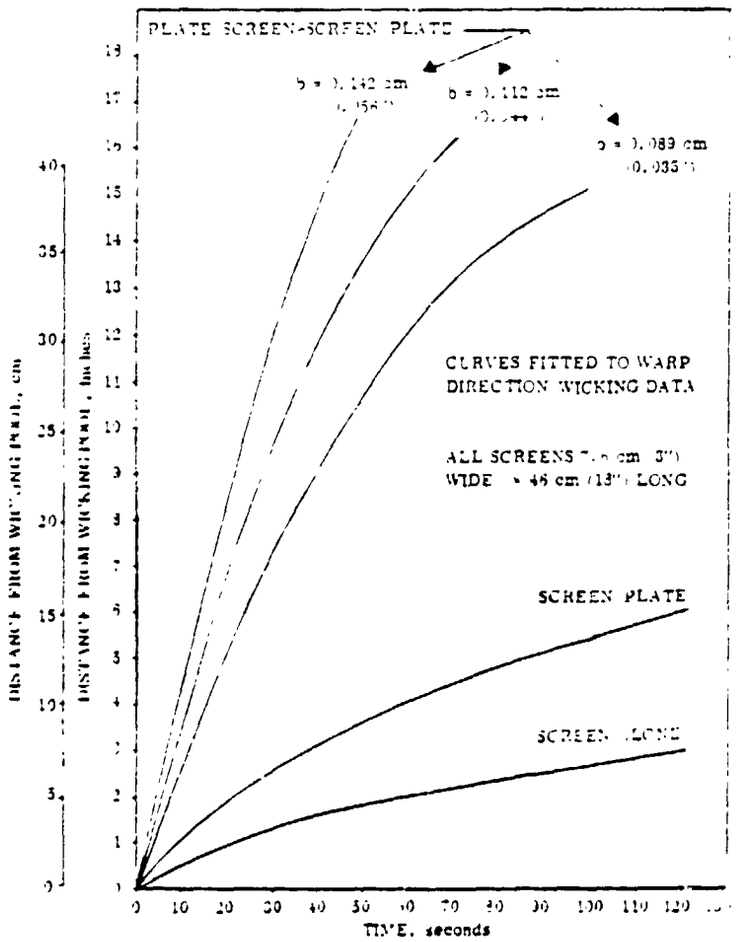

Figure 2-11. Increased Wicking Capability for Plate/Screen-Screen/Plate and Screen/Plate Configuration

The frictional pressure loss is defined

$$\Delta P_f = KL^2/\Delta t \qquad (2\text{-}8)$$

where

K = constant determined analytically for each configuration

L = distance from liquid pool to wicking front

Δt = time from initiation of wicking

Equation 2-7 was evaluated using measured geometry to evaluate ΔP_σ and measured values of L and Δt, over the entire range of L and Δt.

Values of ΔP_X obtained for each configuration are given in Table 2-10. Note the close agreement between the ΔP_X terms found for the 50 × 250 and 200 × 1400 screens.

Wicking capability and wick spacing are functions of the gravity dependence of ΔP_X. Using worst-case interpretations, plate/screen-screen/plate and plate/screen-plate/screen configurations were sized for LO_2 and LH_2 start baskets. Total weight of the passively cooled baskets was found to be 90.2 kg (198.6 lb_m) — a hardware weight savings of 58.6 kg (129 lb_m) over an actively cooled system. In addition, a payload penalty of 189.8 kg (418 lb_m) results from dumping vent fluid overboard for actively cooled capillary devices in the five-burn mission.

2.2.2 THERMAL SUBCOOLING. Thermal subcoolers operate by using a compact heat exchanger, as shown schematically in Figures 2-3 and 2-5 and thermodynamically in Figure 2-4, to remove energy from the liquid leaving the main propellant tanks during engine startup and firing. Work performed in this study examined the weight penalties and configurations for thermal subcoolers designed to replace the LO_2 and LH_2 boost pumps for the existing RL10A-3-3, RL10A-3-3A and the RL10 Category I engine to meet inlet pressure and net positive suction pressure (NPSP) requirements. The analyses included both the start sequence and steady firing of the main engines. NPSP levels investigated ranged from nearly zero to the current baseline requirements (27.6 kN/m^2 (4 psi) for LH_2 and 55.12 kN/m^2 (8 psi) for LO_2). Three system concepts were studied:

1. Current baseline vehicle employing propulsive settling, warm gas pressurization, and boost pumps.

2. A system of thermal subcoolers with propulsive settling.

Table 2-10. Wicking Correction Factors

Configuration	Screen	Spacing		ΔP_σ		ΔP_X		$\Delta P_{X_{mean}}$	
		cm	in.	N/m^2	psf	N/m^2	psf	N/m^2	psf
Plate/screen-screen/plate	50 × 250	.086	.034	51.7	1.08	15.8	.329	18.8	.393
		.113	.0445	39.5	.825	21.1	.44	18.8	.393
		.142	.056	31.4	.656	19.6	.41	18.8	.393
Screen/plate-plate/screen	50 × 250	.051	.02	43.8	.914	24.4	.509	26.4	.551
		.065	.0255	38.8	.811	26.8	.56	26.4	.551
		.086	.034	33.0	.69	26.3	.55	26.4	.551
		.086	.034	33.0	.69	26.8	.56	26.4	.551
		.086	.034	33.0	.69	28.0	.585	26.4	.551
Plate/screen-plate/screen	50× 250	.065	.0255	25.4	.53	5.3	.11	8.8	.183
		.086	.034	20.6	.43	12.3	.256	8.8	.183
		.113	.0445	16.8	.35	8.7	.181	8.8	.183
Pleated screen	50× 250	p = .224 t = .381	.088 .15	46.4	.97	16.3	.34	16.3	.34
Plate/screen-screen/plate	200× 1400	.113	.0445	39.5	.825	18.4	.384	19.0	.397
		.142	.056	31.4	.656	19.6	.41	19.0	.397

3. A system of thermal subcoolers, passively cooled screen acquisition devices, and continuously cooled propellant ducts.

Three realistic engine configurations with NPSP levels covering the desired range were selected for comparison. The first was the baseline D-1S engine, the RL10A-3-3; the other two are Pratt & Whitney engines with lower NPSP requirements; RL10A-3-3A and RL10 Category I. The former was built and tested for use in a pressure-fed Centaur without boost pumps. The latter is the same engine but with reduced chilldown, NPSP, and inlet pressure requirements.

Engine NPSP requirements, line losses (under steady-state and transient conditions), and tank pressure requirements were determined for each option. Tank pressure profiles were generated for the configurations with no pressurization system. Start sequences were developed and analyzed for the concepts not using propellant settling. Thermal analysis of the cooled propellant ducts determined cooling tube sizes and coolant flow rates for both the LO_2 and LH_2 tanks. Coolant flow is taken from the start basket. Analysis techniques described in Reference 2 were used. Work from that study was modified to analyze the thermal subcoolers.

Fin effectiveness was determined for configurations similar to that shown isometrically in Figure 2-5. For heat transfer on the hot side, forced-convection laminar and turbulent heat transfer coefficients for flow over a flat plate were used. The cold side of the subcooler uses vent fluid throttled to an inlet pressure of 26.2 to 34.5 kN/m^2 (3.8 to 5 psia). For fluid quality less than 0.9, Kutateladze nucleate boiling heat transfer coefficients (Reference 7) were used on the cold side.

Subcoolers were designed to subcool the hot side liquid so that fluid entering the engine turbopumps would satisfy pump NPSP requirements. Any pressure drop in the subcooler and propellant duct was counteracted by additional heat removal in the subcooler. A pie-shaped section of each subcooler design was modeled on a thermal analysis computer program to determine the net heat removal and the required size of each configuration. The program was also used for the largest subcooler to determine transient performance. The computed heat removal exceeded that required for all conditions considered.

Weight penalties were determined for all three system concepts for each applicable engine derivative for each of the three missions.

Some of the significant weight penalties were due to tank pressure increase (tank skin delta weight and penalty due to lower tanking density), unsubcooled fluid in the lines (for the cooled feedline concept), thermal subcooler cold-side fluid, and residual fluid in the subcooler cold side. None of the concepts that vent subcooler cold-side fluid offered a weight advantage over the baseline concept. The best subcooler systems of this type were those using the Category I engine. Cooled feedline options were not advantageous because of the unsubcooled LO_2 in the lines in excess of engine chilldown requirements.

Two additional options were considered to alleviate the major weight penalties by pumping the subcooler coolant fluid back into the tank. These options, using settling rockets and capillary devices with uncooled feedlines, eliminated penalties associated with tank pressure increases and vented fluid, but introduced additional complexity into the system.

2.2.3 THERMODYNAMIC VENT MIXER ANALYSES. Centaur/Shuttle integration studies have indicated the importance of controlling tank pressure of a cryogenic stage in the Shuttle payload bay and in low gravity, particularly when the tanks are relatively full. Work performed in this study was the initial analysis and sizing effort required to bring the vent system to fully operational flight status. This is preparatory to the procurement of hardware, flight qualification, and noninterference flight of a LH_2 vent system.

A thermodynamic vent system is a system for venting only vapor in low gravity, regardless of the phase of the fluid entering the system. Shown schematically in Figure 2-12, the system throttles the inlet fluid to a lower temperature and pressure than the surrounding tank fluid. The hot side tank fluid is then pumped over tubes containing the throttled fluid in a heat exchanger to vaporize any liquid initially present in the vent stream. The vapor is then vented overboard. The pump provides forced convection on the hot side of the heat exchanger as well as mixing flow for destratifying tank contents. Destratification is vital if removal of fluid from the pool (for venting) is to result in tank pressure reductions.

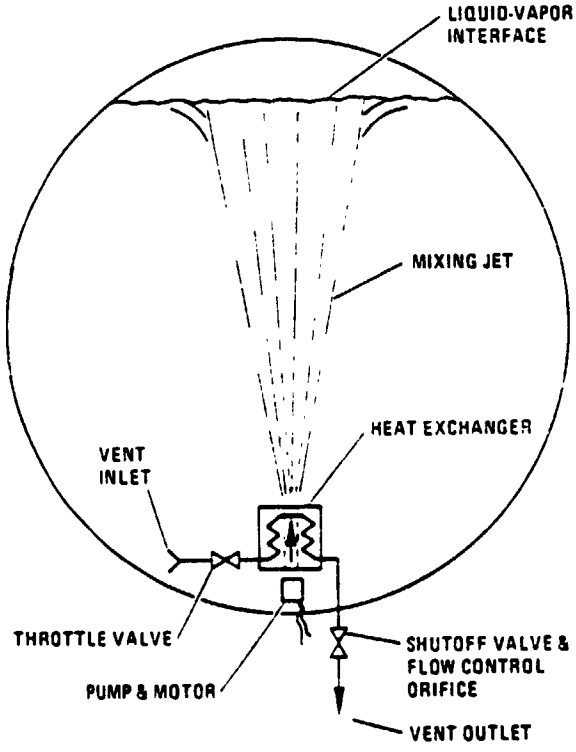

Figure 2-12. Compact Heat Exchanger Vent System Schematic

Results of extensive ground testing have led to the following conclusions:

1. The thermodynamic vent concept will vent only vapor with either vapor or liquid at the vent inlet.

2. The compact heat exchanger concept is lighter weight than the wall heat exchanger.

3. The effectiveness of the compact heat exchanger system could be improved with a better understanding of tank mixing and the use of less conservative mixing correlations.

Because of the importance of understanding tank mixing, effort in this study concentrated on reviewing existing information on mixing of fluids to develop an analysis that can be used to size

mixers for destratification of cryogenic liquids. The mixing correlation providing the best fit of the data was incorporated into the existing Convair Cryogenic Heat Exchanger Analysis Program (CHEAP). This program was then used to size LH_2 thermodynamic vent systems for candidate Centaur and Centaur/Tug derivatives.

2.2.3.1 Mixing Data. Experiments using a jet mixing device to eliminate stratification or to blend fluids have been conducted in the aerospace and petrochemical industry with both cryogenic and non-cryogenic fluids. Ability of the jet to penetrate the stratified layer and the time required to completely mix the tank have been the primary criteria in evaluating the mixing experiments and in sizing the thermodynamic zero-g vent system.

Several experiments were conducted with chemical reactions, where color change or change in concentration were monitored (References 8, 9 and 10). Thermal stratification and mixing tests have been run with pressurized water (Reference 11) and with Freon (Reference 12). Low-gravity mixing tests were run in a drop tower at NASA/LeRC using ethanol and a mixing jet (Reference 13). Cryogenic testing in LH_2 (Reference 14 and 15) and LO_2 (Reference 16) determined destratification with a thermodynamic vent/mixer system.

Considerable scatter was evident in comparing the correlations and mixing data. None of the correlations yielded a good fit of the data. This was felt to be due to differences in experimental procedure and definition of mixing time. The best correlation was the mixing time equation of Okita and Oyama (Reference 10)

$$\theta_m = \frac{5.2\ V\ D_j}{QY^{1/2}\ D_t^{1/2}} \qquad (2\text{-}9)$$

where

θ_m = mixing time, sec

V = tank volume, ft^3

D_t = tank diameter, ft

Q = jet flow rate, ft^3/sec

Y = liquid height, ft

D_j = jet diameter, ft

This correlation was used to size thermodynamic vent mixers for nine Centaur and Centaur/Tug derivatives. The highest weight system, sized for the Centaur D-1T LH_2 tank, was selected because it could handle the venting for all nine vehicles. The weight of the system 6.58 kg (14.50 lbs) was only 2.95 kg (6.5 lbs) higher than

the lowest weight system. Based on the work performed, this lightweight versatile unit is recommended for Centaur/Shuttle thermodynamic vent system requirements.

2.3 RESULTS OF NAS3-20092, "A STUDY OF LIQUID AND VAPOR FLOW INTO A CENTAUR CAPILLARY DEVICE"

Based on the studies performed in NAS3-17802 and NAS3-19693 two areas were identified as being critical technology items for capillary device development. These were capillary device refilling with settled fluid and vapor flow across a wetted screen. Capillary device refilling is required to contain sufficient liquid in preparation for the next coast period and engine start sequence. During coast, capillary device thermal conditioning requires liquid evaporation to intercept incident heating at the screen surface. Vapor must enter the capillary device to replace the liquid evaporated. Analytical and experimental studies were conducted to evaluate refilling and vapor flow across wetted screens.

Propellant feed system alternatives were compared for Centaur D-1S based on weight, reliability, electrical power consumption, and mission profile flexibility.

2.3.1 REFILLING ANALYSIS. Refilling analysis was performed in Reference 2 using conservative assumptions as described in Section 2.1.1.2. This analysis was broadened to include the effects of dynamic pressure, screen wicking, multiple screen barriers, window (standpipe) screens that can be different mesh than the main screens, and time dependent liquid settling (collection). The analysis also included the effects of vehicle mass on the vehicle acceleration as the propellant tanks are being drained. Outflow from the tank was included either as an input or as a calculated value based on feed system pressures. Other analysis features were: calculation of vapor pullthrough height in the basket based on tank outflow rate (and channel geometry), an option for including a standpipe screen in the calculations, options for maintaining the standpipe in either a dry or wetted condition, an option for simulating liquid spilling from the capillary device at initiation of tank outflow (from the start basket), and an option for selecting the type of multiple screen barrier to be used for the main screen in the screen wicking calculations.

A finite difference solution was constructed using the basic screen flow equations and the continuity equation. The screen flow equations are the heart of the computer program developed for analyzing capillary device refilling. The program simulation calculates start basket fluid flows based on boundary conditions of liquid level, system pressure and screen configuration and surface area. Continuity is satisfied by summing the flows into and out of the capillary devices and adjusting the pressure difference between the inside and outside of the basket until the flows balance. This iterative solution is achieved for time step increments until either the total burn time or the pullthrough height is reached.

The pressure loss equations are separately delineated for each of six regions for fluid flow (without liquid impingement). The six regions (for net refilling) are: an unwetted region where vapor flows out of the basket into vapor, a wetted region where vapor flows out of the basket into vapor, a region where the liquid level outside the basket covers the screen and vapor flows into the liquid, a region where no flow occurs across the screen barrier, a region where liquid enters the basket flowing into vapor and a region where liquid enters the basket flowing into liquid. Equations for flow in each of these regions are presented in Reference 17 along with equations for outflow, dynamic pressure caused by liquid impingement and continuity.

2.3.2 REFILLING TESTS. An experimental apparatus was designed and fabricated for obtaining data with which to checkout the computer model. The apparatus, shown in Figure 2-13, consisted of a square Lexan tank with a simulated transparent start basket configuration and a movable cover device for releasing liquid to simulate settling and collection.

The start basket main screen consisted of multiple barriers of 200 × 600 mesh. Standpipe screens of either 200 × 600 mesh or 50 × 250 mesh were used. Two sides of the basket were constructed of Lexan to permit liquid level to be visually observed.

The outer tank was fabricated with back and front sides of Lexan sheet. Within this tank a movable cover (with front and back sides of Lexan) over the basket controlled the collection rate of liquid. A piston/stop arrangement was used to control cover rate and distance travelled.

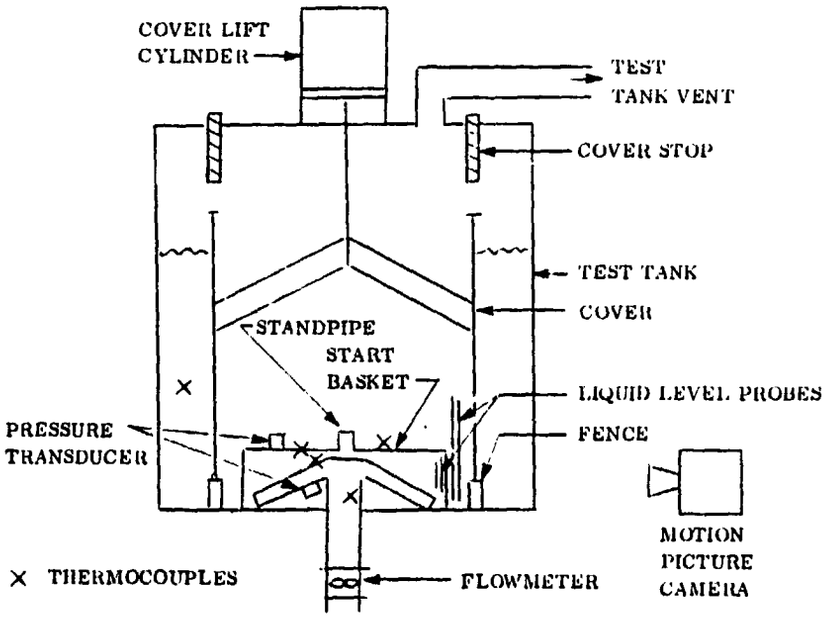

Figure 2-13. Test Apparatus Schematic

Ethanol was used as the test fluid because of its good wettability, low toxicity and low vapor pressure at room temperature. Surface geometry was recorded photographically on 16 mm color movie film. A scale with 0.1 mm divisions was mounted on the start basket Lexan surface. Liquid level inside and outside the basket was measured using General Dynamics Convair fabricated parallel plate capacitance probes. Variable reluctance type pressure transducers were used to measure the pressure difference across both the start basket and channel. Flow rate out of the basket was measured with a turbine flowmeter in the outlet line. Temperatures at selected locations on the start basket, channels and outlet line were measured using chromel constantan thermocouples.

Test variables were outflow rate, top screen (standpipe) configuration, initial start basket wetting, liquid collection rate and refilling geometry. Analog recordings were obtained for each run. Data channels recorded were outer chamber liquid level, start basket liquid level, start basket pressure drop, channel pressure drop, channel outflow rate, and the six selected temperatures. All quantitative data was obtained from the analog recordings. Motion picture runs were used for qualitative observations and for assistance in determining boundary conditions such as settling flow pattern and screen wetting during refill.

A total of twenty-nine test runs were made. Results were obtained over a wide spectrum of refilling times ranging from no refilling, with the 200 × 600 mesh screens, to rapid refilling with the 50 × 250 mesh standpipe and initially dry screens.

Test data was used to correlate computer program predictions. Five test runs were selected for computer program simulation. Computer runs were made with both air and ethanol vapor as the gas inside and surrounding the basket. The data was best correlated with air properties for vapor flow across the start basket. Tank liquid level versus time was obtained from test data as an input for each computer run. A typical comparison of the data and model are shown in Figure 2-14. Correlation was obtained by fixing the initial basket level and varying the standpipe unwetted area until the basket level at the final time was matched. In Figure 2-14, AST is the screen area of the standpipe. DBP2 is the bubble point of the standpipe screen. DBP is the effective bubble point of the main screens. NW is a flag that determines wetting of the screen, not covered by liquid, away from the standpipe. If NW = 1, wetting of the screen does not occur above the liquid level outside the basket. If NW = 2, the basket is wetted to the base of the standpipe. (If NW = 3, a subroutine is used to calculate screen wetting based on screen/plate wicking.) NDR is a flag that keeps the standpipe screen dry if not equal to zero. If NDR = 0, the standpipe screen is wet. OA is the main screen open area fraction. (Screen is backed up by perforated plate).

Based on the correlation obtained with the five test runs, the program was used to predict refilling for the Centaur D-1S LO_2 and LH_2 start baskets. These predictions indicated that refilling would be accomplished successfully for the two worst case mission conditions considered. (The shortest burn and the lowest g-level burn were

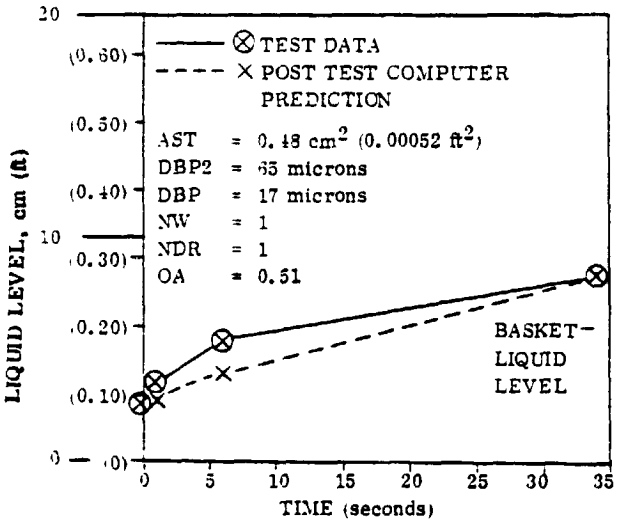

Figure 2-14. REFILL Computer Program Simulation of Test Run No. 15

the cases analyzed.) Based on the program versatility and the correlation with ground test data, the refilling computer program is recommended for use as a design tool to determine start basket volume and geometry.

2.3.3 VAPOR INFLOW ANALYSIS. In order for cryogenic capillary devices to function properly between engine restarts, screen retention capability must be maintained by keeping screens in a wetted condition. For partial acquisition devices, such as the LO_2 and LH_2 start baskets designed for the Centaur D-1S, the screen surfaces will dry out due to heat input unless liquid is continuously supplied to the screen. Wicking can be used to supply this liquid as discussed in detail in Section 2.2.1. In order to replace liquid evaporated from the screen, vapor can enter the contained volume. Unless this vapor can be directed to specific areas of the start basket, the vapor will detrimentally affect wicking flow and screen retention capability.

Using a screen window can successfully avoid the adverse effects of vapor penetration into a multiple screen liner device. The window enables communication to exist between the vapor in the tank and the inner volume of the start basket by making the bubble point of the window screen larger than that of the multiple screens. This allows the region between the multiple screen barrier to be free of vapor and the multiple screens will remain wetted and not dry out.

Vapor flow across wetted screened windows was examined in detail during this study. An extensive program of small scale bench tests was conducted in order to verify and correlate the equations. Initial test results were encouraging and used as a basis for design of the experimental configuration and conduct of the subsequent tests. These succeeding tests produced results that had a wide variance from run to run.

The equations believed to govern the operation of a single screen window are presented in Reference 17. These equations define parameters that describe the ability of the window screen to rewet after vapor enters the inner volume. The window screen will remain wetted as long as its wicking capability is greater than the equivalent incident heat flux on the entire screen surface. The important variables are the liquid level in the inner region and the pressure difference across the window screen and along the window screen.

2.3.4 VAPOR INFLOW TESTING. A series of tests were run in order to evaluate the equations presented in Reference 17. Initial tests with a single test specimen using hexane provided repeatable results that were used to formulate the analytical model. Based on these results six new specimens were built and tested with hexane. The configurations were designed to yield parametric data on the screen wetting process when subjected to vapor flow. Results obtained were less repeatable than the first test series and showed generally poorer wicking performance. Some of the problems were felt to be due to control of wicking between the main screen and window-screen, reduced volume under the window and increased screen deflection because of the increased screen span between supports. New specimens were fabricated with reduced span, improved main screen/window screen wicking and increased volume under the window. The third test series was conducted with hexane using a bell jar for improved environmental control with the new test specimen as well as the original specimen. Somewhat better results were obtained under these conditions. Two additional boxes were then fabricated with different window lengths and tested in the fourth test series using hexane, ethanol and Freon TF. The test data was not as consistent as that obtained in the third test series. In the fifth test series two of the boxes were modified and tested with hexane and Freon TF. One of the boxes used Teflon dams to promote unidirectional wicking. The other box used screens with higher retention capability than previously tested.

Test results obtained in the five test series were examined, reduced and compared to the analytical models. Unfortunately, for this data analysis, no quantitative data was available for the first test series and the early runs of the second test series. Only data from test series 2, 3, 4 and 5 were available for analysis and correlation.

Thermal conditioning calculations were performed to determine whether the window screen on the Centaur D-1S LO_2 and LH_2 basket would dry out when subjected to heating. Required values of F_σ were determined from

$$F_\sigma = \frac{\dot{Q}/A_{\text{incident}}}{Q/A_{\text{wicking capability}}} \qquad (2\text{-}10)$$

F_σ is a parameter obtained from test results and is a function of the pressure differentials across the basket at vapor breakthrough and recovery.

For the LO_2 standpipe the worst case F_σ was found to be a maximum of 0.0076. For the LH_2 standpipe the worst case F_σ was found to be a maximum of 0.058. Both these values are well below the considerable majority of F_σ's found from test data.

The other important vapor flow parameter is the critical height of vapor in the inner basket volume at which breakdown could occur. This was determined by computing the maximum vapor volume that could be generated by incident heating to the start basket. This volume was then converted to a liquid level in the basket below the top of the standpipe and compared to the values obtained during testing. Only one value out of

30 runs was less than that required to make the window screen operate properly. Based on these calculations, the Centaur D-1S start basket window screens should be capable of remaining wet during the complete set of mission conditions.

The conclusion of the vapor inflow testing and analysis was that the data obtained can be used as a rough estimate to find the limits of the thermal conditioning capability of a given configuration. For detailed thermal conditioning design data, additional experimental work will be required. This work is described in Reference 17, Section 3.4.

2.3.5 PROPELLANT FEED SYSTEM COMPARISONS. Feed system alternatives were developed for pressure fed engines and combinations of feed system components in order to determine the optimum propellant feed system for the Centaur D-1S. Comparisons were made between propellant settling and capillary acquisition, thermal subcooling and pressurization for boost pump NPSP (net positive suction pressure), boost pumps, thermal subcooling and pressurization for turbopump NPSP, uncooled and cooled propellant ducts, and pumping coolant back into the tank or dumping coolant overboard. Capillary device designs used for the Centaur D-1S, reflected the refilling and vapor inflow analysis described in Section 2.3.1 and 2.3.2.

Comparisons were made on the basis of payload penalty, hardware weight, reliability, electrical power consumption and mission profile flexibility. The comparisons were made for three engine candidates; the existing RL10A-3-3 and two lower NPSP alternatives the RL10A-3-3A and the RL10 Category 1. Characteristics for these two advanced engines are described in Reference 18. Three missions were considered for each engine candidate, a one burn planetary mission, a two burn synchronous equatorial mission and a five burn low earth orbit mission (Tables 1-1, 1-2 and 1-3, respectively). A total of ten feed system concepts were compared for each of the three engines and three missions.

2.3.5.1 Selection of Feed System Alternatives. In order to select the most promising feed system alternatives for comparison, a matrix of system candidates was constructed by selecting an alternative from each of the following subsystems or operations.

A. Acquisition

   1. Propellant Settling
   2. Capillary Device

B. Boost Pump NPSP

   1. Boost Pump Pressurization
   2. Thermal Subcooling of Boost Pump Propellants
   3. No Boost Pump

C. Turbopump NPSP

1. Boost Pump
2. Thermal Subcooling of Turbopump Propellants
3. Pressurization

D. Propellant Duct Cooling

1. Uncooled
2. Cooled

E. Coolant Handling

1. No Coolant Required
2. Coolant Pumped Back Into the Tank
3. Coolant Dumped Overboard

Selecting all the possible combinations produced 108 alternatives. Infeasible combinations were then identified. For example, boost pumps cannot be used with cooled propellant ducts because subcoolers before the boost pumps are impractical. Pressurization and capillary acquisition were shown to be infeasible in NAS3-17802. Other incompatibilities are subcoolers before turbopumps or pressurization with a boost pump; no coolant required and a cooled feedline, thermal subcooler before the turbopump, or thermal subcooler before the boost pump; turbopump NPSP from a boost pump and no boost pump; coolant pumped or coolant dumped with uncooled duct and a pressure fed system; no cooling required with coolant pumped or dumped; and coolant pumped or dumped with no subcoolers or cooled duct. Candidates using cooled propellant ducts and not having capillary devices are also infeasible because liquid could not positively be contained within the duct or supplied for cooling the propellant duct without a capillary device.

The screening process resulted in twelve combinations that were feasible. These are listed in Table 2-11. Candidates selected for additional analysis are circled. Reasons for selecting these ten concepts are described in the following paragraphs. Comparisons performed in contracts NAS3-17802 and NAS3-19693 showed that thermal subcoolers for cooling propellants prior to the boost pump have weight advantages compared to boost pump pressurization, pumping cooling fluid back into the tank was advantageous over dumping fluid overboard, boost pumps were lighter than thermal subcooling for propellant prior to the turbopump and uncooled propellant ducts were lower in weight penalty than cooled propellant ducts. These comparisons were used as guidelines in selecting the feed system alternatives to consider. Several key comparisons were desirable in order to determine the best feed system candidate.

A critical comparison to be made was between capillary acquisition and settling. Several pairs of concepts in Table 2-11 could have been compared for this purpose, i.e., B and K, C and L, D and M, or E and N. Based on the comparisons done on the previous contracts, concepts B and K should be the lowest weight of all these pairs

Table 2-11. Feed System Candidates

	Concept											
	Ⓐ	Ⓑ	C	Ⓓ	Ⓔ	Ⓗ	Ⓚ	Ⓛ	Ⓜ	Ⓝ	Ⓞ	Ⓟ
A. Acquisition												
1. Propellant Settling	x	x	x	x	x	x						
2. Capillary Device							x	x	x	x	x	x
B. Boost Pump NPSP												
1. Boost Pump Pressurization	x											
2. Thermal Subcooling Propellant for the Boost Pump		x	x				x	x				
3. No Boost Pump				x	x	x			x	x	x	x
C. Turbopump NPSP												
1. Turbopump NPSP - Boost Pump	x	x	x				x	x				
2. Turbopump NPSP - Thermal Subcooler				x	x				x	x	x	x
3. Turbopump NPSP - Pressurization						x						
D. Propellant Duct Cooling												
1. Uncooled Propellant Duct	x	x	x	x	x	x	x	x	x	x		
2. Cooled Propellant Duct											x	x
E. Coolant Handling												
1. No Coolant Required	x					x						
2. Coolant Pumped Back Into The Tank		x		x			x		x		x	
3. Coolant Dumped Overboard			x		x			x		x		x

and was selected as the primary comparison pair for propellant settling versus capillary acquisition.

Concepts A and B were selected for comparing pressure fed boost pumps to thermally subcooling of propellants before the boost pumps.

Concepts B, D and H were compared for use of a boost pump, thermal subcooler, or pressure feed for supplying turbopump NPSP.

Another comparison involved the propellant duct cooling. Uncooled propellant ducts, cooled propellant ducts with cooling fluid dumped overboard and cooled propellant ducts with cooling fluid pumped back into the tank were compared by considering concepts O, N and P.

Comparison of subcooling coolant flow being dumped or pumped could have been made for subcooling propellant for the boost pump by comparing concepts B and C or concepts K and L. Concepts K and L were evaluated for this purpose since most of the data for this comparison had already been generated on NAS3-17802.

For comparing pumping or dumping subcooler flow for providing turbopump NPSP, concepts D and E and concepts O and P were compared.

Based on the considerations described in the preceding paragraphs analysis of concepts A, B, D, E, H, K, L, N, O and P will be required to provide the necessary comparisons. These concepts concept. are circled in Table 2-11. Candidates that were analyzed previously in NAS3-17802 (Reference 2) and NAS3-19693 (Reference 6) have their letters underlined.

2.3.5.2 Payload Penalty. Payload penalty calculations were performed using payload sensitivity factors given in Reference 2, Table 2-1. All hardware weight and fluid penalty elements that could be different between the ten concepts were considered in the comparison. Relative payload penalties were found for each applicable concept for the three missions and three engine candidates by comparing twenty one weight elements. A typical tabulation of this data for the five burn mission for the RL10A-3-3 engine is shown in Table 2-12. Weights for concept H are not shown in Table 2-12 because the high NPSH requirements for the current RL10A-3-3 engine make a pressure fed system infeasible.

Comparing the payload penalties of the ten concepts yields the following observations. Settling is superior to capillary devices for the missions considered. Subcooling propellants for boost pumps by thermal or pressure means is a close trade-off, with thermal subcooling preferred for the multiburn missions. Pumping coolant back into the tank is better than dumping overboard. Uncooled propellant ducts are better than cooled propellant ducts and boost pumps are the best method of supplying turbopump NPSP. Based on these comparisons of relative payload weight penalties, feed system concepts A or B appear best for the Centaur D-1S application. (Feed system concept A is the baseline system. Feed system concept B is the baseline system with the substitution of a thermal subcooler instead of main tank pressurization.) Capillary devices would fare better in the comparisons if missions of more than five burns were considered.

2.3.5.3 Hardware Weight Comparisons. Hardware weight comparisons were made for the feed systems for the three engine candidates and the three missions. Twelve hardware weight elements were analyzed; capillary device, pressurization system, propellant supply duct, hardware to keep ducts wet, subcooler, boost pump, settling system, sump assembly, coolant pumping system, other hardware, tank skin delta and thrust barrel revisions. Hardware weight comparisons are not as meaningful as equivalent payload weight penalties because they neglect fluid weight differences.

Comparison of the feed system elements shows that capillary devices are heavier than settling for all three missions that were considered for this study. Boost pumps with propellant thermally subcooled have lower hardware weight than pressure fed boost pumps. Boost pumps have the lowest hardware weight of the turbopump NPSP supply methods. Uncooled ducts have the lowest hardware weight of the propellant duct thermal conditioning alternatives. Pumping coolant back into the tank is an option having greater hardware weight than dumping coolant overboard.

Table 2-12. Payload Weight Penalties for System Comparisons, kg_m (lb_m), Five Burn Mission, RL10A-3-3 Engine

WEIGHT PENALTY ELEMENT / FEED SYSTEM CONCEPT		A: Settling, Pressurization Boost Pump, Uncooled Duct, No Coolant Required	B: Settling, Thermal Subcooler Before Boost Pump, Uncooled Duct, Coolant Pumped	D: Settling, Thermal Subcooler Before Turbopump, Uncooled Duct, Coolant Pumped	E: Settling, Thermal Subcooler Before Turbopump, Uncooled Duct, Coolant Dumped	H: Settling, Pressure Fed Engine, Autogenous + Amb. Stored He, Uncooled Duct, No Coolant Reqd.	H_1: Settling, Pressure Fed Engine, Autogenous + Cryo Stored He, Uncooled Duct, No Coolant Reqd.	H_2: Settling, Pressure Fed Engine, Cryo Stored GHe for LH_2, Uncooled Duct, No Coolant Reqd.	K: Capillary Device, Thermal Subcooler Before Boost Pump, Uncooled Duct, Pumped Coolant	L: Capillary Device, Thermal Subcooler Before Boost Pump, Uncooled Duct, Dumped Coolant	N: Capillary Device, Thermal Subcooler Before Turbopump, Uncooled Duct, Coolant Dumped	O: Capillary Device, Thermal Subcooler Before Turbopump, Cooled Duct, Coolant Pumped	P: Capillary Device, Thermal Subcooled Before Turbopump, Cooled Duct, Coolant Dumped
1. Capillary Device	LH_2	-	-	-	-				85 (187)	85 (187)	102 (225)	102 (225)	102 (225)
	LO_2	-	-	-	-				20 (45)	20 (45)	21 (47)	21 (47)	21 (47)
2. Lower Tanking Density	LH_2	-	-	86 (189)	86 (189)				-	-	86 (189)	86 (189)	86 (189)
	LO_2	-	-	505(1113)	505(1113)				-	-	505(1113)	505(1113)	505(1113)
3. Pressurization System		165 (364)	43 (94)	43 (94)	43 (94)				43 (94)	43 (94)	43 (94)	43 (94)	43 (94)
4. Propellant Supply Duct	LH_2	10 (23)	10 (23)	10 (23)	10 (23)				10 (23)	10 (23)	10 (23)	10 (23)	10 (23)
	LO_2	10 (23)	10 (23)	10 (23)	10 (23)				10 (23)	10 (23)	10 (23)	10 (23)	10 (23)
5. Supply Duct Chilldown Propellant	LH_2	-	-	6 (14)	6 (14)				-	-	6 (14)	-	-
	LO_2	-	-	10 (23)	10 (23)				-	-	10 (23)	-	-
6. Supply Duct Cooling Dumped Overboard	LH_2	-	-	-	-				-	-	-	-	7 (16)
	LO_2	-	-	-	-				-	-	-	-	74 (163)
7. Hardware to Keep Ducts Wet	LH_2	-	-	-	-				-	-		16 (36)	16 (36)
	LO_2	-	-	-	-				-	-	-	5 (12)	5 (12)
8. Excess LO_2 in Lines Over Chilldown		-	-	-	-				-	-	-	226 (497)	226 (497)
9. Engine Chilldown Propellant	LH_2	20 (43)	20 (43)	20 (43)	20 (43)				20 (43)	20 (43)	20 (43)	20 (43)	20 (43)
	LO_2	3 (7)	3 (7)	3 (7)	3 (7)				3 (7)	3 (7)	3 (7)	3 (7)	3 (7)
10. Subcooler	LH_2	-	9 (19)	49 (107)	49 (107)				9 (19)	9 (19)	49 (107)	49 (107)	49 (107)
	LO_2	-	11 (24)	20 (43)	20 (43)				11 (24)	11 (24)	20 (43)	20 (43)	20 (43)
11. Subcooler Cooling Fld. Dumped Overboard	LH_2	-	-	-	144 (318)				-	17 (38)	144 (318)	-	144 (319)
	LO_2	-	-	-	520(1146)				-	54 (119)	520 (1146)	-	520(1146)
12. Boost Pump	LH_2	38 (85)	39 (85)	-	-				39 (85)	39 (85)	-	-	-
	LO_2	29 (64)	29 (64)	-	-				29 (64)	29 (64)	-	-	-
13. H_2O_2 Usage, Boost Pump		8 (18)	8 (18)	-	-				8 (18)	8 (18)	-	-	-
14. Settling System Including H_2O_2 Penalty		75 (165)	75 (165)	75 (165)	75 (165)				-	-	-	-	-
15. Sump Assembly	LH_2	6 (14)	6 (14)	3 (7)	3 (7)				6 (14)	6 (14)	3 (7)	3 (7)	3 (7)
	LO_2	8 (17)	8 (17)	7 (15)	7 (15)				8 (17)	8 (17)	7 (15)	7 (15)	7 (15)
16. Pumping Sys. to Return Coolant to Tank Incl. Bellolf, Batt. & Hdwr.	LH_2	-	6 (13)	12 (27)	-				6 (13)	-	-	13 (29)	-
	LO_2	-	5 (12)	10 (23)	-				5 (12)	-	-	12 (27)	-
17. Volume Penalty Due to Hardware Added	LH_2	-	-	-(1)	-(1)				1 (2)	1 (2)	2 (3)	2 (3)	2 (3)
	LO_2	-	2 (4)	3 (7)	3 (7)				6 (14)	6 (14)	8 (17)	8 (17)	8 (17)
18. Fluid Residuals Cold Side Subcooler	LH_2	-	4 (8)	19 (42)	19 (42)				4 (8)	4 (8)	19 (42)	19 (42)	19 (42)
	LO_2	-	34 (74)	46 (100)	46 (100)				34 (74)	34 (74)	46 (100)	46 (100)	46 (100)
19. Thrust Barrel Revisions		-	-	-	-				5 (11)	5 (11)	5 (11)	5 (11)	5 (11)
20. Other Hardware		3 (7)	3 (7)	-	-				8 (18)	8 (18)	5 (11)	5 (11)	5 (11)
21. Tank Skin & Weight Over Baseline		-	-	97 (213)	97 (213)				-	-	97 (213)	97 (213)	97 (213)
		-	-	49 (109)	49 (109)				-	-	49 (109)	49 (109)	49 (109)
TOTALS		376 (830)	325 (714)	1083(2388)	1725(3802)				370 (815)	430 (948)	1750(3859)	1382(3043)	2102(4630)

2.3.5.4 Relative Reliability. Relative reliability for each of the ten concepts identified in Table 2-11 was determined by analyzing each major subsystem component to determine mean missions between failures (MMBF). The reliability analysis used Concept A as the baseline with other concepts evaluated as modifications to this concept. The results of the reliability analyses, presented in Table 2-13 indicate the relative reliability and mean missions between failures for each concept.

Concept H has the highest reliability rating; this is achieved by replacing both boost pumps with a pressurization system for turbopump NPSP. The pressurization system has many components, however the reliability achieved by redundancy exceeds that of two boost pumps. The reliability of all acquisition systems is lower than that of all settling systems. This is mainly due to the additional valving required for venting liquid or vapor back into tank from the sump area. Cooling the feedline reduces the reliability compared to an uncooled feedline. Pumping coolant back into the tank also degrades reliability (compared to dumping coolant overboard).

2.3.5.5 Electrical Power Consumption. Electrical power consumption was computed for each concept. Power consumption for the valves and sensors were neglected. The two main power requirements are for pumping cooling fluid back into the tank and for warming cryostored helium to usage temperature. Heat exchanger power requirements are relatively high. The cryostored pressurant option has the highest power requirements. The next highest power requirements are for pumping turbopump thermal subcooler fluid and propellant duct cooling fluid back into the tanks (Concept O). This consumption is slightly greater than Concepts D and M which only pump turbopump

Table 2-13. Relative Reliability of Propellant Feed System Concepts

Concept	One Burn		Two Burn		Five Burn	
	R*	MMBF**	R	MMBF	R	MMBF
A	0.999271	1371	0.998957	958	0.998792	827
B	0.999025	1025	0.998605	716	0.998384	618
D	0.999466	187	0.999236	1308	0.999114	1128
E	0.999582	2392	0.999403	1675	0.999307	1443
H (RL10A-3-3A)	0.999670	3030	0.999503	2012	0.999415	1709
H (RL10-Cat I)	0.999676	3086	0.999524	2100	0.999425	1739
K	0.998853	871	0.998360	609	0.998101	526
L	0.998969	969	0.998527	678	0.998294	586
N	0.998528	679	0.997897	475	0.997564	410
O	0.997910	478	0.997013	334	0.996542	289
P	0.997927	482	0.997205	357	0.996734	306

* Reliability

** MMBF = mean missions between failure

subcooler fluid. Concepts B and K, pumping boost pump subcooler fluid back into the tank, have lower power consumption than the other concepts requiring electrical power. Concepts A, E, L, N and P do not require any electrical power consumption.

2.3.5.6 Mission Profile Flexibility. Mission profile flexibility assessments were made. For systems using settling, added start sequence time will be required to accomplish settling. This will have an impact on the existing mission profiles for the Centaur D-1S. Main engine firing with capillary devices can be initiated more quickly than with settling thrusters.

2.3.5.7 Systems Comparison Conclusions and Recommendations. For the Centaur D-1S, feed systems using capillary devices have the greatest mission profile flexibility. Feed systems having the lowest hardware weight are those using propellant settling and thermal subcoolers before the boost pumps with coolant pumped back into the tank (Concept B). Feed systems having the lowest payload weight penalty are Concepts A and B. Concept A uses propellant settling and pressure fed boost pumps. For longer missions than those required by the Centaur D-1S vehicle, capillary device payload weight penalty will be less than that of propellant settling. Concepts with no electrical power consumption are Concepts A, E, L, N and P. The highest reliability concept is Concept H utilizing pressure fed turbopumps.

The study showed that several areas are worthy of investigation depending on the direction taken by new vehicle design requirements. If high reliability is the major criteria, then pressure fed vehicles should be studied. If low payload penalty and low power consumption are most significant then the baseline Centaur D-1S using propellant settling and boost pumps (Concept A) is best. If lowest hardware weight is most important and missions of two burns or less are required (payload penalty is then also lowest) then propellant settling with thermal subcooling and coolant returned to the tank should be selected. For missions greater than five burns, (approximately 10 burns) capillary devices are attractive (using thermal subcoolers before boost pumps with coolant returned to the tank, Concept K).

The study showed that the baseline system is attractive and, under a specific set of assumptions, pressure fed turbopumps, thermal subcoolers before the boost pumps with coolant pumped back into the tank and capillary devices are worthy of additional study.

2.4 PROPELLANT ACQUISITION FOR ORBITAL TRANSFER VEHICLES

An additional task was added to NAS3-20092 to determine the preferred approach to propellant acquisition for two types of orbital transfer vehicles (OTVs). To this end, capillary acquisition device systems were analyzed for four selected tankages and compared with propellant settling systems for the same vehicles and missions. The vehicles were an All-Propulsive Orbit Transfer Vehicle (APOTV) which is ground-based and a larger Personnel Orbit Transfer Vehicle (POTV) which is space-based. Both vehicles will be considered as single or dual (tandem stages). The mission will be the LEO (270 n.mi.) to GEO transfer and return. The procedures and systems for this task were established in the prior studies reported in Sections 2.1, 2.2, and 2.3. In prior studies the D-1S vehicle was used. In this task the vehicles are less well-defined. A settling system using N_2O_4/MMH propellants with I_{sp} of 260 was selected. Three systems are selected for comparison: settling with subcooling of propellants to meet boost pump NPSP requirements and coolant pumped back into the tank, settling with pressurization and no subcooling, and capillary device with subcooling of propellants to meet boost pump NPSP and coolant pumped back into the tank. For these three systems, only those components are considered in the comparison which vary among these systems, excluding some components considered in earlier studies.

2.4.1 VEHICLE AND MISSION DEFINITION. The vehicles to be considered for this study are shown in Figure 2-15 and 2-16. They are representative of the type of geometric tankage expected for OTVs. Dual stage vehicles consist of two similar single stage vehicles although number of engines and total thrust may vary between stages. Weights and mass fractions of the smaller All Propulsive Orbital Transfer Vehicle (APOTV) and larger Personnel Orbital Transfer Vehicle (POTV) are shown in Table 2-14. Round trip payloads will assume the delivered payload equals the returned payload. Delivery only payloads assumed only the stage was returned to low-earth orbit. Only half of the cases were calculated as representative of the 1990 timeframe; single stages for round trip missions were deleted because they do not satisfy manned requirements and dual stages for delivery only is unlikely.

In order to make comparisons, which are based on payload weight, between settling and capillary acquisitions for these vehicles, the sensitivity factors or payload partials must be determined. The following paragraphs present the ground rules used to determine the partials, and how each partial is used with the acquisition systems to be compared.

Figures 2-17 and 2-18 describe pictorially the mission profiles used for this analysis. One stage and two stage vehicles primarily account for the differences shown. The ΔV for the various burns are tabulated in Table 2-15. Using these profiles, Tables 2-16 through 2-19 were developed to define the propellant and dry weights used for each vehicle and the resultant propellants available at the end of each burn. The latter is used to calculate propellant settling requirements for each subsequent propulsive burn. A specific impulse of 470 seconds is used and 2 percent of the propellants are

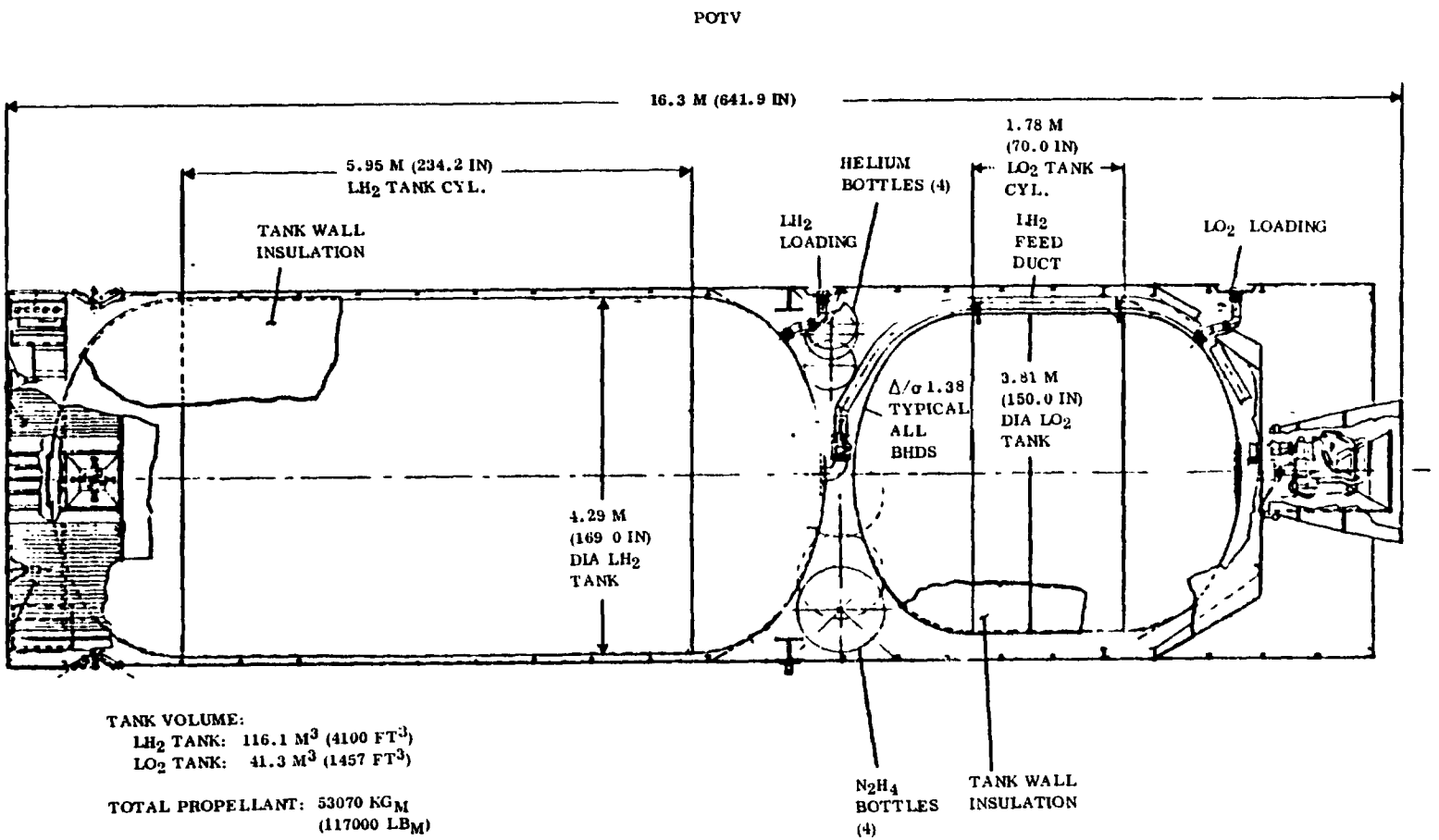

Figure 2-15. Typical Characteristics of Personnel Orbital Transfer Vehicle (POTV)

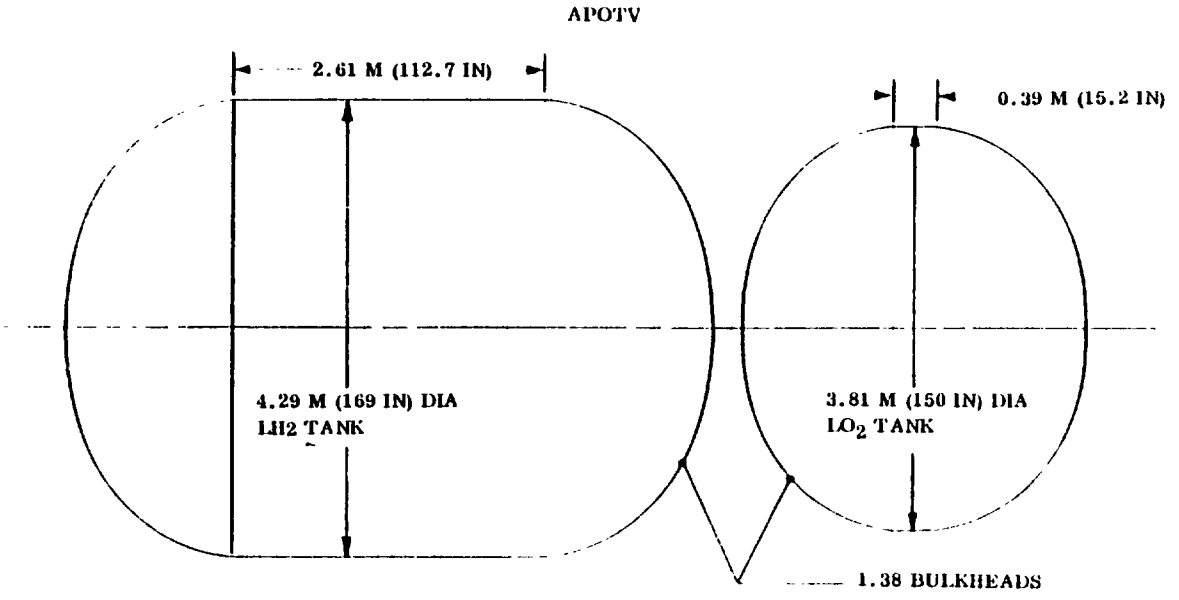

TANK VOLUME:

LH_2 TANK: 71.4 M^3 (2523 FT^3)
LO_2 TANK: 25.3 M^3 (897 FT^3)

TOTAL PROPELLANT: 32,659 KG_M (72,000 LB_M)

Figure 2-16. Typical Characteristics of All Propulsive Orbital Transfer Vehicle (APOTV)

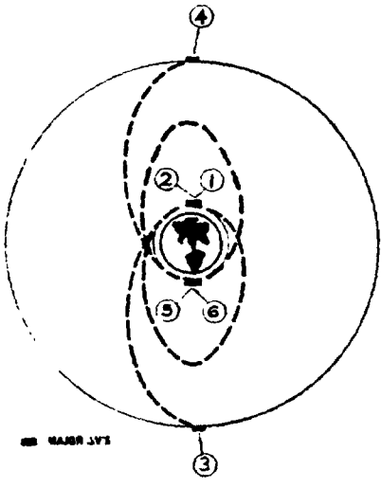

Single Stage

1. ΔV_1 boost from LEO to phasing orbit
2. ΔV_2 boost from phasing orbit to transfer orbit
3. ΔV_3 boost from transfer orbit to GEO
4. ΔV_4 retro burn from GEO to transfer orbit
5. ΔV_5 retro burn from transfer orbit to phasing orbit
6. ΔV_6 retro burn from phasing orbit to LEO

Figure 2-17. Mission Profile LEO to GEO and Return for Single Stage OTV

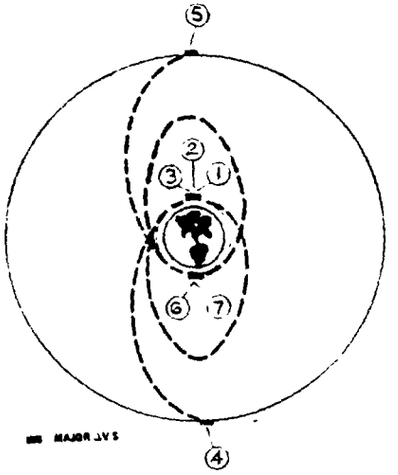

Dual Stage

1. ΔV_1 (Stage 1) boost from LEO to phasing orbit
2. ΔV_2 (Stage 1) initial boost from phasing orbit to transfer orbit
3. ΔV_3 (Stage 1) retro burn from phasing orbit to LEO with ΔV_1 (Stage 2) following sequentially after staging to boost Stage 2 from phasing orbit to transfer orbit
4. ΔV_2 (Stage 2) boost from transfer orbit to GEO
5. ΔV_3 (Stage 2) retro burn from GEO to transfer orbit
6. ΔV_4 (Stage 2) retro burn from transfer orbit to phasing orbit
7. ΔV_5 (Stage 2) retro burn from phasing orbit to LEO

Figure 2-18. Mission Profile LEO to GEO and Return for Dual Stage OTV

Table 2-14. Propellant and Dry Weights Used for all Stages

	Mass Fraction	Propellants	Dry Weight	Payload
APOTV	0.9	32,659 kg_m (72,000 lb_m)	3,629 kg_m (8,000 lb_m)	8,074 kg_m (17,800 lb_m)
POTV	0.92	53,070 kg_m (117,000 lb_m)	4,536 kg_m (10,000 lb_m)	18,126 kg_m (38,960 lb_m)

Table 2-15. Mission Profile Velocity Requirements for Synchronous Missions

	ΔV Requirement, ft/sec
1. LEO First Injection Burn (Phasing Orbit)	4,270
2. LEO Second Injection Burn	3,586
Estimated Gravity Losses	190
3. GEO Circularization Burn	5,798
4. GEO Deorbit Burn	5,798
5. LEO Phasing Orbit Burn	3,586
6. LEO Circularization Burn	4,270
Estimated Losses	50
7. Flight Performance Reserves, 2 Percent of Total ΔV	556

Table 2-16. Mission Profile and Propellant Usage for APOTV (Delivery Only) Single Stage

Event/ Time (hr.)	Initial Mass kg_m (lb_m)		Burn Time, sec	Propellant Burned, kg_m (lb_m)		Final Mass, kg_m (lb_m)		Initial Percent Full	Initial Acceleration, g
MES1	Vehicle	44,361 (97,800)				33,569	(74,006)		
(T=0)	LO_2	27,993 (61,714)	559.1	9,270	(20,436)	18,687	(41,198)	97	0.204
	LH_2	4,666 (10,286)		1,523	(3,358)	3,108	(6,852)	92	
MES2	Vehicle	33,569 (74,006)				26,337	(58,064)		
(T=3.1)	LO_2	18,687 (41,198)	374.6	6,211	(13,692)	12,455	(27,458)	64	0.270
	LH_2	3,108 (6,852)		1,021	(2,250)	2,073	(4,571)	61	
MES3	Vehicle	26,337 (58,064)				17,872	(39,400)		
(T=8.35)	LO_2	12,454 (27,457)	438.6	7,271	(16,030)	5,161	(11,379)	43	0.344
	LH_2	2,073 (4,571)		1,195	(2,634)	868	(1,913)	41	
MES4	Vehicle	9,798 (21,600)				6,719	(14,813)		
(T=	LO_2	5,147 (11,348)	159.5	2,644	(5,829)	2,496	(5,502)	18	0.926
128.35)	LH_2	868 (1,913)		435	(958)	431	(950)	17	
MES5	Vehicle	6,719 (14,813)				5,385	(11,871)		
(T=	LO_2	2,494 (5,499)	69.1	1,146	(2,527)	1,344	(2,962)	8.6	1.35
133.6)	LH_2	431 (950)		188	(415)	242	(534)	8.4	
MES6	Vehicle	5,385 (11,871)				3,987	(8,790)		
(T=	LO_2	1,342 (2,959)	72.4	1,200	(2,646)	137	(303)	4.6	1.68
136.7)	LH_2	242 (534)		197	(435)	46	(101)	4.7	

Main Engine Thrust = 9,080 kg_f (20,000 lb_f)
Mixture Ratio = 6.08
I_{sp} = 470 sec
Dry Weight = 3,629 kg_m (8,000 lb_m)
Payload Weight = 8,074 kg_m (17,800 lb_m)
Burnout Acceleration = 2.28 g's.

Table 2-17 Mission Profile and Propellant Usage for APOTV (Round Trip) Dual Stage

Event / Time (hr.)		Initial Mass kg_m (lb_m)		Burn Time, sec	Propellant Burned, kg_m (lb_m)		Final Mass, kg_m (lb_m)		Initial Percent Full	Initial Acceleration, g
FIRST STAGE										
MES1	Vehicle	79,637	(175,570)				60,087	(132,471)		
(T=0)	LO_2	27,993	(61,714)	1013	16,792	(37,021)	11,138	(24,555)	97	0.114
	LH_2	4,666	(10,286)		2,757	(6,078)	1,858	(4,096)	92	
MES2	Vehicle	60,088	(132,471)				49,972	(110,169)		
(T=3.1)	LO_2	11,138	(24,555)	524 1	8,689	(19,157)	2,424	(5,345)	38	0.151
	LH_2	1,858	(4,096)		1,427	(3,145)	420	(927)	36	
MES3	Vehicle	6,622	(14,599)				3,964	(8,739)		
(T=3.2)	LO_2	2,424	(5,345)	137.7	2,283	(5,033)	137	(301)	8.3	1.37
	LH_2	420	(927)		375	(827)	46	(101)	8.1	
SECOND STAGE										
MES1	Vehicle	43,350	(95,570)				41,264	(90,972)		
(T=3.3)	LO_2	27,993	(61,714)	108.1	1,791	(3,949)	26,195	(57,749)	97	0.209
	LH_2	4,666	(10,286)		294	(649)	4,359	(9,609)	92	
MES2	Vehicle	41,264	(90,972)				27,900	(61,508)		
(T=8.35)	LO_2	26,195	(57,749)	692.4	11,479	(25,307)	14,672	(32,346)	90	0.220
	LH_2	4,359	(9,609)		1,886	(4,157)	2,442	(5,384)	86	
MES3	Vehicle	27.900	(61,508)				18,912	(41,693)		
(T=	LO_2	14,669	(32,339)	465.7	7,720	(17,019)	6,923	(15,262)	51	0.325
128.35)	LH_2	2,442	(5,384)		1,268	(2,796)	1,161	(2,559)	48	
MES4	Vehicle	18,912	(41,693)				15,016	(33,105)		
(T=	LO_2	6,922	(15,261)	201.8	3,346	(7,377)	3,567	(7,863)	24	0.480
133.6)	LH_2	1,161	(2,559)		549	(1,211)	608	(1,340)	23	
MES5	Vehicle	15,016	(33,105)				11,033	(24,324)		
(T=	LO_2	3,566	(7,862)	206.3	3,421	(7,542)	137	(301)	12	0.604
136.7)	LH_2	608	(1,340)		562	(1,239)	45	(100)	12	

First Stage
Main Engine Thrust = 9,080 kg_f (20,000 lb_f)
Mixture Ratio = 6.08
I_{sp} = 470 sec
Dry Weight = 3,629 kg_m (8,000 lb_m)
Payload Weight = 7,062 kg_f (15,370 lb_m)
Burnout Acceleration = 2.29 g's

Second Stage
Main Engine Thrust = 9,080 kg_f (20,000 lb_f)
Mixture Ratio = 6.08
I_{sp} = 470 sec
Dry Weight = 3,629 kg_m (8,000 lb_m)
Payload Weight = 7,062 kg_f (15,570 lb_m)
Burnout Acceleration = 0.922 g's

Table 2-18. Mission Profile and Propellant Usage for POTV (Delivery Only) Single Stage

Event/ Time (hr.)	Initial Mass kg_m (lb_m)		Burn Time, sec	Propellant Burned, kg_m (lb_m)		Final Mass, kg_m (lb_m)		Initial Percent Full	Initial Acceleration, g
MES1	Vehicle	75,732 (166,960)				58,215	(128,342)		
(T=0)	LO_2	45,489 (100,286)	453.8	15,040	(33,158)	30,390	(66,999)	97	0.239
	LH_2	7,561 (16,714)		2,477	(5,460)	5,048	(11,130)	92	
MES2	Vehicle	58,215 (128,342)				45,504	(100,320)		
(T=3.1)	LO_2	30,390 (66,998)	329.3	10,913	(24,060)	19,438	(42,854)	65	0.312
	LH_2	5,048 (11,130)		1,797	(3,962)	3,227	(7,114)	61	
MES3	Vehicle	45,504 (100,320)				30,623	(67,512)		
(T=8.35)	LO_2	19,438 (42,853)	385.5	12,777	(28,169)	6,623	(14,602)	41	0.399
	LH_2	3,227 (7,114)		2,104	(4,639)	1,105	(2,436)	39	
MES4	Vehicle	12,497 (27,552)				8,553	(18,856)		
(T=	LO_2	6,606 (14,563)	102.6	3,402	(7,500)	3,195	(7,043)	14	1.45
128.35)	LH_2	1,105 (2,436)		560	(1,235)	542	(1,196)	13	
MES5	Vehicle	8,553 (18,856)				6,836	(15,070)		
(T=	LO_2	3,193 (7,040)	44.5	1,475	(3,251)	1,713	(3,776)	6.8	2.12
133.6)	LH_2	542 (1,196)		243	(535)	299	(660)	6.5	
MES6	Vehicle	6,836 (15,070)				5,037	(11,105)		
(T=	LO_2	1,711 (3,773)	46.6	1,544	(3,405)	161	(355)	3.6	2.65
136.7)	LH_2	299 (660)		254	(560)	47	(103)	3.6	

Main Engine Thrust = 18,160 kg_f (40,000 lb_f)
Mixture Ratio = 6.08
I_{sp} = 470 sec

Dry Weight = 4,536 kg_m (10,000 lb_m)
Payload Weight = 18,126 kg_m (39,960 lb_m)
Burnout Acceleration = 3.60 g's

Table 2-19. Mission Profile and Propellant Usage for POTV (Round Trip) Dual Stage

Event/ Time (hr.)	Initial Mass kg_m (lb_m)			Burn Time, sec	Propellant Burned, kg_m (lb_m)		Final Mass, kg_m (lb_m)		Initial Percent Full	Initial Acceleration, g
FIRST STAGE										
MES1	Vehicle	128,394	(283,060)				106,949	(235,782)		
(T=0)	LO_2	45,489	(100,286)	370.3	18,415	(40,599)	27,002	(59,530)	97	0.212
	LH_2	7,581	(16,714)		3,030	(6,679)	4,487	(9,393)	92	
MES2	Vehicle	106,949	(235,782)				78,460	(172,974)		
(T=3.1)	LO_2	27,002	(59,530)	492.0	24,465	(53,936)	2,464	(5,433)	57	0.254
	LH_2	4,487	(9,893)		4,024	(8,872)	427	(941)	54	
MES3	Vehicle	7,672	(16,914)				4,968	(10,952)		
(T=3.2)	LO_2	2,464	(5,433)	46.7	2,322	(5,120)	134	(296)	5.2	3.55
	LH_2	427	(941)		382	(842)	46	(101)	5.1	
SECOND STAGE										
MES1	Vehicle	70,788	(156,060)				68,352	(150,690)		
(T=3.3)	LO_2	45,489	(100,286)	63.1	2,092	(4,611)	43,389	(95,657)	97	0.256
	LH_2	7,581	(16,714)		344	(759)	7,218	(15,913)	92	
MES2	Vehicle	68,352	(150,690)				46,157	(101,758)		
(T=8.35)	LO_2	43,389	(95,657)	574.9	19,059	(42,019)	24,257	(53,477)	92	0.265
	LH_2	7,218	(15,913)		3,136	(6,913)	4,031	(8,886)	88	
MES3	Vehicle	46,157	(101,758)				31,231	(68,852)		
(T=	LO_2	24,254	(53,470)	386.6	12,817	(28,257)	11,394	(25,119)	51	0.393
128.35)	LH_2	4,031	(8,886)		2,109	(4,649)	1,899	(4,187)	49	
MES4	Vehicle	31,231	(68,852)				24,759	(54,588)		
(T=	LO_2	11,393	(25,118)	167.6	5,556	(12,249)	5,822	(12,835)	24	0.581
133.6)	LH_2	1,899	(4,187)		914	(2,015)	980	(2,160)	23	
MES5	Vehicle	24,761	(54,588)				18,156	(40,027)		
(T=	LO_2	5,821	(12,834)	171.1	5,672	(12,504)	137	(301)	12	0.733
136.7)	LH_2	979	(2,160)		933	(2,057)	46	(101)	12	

First Stage
Main Engine Thrust = 27,240 kg_f (60,000 lb_f)
Mixture Ratio = 6.08
I_{sp} = 470 sec
Dry Weight = 4,536 kg_m (10,000 lb_m)
Payload Weight = 13,181 kg_m (29,060 lb_m)
Burnout Acceleration = 5.48 g's

Second Stage
Main Engine Thrust = 18,160 kg_f (40,000 lb_f)
Mixture Ratio = 6.08
I_{sp} = 470 sec
Dry Weight = 4,536 kg_m (10,000 lb_m)
Payload Weight = 13,181 kg_m (29,060 lb_m)
Burnout Acceleration = 0.999 g's

used for flight performance reserves. No accounting was made for RCS propellants or main propellants used at GEO in this preliminary study.

Table 2-20 shows the payload sensitivity factors for the above cases. The dry weight partials will be used for added hardware weight, and helium and auxiliary propellant residuals. Propellant weight partials are used for the displacement of propellant volume by hardware, i.e., subcooler. Propellant residual partials are used for any residual propellant created by an acquisition system. All partials are multiplied by the quantity weight or velocity to obtain payload weight which is compared between systems, i.e., $\partial P/\partial x$ where P is payload weight and x is the determined weight or velocity.

Consumed auxiliary propellants for settling are determined in two parts. The single velocity partial is used for any velocity added. Consumed auxiliary or settling propellant weight is used with the corresponding burn value. For example, settling propellants used prior to the third burn are multiplied by the burn number 3 partial.

A computer program, written under IRAD funding (Ref. 19), was used to develop the propellant usage schedules presented in Tables 2-16 through 2-19. The program, known as LOXPRES, calculates oxygen tank conditions for a single or multiple burn mission.

Table 2-20. Payload Sensitivity Factors for Geosynchronous Orbits

Vehicle:	APOTV, Prop = 72,000 lbs				POTV, Prop = 117,000 lbs			
Payload Delivery Mode:	Delivery Only		Round Trip		Delivery Only		Round Trip	
Stages:	Single	Dual*	Single*	Dual	Single	Dual*	Single*	Dual
CRITERIA								
Dry Weight								
1st Stage		-0.668		-0.24		-0.67		-0.27
2nd Stage	-3.68	-3.76	-1.0	-1.0	3.68	-3.74	-1.0	-1.0
Propellant Weight								
1st Stage		0.59		0.15		0.61		0.15
2nd Stage	0.66	0.73	0.18	0.21	0.66	0.71	0.17	0.20
Propellant Residuals								
1st Stage		-1.26		-0.39		-1.28		-0.42
2nd Stage	-4.34	-4.49	-1.18	-1.21	-4.34	-4.45	-1.17	-1.2
Auxiliary Propellant Used Prior to Burn								
Stage 1								
Burn No. 2		-0.2		-0.04		-0.2		-0.06
Burn No. 3		-0.26		-0.08		-0.28		-0.1
Stage 2								
Burn No. 2	-0.2	-0.42	-0.04	-0.1	-0.2	-0.44	-0.05	-0.11
Burn No. 3	-0.45	-0.99	-0.12	-0.26	-0.46	-1.0	-0.12	-0.26
Burn No. 4	-1.0	-1.83	-0.27	-0.48	-1.0	-1.82	-0.27	-0.49
Burn No. 5	-1.80	-2.6	-0.49	-0.7	-1.82	-2.6	-0.49	-0.7
Burn No. 6	-2.6		-0.7		-2.6		-0.7	
Velocity	5.32	5.82	1.0	1.93	5.12	9.21	1.64	3.21

Note: Values are ∂ payload/∂ x where x is weight or velocity

$\Delta V = I_{sp}\, g_c\, \ln (m_i/m_f)$

* Missions not considered in this study.

LOXPRES was developed with the intent that it be used as a preliminary design tool. With this purpose in mind the input data necessary to execute the program was kept simple. The input variables require only a basic knowledge of the vehicle geometry and mission definition.

LOXPRES calculates the helium mass necessary to provide the required net positive suction pressure (NPSP) for the oxygen tank before and during main engine firing. The mass of oxygen boiloff during coast and main engine firing, as well as the resulting tank pressure profile is also calculated. Simplifications exist in the program logic which relate propellant vapor pressure decay during outflow empirically to Centaur flight data and coast pressure rise rates to normalized expressions derived from a rigorous equilibrium solution. These simplifications do not, however, greatly compromise the results obtained.

Note that currently the LO_2 weight varies between burns by the vaporization due to tank heating occurring during coast periods. Hydrogen weight delta between burns will be somewhat smaller. The H_2 pressurization and boiloff code development schedule did not permit inclusion of these effects for H_2. Although the magnitude of these numbers are not large, they are the significant numbers that must be considered in our comparison between settling and capillary acquisition. The tables presented are also required to define propellants which must be settled for each burn. The tables will support that phase of the task and enable us to determine required propellants for settling for the established mission profiles. Tank geometries as a function of station were defined for the four vehicle tanks to support analysis of the start basket behavior.

2.4.2 PROPELLANT ACQUISITION WITH CAPILLARY DEVICES. Capillary acquisition devices provide propellant to initiate the main engine start sequence by maintaining wetted screen barriers over the engine outlet, affording a collected propellant available at all times. This start basket is refilled each burn. Cryogenic capillary devices are not used with main tank pressurization because of capillary device interactions with the warm pressurant gas. These devices therefore require a thermal subcooler to provide subcooled liquid to meet NPSP requirements. Subcoolers may be used in conjunction with boost pumps — a constant requirement for engine start and operation — or without boost pumps where they must be designed for higher performance (larger units than above) to meet the transient start conditions. This study assumed that electrically-driven tank-mounted boost pumps would be a preferred option since without them subcooler weights and penalties increase two-fold or more.

Sufficient design and analysis were performed to define the system size, the operational characteristics of the start basket including refilling times and the weights of the systems.

2.4.2.1 Capillary Device Analysis. Calculations were performed to size capillary devices for LO_2 and LH_2 tanks for the APOTV and POTV vehicles. The start sequence and thermal conditioning volume requirements were determined. Thermal conditioning requirements were based on estimates of total basket volume and

basket surface area. This estimate will be verified with the actual total volume and surface areas determined by calculating and summing the start sequence, thermal conditioning (start basket), subcooler start up, channel volume and residual volume.

Start sequence calculations were performed to determine main engine settling time and settling during the start sequence. Five times the free fall time was used as the settling and collection criteria.

Subcooler filling volume was based on scaling of subcooler requirements from Reference 2 using engine flow rate and anticipated NPSP requirements as the scaling parameters.

Capillary device thermal conditioning requirements were determined using worst case incident heating on the start basket. Heat fluxes across the tank wall were assumed to be 0.2 Btu/hr ft^2 for LH_2 and 0.3 Btu/hr ft^2 for LO_2 (Ref. 20). Both forced convection (due to mixing) and free convection heat transfer coefficients were calculated and applied to the start basket conical surface area. Mixing flows were defined from space system mixing design correlations developed by Poth (Ref. 11). These utilize a factor $V_o d_o$ to define the strength of the jet. Worst case coefficients for heat transfer to the basket due to forced convection were defined from jet impingement or flow over a flat plate. These flows were applied to the basket conical surface area and were assumed to persist for extended periods to evaluate total generation load for dryout. The free convection flows were low except for main engine firings which were of duration short enough to neglect for vapor volume generation requirements. Conversely, they could be significant for wicking strength design.

Channel and residual volume requirements were conservatively calculated to determine the required channel dimensions and basket liquid level prior to refilling initiation. The liquid in the basket must be sufficient to prevent vapor from entering the channel prior to burnout. Worst case start sequence and thermal conditioning volumes were used. Assumptions are conservative because liquid will cover the screen at a point where low pressure exists. The channels must function as follows. They must maintain contact with the liquid in the basket at the initiation of the start sequence and prevent vapor ingestion during settling of start basket fluid. (Initially liquid is positioned at the top of the basket due to drag, with thermal conditioning volume removed from the start basket). After start basket fluid is settled, the basket drains through the channels until refilling is initiated. It is for this period under main engine thrust that the channels are sized and "residual" liquid quantities are determined.

Capillary devices are assumed to be topped by 6° cones and follow the elliptical bulkhead (spaced at 1") until the conical region commences. Each cone is topped with a standpipe, sized to minimize vapor trapped during refilling. The standpipe screen is a single layer of screen that allows vapor to enter the capillary device during thermal conditioning and vapor to leave during refilling. Standpipe screen mesh is sized for retention purposes to meet worst case RCS acceleration between burns. Multiple layers of screen are used

for wicking over the remainder of the basket. Screens are spaced at 0.053 cm (0.021 in) which is the spacing determined in Reference 6. Main screen mesh is sized based on retention capability to hold liquid during all cases of engine firing prior to the last burn of each mission. For refilling purposes, burn 1 of the three-burn mission and burn 5 of the six-burn mission were analyzed for both APOTV and POTV LO_2 and LH_2 capillary devices. This analysis produced the capillary device characteristics presented in Table 2-21. Figure 2-19 is provided to illustrate specific dimensions for Table 2-21.

Refilling Calculations - Refilling capability is a major design criteria in start basket analysis. Two factors affecting start basket refill are the imposed g-level and the time available for refilling. Refilling of the start basket configurations presented in Section 2.4.3.2 was analyzed using the REFILL computer program. Burn 1 of the three-burn mission and burn 5 of the six burn mission were analyzed for both APOTV and POTV LO_2 and LH_2 capillary devices. Burn 1 of the three-burn mission was selected for analysis because it provided the lowest g-level (APOTV-0.114 g's, 1013 sec burn; POTV-0.212 g's, 370 sec burn) at which refilling would occur.

Burn 5 of the six burn mission was selected since this was the shortest burn, and therefore, had the least amount of time (APOTV-69.1 sec, POTV-44.5 sec) for refilling to occur. Mission burn conditions were given in Tables 2-15 through 2-18.

Main screen mesh requirements assume that a large portion of the start basket is covered by main tank liquid during the start sequence.

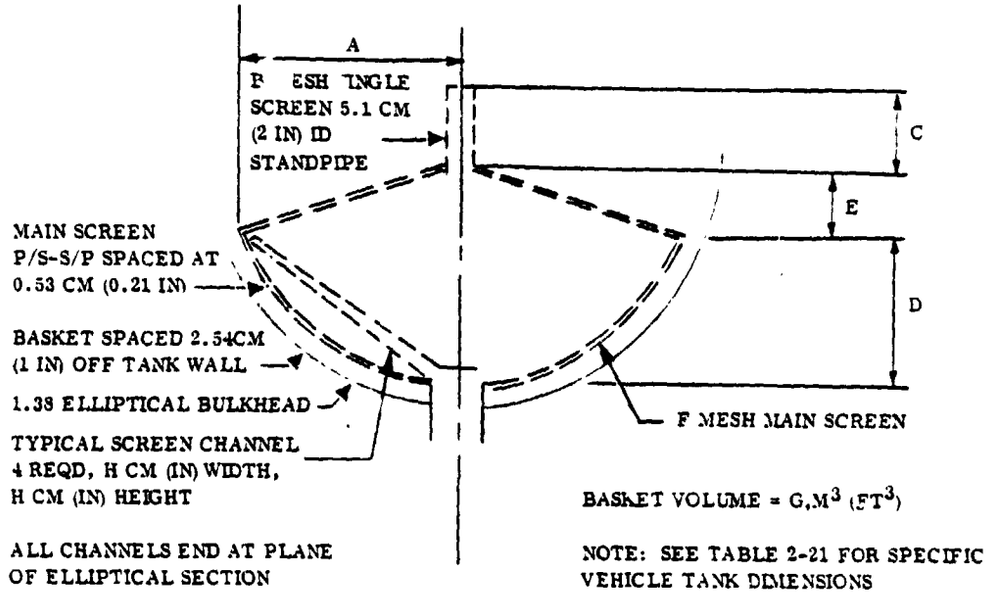

Figure 2-19. Capillary Device Schematic

Table 2-21. Capillary Device Characteristics

	Volumetric Requirement	POTV LO_2	APOTV LO_2	POTV LH_2	APOTV LH_2
	Start Sequence, m^3 (ft^3)	0.306 (10.81)	0.143 (5.05)	1.40 (49.33)	0.652 (23.02)
	Thermal Conditioning, m^3 (ft^3)	0.010 (0.37)	0.007 (0.25)	0.411 (14.5)	0.198 (7.0)
	Subcooler, m^3 (ft^3)	0.005 (0.19)	0.003 (0.10)	0.024 (0.83)	0.012 (0.42)
	Residual Margin, m^3 (ft^3)	0.002 (0.06)	0.001 (0.03)	0.024 (0.83)	0.006 (0.20)
	Channel Volume, m^3 (ft^3)	0.014 (0.51)	0.011 (0.40)	0.065 (2.3)	0.046 (1.62)
G	Total Volume, m^3 (ft^3)	0.337 (11.9)	0.165 (5.83)	1.92 (67.8)	0.912 (32.2)
	Characteristics Dimensions				
A	Radius, cm (in)	85.1 (33.5)	66.0 (26.0)	142.2 (56.0)	119.4 (47.0)
D	Ellipsoidal Ht, cm (in)	17.5 (6.9)	11.9 (4.7)	42.9 (16.9)	28.4 (11.2)
	Ellipsoidal Volume, m^3 (ft^3)	0.246 (8.7)	0.116 (4.1)	1.57 (55.5)	0.694 (24.5)
E	Cone Ht, cm (in)	9.9 (3.9)	8.4 (3.3)	16.5 (6.5)	13.0 (5.1)
	Cone Volume, m^3 (ft^3)	0.091 (3.2)	0.049 (1.73)	0.348 (12.3)	0.218 (7.7)
C	Standpipe Ht, cm (in)	4.6 (1.8)	7.9 (3.1)	11.9 (4.7)	20.1 (7.9)
	Total Height, cm (in)	32.0 (12.6)	28.2 (11.1)	71.4 (28.1)	61.5 (24.2)
H	Channel Dimensions, cm (in)	1.3 × 30.5 (1/2 × 12)	1.3 × 30.5 (1/2 × 12)	5.1 × 12.7 (2 × 5)	5.1 × 12.7 (2 × 5)
H	Channel Vertical Height, cm (in)	10.2 (4)	7.6 (3)	26.7 (10.5)	18.5 (7.3)
	Channel Mesh	325 × 2300	325 × 2300	325 × 2300	325 × 2300
F	Main Screen Mesh	24 × 110	24 × 110	24 × 110	24 × 110
	Main Screen Micron Rating	138	138	138	138
B	Standpipe Mesh	14 × 88	14 × 88	14 × 88	14 × 88
	Standpipe Micron Rating	245	245	245	245

NOTE: Four channels are required; main screen is two layers of P/S-S/P spaced at 0.053 cm (0.021 in). Standpipe is a single screen layer 5.1 cm (2 in) diameter tube. The basket is spaced 2.54 cm (1 in) off the wall.

The results of this refilling analysis are presented in Table 2-22. The settling times listed are worst case. In running the computer program REFILL, it was assumed that the propellants were completely settled before basket refilling occurred, therefore, the refilling times are conservative. The total refilling times indicate that there will be no problem in adequately refilling the start baskets. A convergence problem in REFILL prevented determination of a refilling time for the LO_2 basket in the POTV for burn 5, however, no problem in refilling is anticipated.

2.4.2.2 Subcooler Sizing Analysis. A thermal subcooler sizing analysis was performed to determine subcooler weights and associated payload weight penalties for APOTV and POTV vehicles. Subcooler system weights were generated to enable a comparison between settling with tank pressurization (Concept A, Ref. 17), settling with subcooling of boost pump propellants (Concept B, Ref. 17) and capillary acquisition with subcooling of boost pump propellants (Concept K, Ref. 17).

Table 2-22. Start Basket Refilling Times

Configuration	Mission Burn Time, sec	$(a/g_o)_{init.}$	Setting Time, sec	Refilling Time, sec	Total Refilling Time, sec
APOTV LH_2 Burn 1	1013.0	0.114	11	29.5	40.5
APOTV LH_2 Burn 5	69.1	1.35	11	1.38	12.4
APOTV LO_2 Burn 1	1013.0	0.114	7	6.0	13.0
APOTV LO_2 Burn 5	69.1	1.35	7	0.23	7.2
POTV LH_2 Burn 1	370.3	0.212	9	46.5	55.5
POTV LH_2 Burn 5	44.5	2.12	9	0.31	9.3
POTV LO_2 Burn 1	370.3	0.212	6	13.0	19.0
POTV LO_2 Burn 5	44.5	2.12	6	-	-

A. Sizing Approach

The subcooler sizing approach for this study is to match heat removal requirements for a desired NPSP to the size of subcooler which will provide this heat removal at the minimum expected operating tank pressure. The equation giving required heat removal as a function of NPSP is

$$\dot{Q}_r = \dot{m} C_p \, \Delta T/\Delta P \, (\text{NPSP} + \text{losses}) \qquad (2\text{-}11)$$

where

$\dot{Q}_r$ = required rate of heat removal, watt (Btu/sec)

$\dot{m}$ = flow rate of liquid through subcooler hot side, kg_m/sec (lb_m/(sec)

C_p = liquid propellant specific heat, Joule/kg_m-K (Btu/lb_m-F)

$\Delta T/\Delta P$ = ratio of temperature change to pressure change, K/kN/m^2 (F/psi)

NPSP = required inlet net positive suction pressure, kN/m^2 (psi)

losses = pressure drop in subcooler, kN/m^2 (psi)

Subcooler heat removal performance was determined parametrically as a function of tank pressure in Reference 2 for the three defined LO_2 and LH_2 subcooler sizes. Subcooler sizes for this study were extrapolated from the parametric curves using the specific calculation steps described later in detail. This approach

was used iteratively since the "losses" term of the above equation depends on the size of subcooler providing the NPSP.

B. Assumptions and Groundrules

1. Required delivered NPSP values are 6.9 kN/m^2 (1.0 psi) for LO_2 and 3.45 kN/m^2 (0.5 psi) for LH_2.

2. Subcoolers are sized to provide NPSP for propellant acquisition by settling (Concept B, Ref. 17) and by capillary device (Concept K, Ref. 17). It is assumed that factors affecting subcooler size (tank pressure, flow rates, etc.) are the same for both of these approaches, so a single set of subcooler weights applies to both approaches.

3. Minimum tank operating pressures during the time the subcoolers must function are estimated to be 110.3 kN/m^2 (16 psia) for the LO_2 tank and 89.6 kN/m^2 (13 psia) for the LH_2 tank based on 137.8 kN/m^2 (20 psia) initial pressure in both tanks. To determine subcooler system weight sensitivity to tank pressure, minimum pressures of 75.8 kN/m^2 (11 psia) in the LO_2 tank and 68.9 kN/m^2 (10 psia) in the LH_2 tank were also evaluated. This is shown in Table 2-23 where the comparison with nominal tank pressures can be made.

4. Both LH_2 and LO_2 subcoolers are similar in design to the LO_2 subcooler of Reference 6. Larger subcooler heat transfer areas are achieved by adding more passes to the configuration (see Figure 3-9 of Reference 6).

5. Vehicle stage thrusts are as follows:

APOTV		POTV	
Single:	9072 kg_f (20,000 lb_f)	Single:	18,144 kg_f (40,000 lb_f)
Dual:	1st - 9072 kg_f (20,000 lb_f)	Dual:	1st - 27,2 kg_f (60,000 lb_f)
	2nd - 9072 kg_f (20,000 lb_f)		2nd - 18,1 kg_f (40,000 lb_f)

6. Propellant flow rates are those for the RL10A-3-3 engine multiplied by the factor: stage thrust/13,608 kg_f (30,000 lb_f)

Stage Thrust K kg_f (K lb_f)	LO_2 $\dot{m}$ kg_m/sec (lb_m/sec)	LH_2 $\dot{m}$ kg_m/sec (lb_m/sec)
9.072 (20)	17.1 (37.6)	3.39 (7.47)
18.144 (40)	34.1 (75.2)	6.80 (14.9)
27.216 (60)	51.2 (112.8)	10.2 (22.4)

Table 2-23. Subcooler Related Weight Penalties, kg_m (lb_m) at Two Potential Tank Operating Pressures

FINAL TANK PRESSURE		LO_2 110 kN/m² (16 psia) LH_2 89.6 kN/m² (13 psia)						LO_2 75.8 kN/m² (11 psia) LH_2 68.9 kN/m² (10 psia)		
VEHICLE SIZE		Thrust 9,080 kgf (20,000 lbf) Single APOTV	Thrust 18,160 kgf (40,000 lbf) Single POTV	Thrust 27,240 kgf (60,000 lbf) 1st Stage, POTV	Thrust 18,160 kgf (40,000 lbf) 2nd Stage. POTV	Thrust 9,080 kgf (20,000 lbf) 1st Stage, APOTV	Thrust 9,080 kgf (20,000 lbf) 2nd Stage, APOTV	Thrust 9,080 kgf (20,000 lbf) Single APOTV	Thrust 15,160 kgf (40,000 lbf) Single POTV	Thrust 27,240 kgf (60,000 lbf) 1st Stage, POTV
WEIGHT PENALTY ELEMENT										
10. Subcooler	LH_2	13 (28)	29 (65)	34 (76)	111 (244)	9 (19)	48 (105)	26 (58)	75 (166)	90 (198)
	LO_2	16 (35)	33 (73)	37 (82)	124 (274)	10 (23)	60 (132)	34 (76)	85 (188)	134 (295)
16. Pumping System to Return Coolant to Tank	LH_2	9 (20)	10 (22)	7 (15)	37 (82)	6 (13)	34 (75)	9 (20)	10 (22)	7 (15)
	LH_2	10 (23)	13 (29)	11 (24)	49 (109)	7 (15)	39 (86)	10 (23)	13 (29)	11 (24)
17. Volume Penalty Due to Hardware Added	LH_2	Neg.	Neg.	1 (2)	1 (2)	1 (1)	1 (1)	Neg.	1 (1)	4 (8)
	LO_2	1 (3)	3 (5)	14 (30)	9 (20)	5 (10)	5 (12)	3 (6)	6 (14)	54 (119)
18. Fluid Residuals Cold Side Subcooler	LH_2	3 (6)	5 (12)	10 (22)	20 (44)	3 (6)	10 (22)	5 (12)	15 (33)	29 (64)
	LO_2	54 (118)	114 (252)	209 (461)	434 (957)	57 (126)	204 (449)	120 (264)	294 (649)	753 (1661)
TOTALS		106 (233)	208 (458)	323 (712)	786 (1732)	96 (213)	400 (882)	208 (459)	500 (1102)	1081 (2384)

NOTE: SETTLING OR CAPILLARY DEVICE, THERMAL SUBCOOLING, BOOST PUMP, UNCOOLED DUCT, COOLANT PUMPED.

7. Propellant properties used in the analysis:

	LO_2		LH_2	
	110.3 kN/m_2 (16 psia)	75.8 kN/m^2 (11 psia)	89.6 kN/m^2 (13 psia)	68.9 kN/m^2 (10 psia)
C_ρ joule/kg F (Btu/lb-F)	1696 (0.405)	1691 (0.404)	9462 (2.26)	9085 (2.17)
$\Delta T/\Delta P$ K/kN/m^2 (F/psi)	0.083 (1.03)	0.120 (1.49)	0.037 (0.460)	0.046 (0.571)

8. Payload partials (i.e., pound of payload penalty per pound of dry weight added, per pound of propellant not tanked, per pound of residuals, etc.) are different for delivery and round trip missions and for single and dual stage vehicles (see Table 2-20). In this study subcooler weights are treated as pounds of dry weight added. Payload penalty for propellant not tanked was calculated using the appropriate propellant weight factor.

C. LO_2 Subcooler Sizing Steps

1. Calculate required heat removal, $\dot{Q}_r$, using Equation 2-11 and estimating losses (pressure loss within subcooler).

2. Determine size of subcooler which will provide this heat removal.

   a. Extrapolate parametric curves of LO_2 heat removal down to 110.3 kN/m^2 (16 psia) (see Figure 2-20).

   b. Calculate equivalent subcooler hot side heat exchanger areas for each of three LO_2 subcoolers of Reference 6. Fin areas are multiplied by respective fin efficiencies.

   c. Plot a working curve of heat removal rate at 110.3 kN/m^2 (16 psia) versus heat exchanger area from three LO_2 subcoolers of Reference 6 (upper left curve of Figure 2-20).

   d. From this curve pick off heat exchanger area for required heat removal rate.

3. Determine pressure drop in subcooler for this size.

   a. Plot a working curve of LO_2 subcooler pressure drop vs heat exchange area using three subcoolers of Reference 6.

   b. Pick off pressure drop from curve.

4. If subcooler pressure drop is different from that estimated in Step 1, replace estimate with calculated value and do Steps 1 - 3 again. Iterate until pressure drops match.

5. When required heat removal equals heat removal performance, design point has been achieved. Determine subcooler weight.

   a. Plot a working curve of subcooler weight vs heat transfer area (upper right curve of Figure 2-20.

   b. Pick subcooler weight from curve.

D. LH_2 Subcooler Sizing Steps

1. Calculate required heat removal, $\dot{Q}_r$, using Equation 2-11 and estimating losses (pressure loss within subcooler).

2. Determine size of subcooler which will provide this heat removal.

   a. Extrapolate parametric curves of LH_2 heat removal down to 89.6 kN/m^2 (13 psia) (see Figure 2-21).

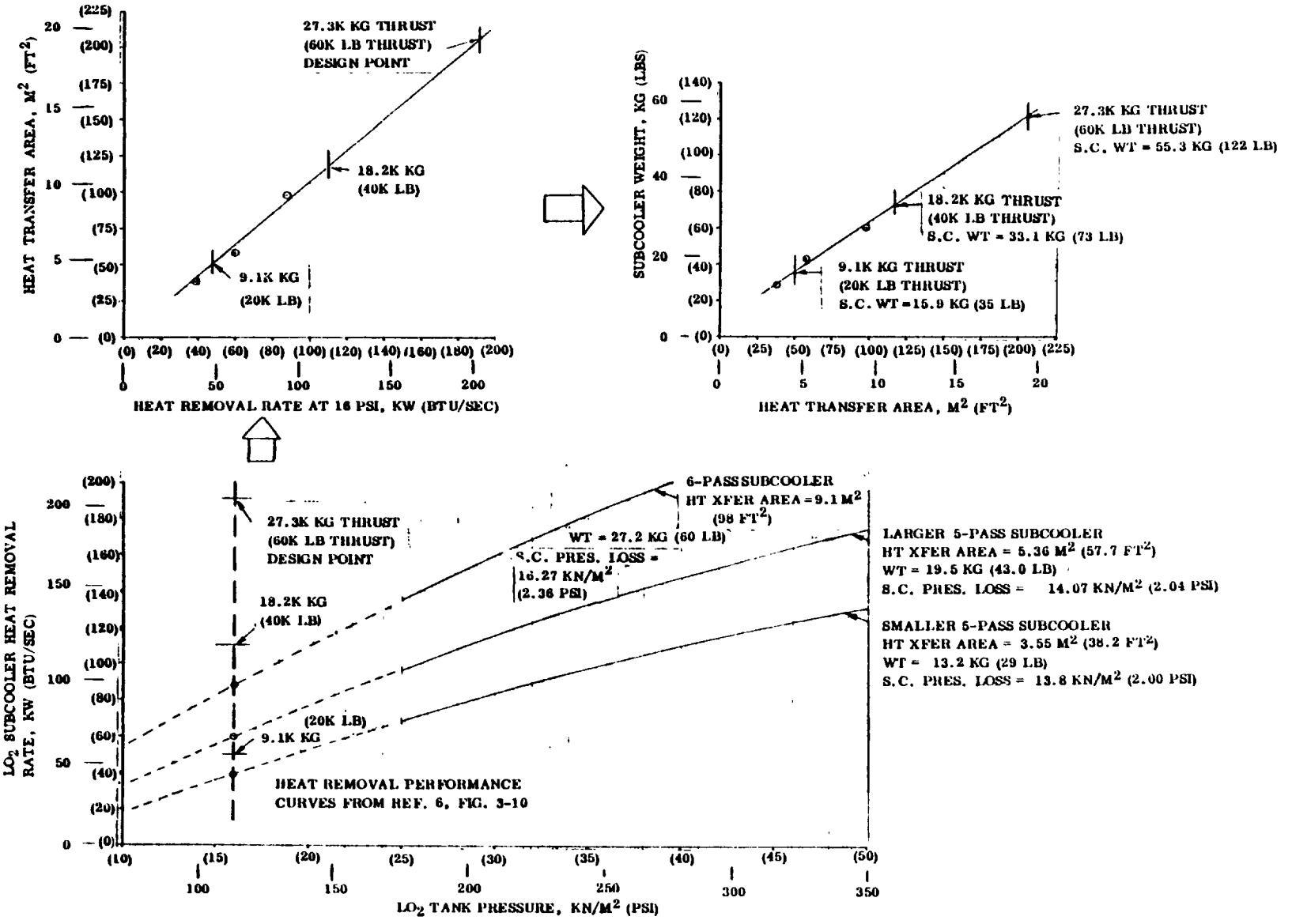

Figure 2-20. LO_2 Subcooler Sizing for APOTV and POTV Vehicles

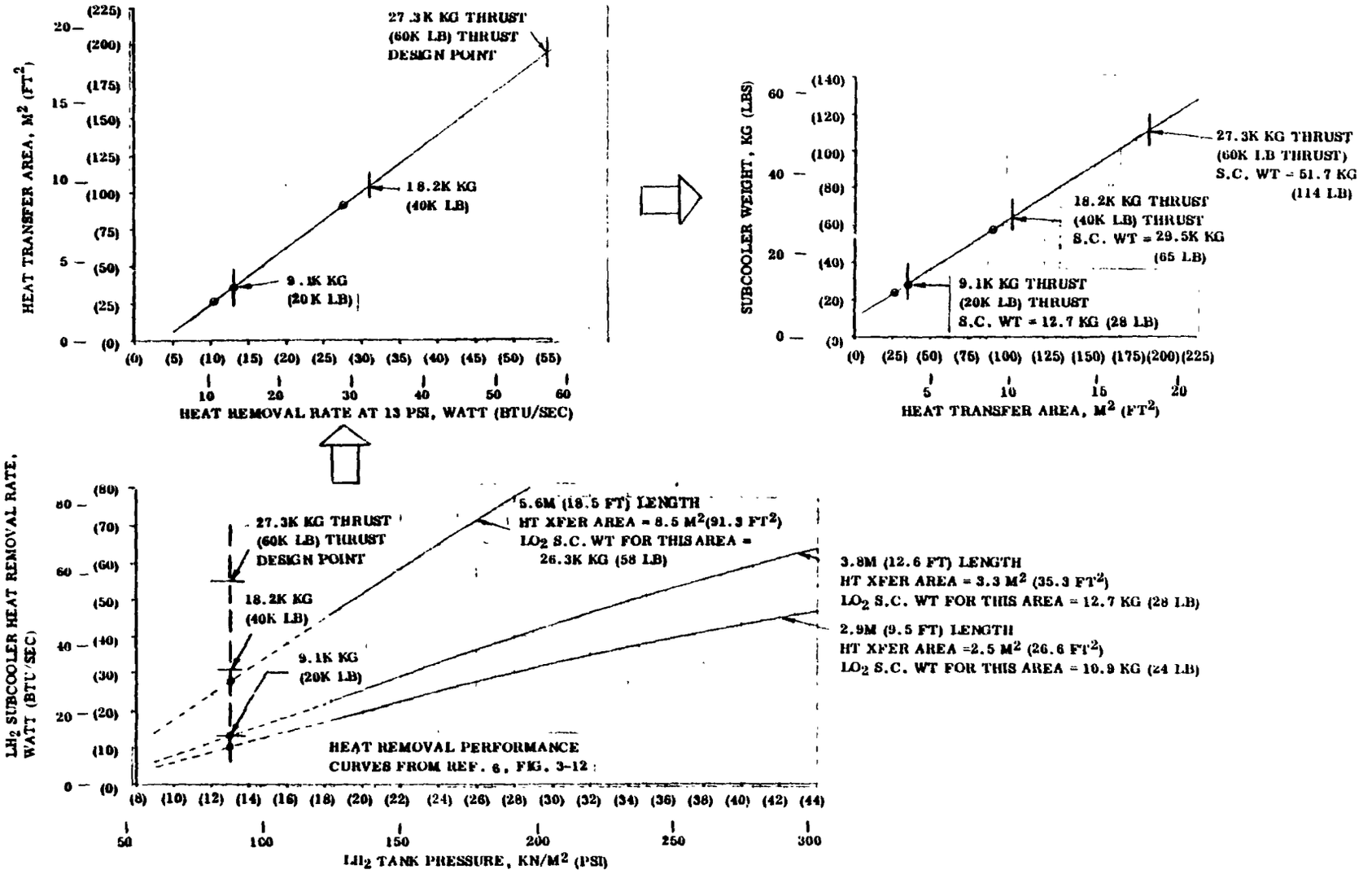

Figure 2-21. LH_2 Subcooler Sizing for APOTV and POTV Vehicles

b. Calculate equivalent subcooler hot side heat exchanger areas for each of three LH_2 subcoolers of Reference 6. Fin areas are multiplied by respective fin efficiencies.

c. Plot a working curve of heat removal rate at 89.6 kN/m^2 (13 psia) versus heat exchanger area from three LH_2 subcoolers of Reference 6 (upper left curve of Figure 2-21.

d. From this curve pick off heat exchanger area for required heat removal rate.

3. Determine LH_2 pressure drop in subcooler of LO_2 type design for this size.

a. Use the working curve of LO_2 subcooler pressure drop vs heat exchange area.

b. Pick off pressure drop from curve.

c. Adjust pressure drop for LH_2 properties ($LH_2\ \Delta P = 0.63\ LO_2\ \Delta P$)

4. If subcooler pressure drop is different from that estimated in Step 1, replace estimate with calculated value and do Steps 1 - 3 again. Iterate until pressure drops match.

5. When required heat removal equals heat removal performance, design point has been achieved. Determine subcooler weight.

a. Plot a working curve of LH_2 subcooler weight vs heat transfer area (upper right curve of Figure 2-21.

b. Pick subcooler weight from curve.

E. Factors Affecting Subcooler Size

Using subcoolers to supply NPSP requirements to the boost pumps obviates the need for main tank pressurization. However, the resulting lower tank pressures have a negative effect on both subcooler heat removal requirements and heat removal performance. Required heat removal, $\dot{Q}_r$, given by Equation 2-11 is seen to be a function of $\Delta T/\Delta P$, the slope of the LO_2 or LH_2 saturation curve, which increases with decreasing pressure. Lower tank pressures decrease subcooler performance by providing lower fluid temperature on the hot side. This is illustrated in the lower curves of Figures 2-20 and 2-21 which show performance decreasing with decreasing pressure.

Stage thrust values for this study are 9,072 kg_f (20,000 lb_f) (APOTV), 13,144 kg_f (40,000 lb_f) (POTV) and 27,216 kg_f (60,000 lb_f) (POTV) as compared to the 13,608 kg_f (30,000 lb_f) thrust of Centaur. The propellant flow rate, $\dot{m}$, appearing in

Equation 2-11 is a direct function of stage thrust (for the same I_{sp} engines). Consequently, the required heat removal for the larger POTV stages is at least double and triple that for the 9,072 kg_f (20,000 lb_f) thrust APOTV stage due just to the $\dot{m}$ term.

Considering both the lower tank pressures and higher flow rates listed above (on two stages), the subcoolers of this study are of the same approximate size, or even larger than those of Reference 6, even though the required NPSP output is less. Compounding the problem, the larger subcooler pressure drop losses occurring with the higher heat load subcoolers further increases subcooler size.

Note that the subcooler weight versus heat transfer area curves at the top right of Figures 2-20 and 2-21 are extrapolations of the three closely spaced points developed in Reference 6. The subcooler sizes and weights determined by this analysis should therefore be considered conceptual only. They are however valid for system weight comparisons. The weights for the three stages in order of increasing thrust are for LH_2 subcooler 13 kg_m (28 lb_m), 28 kg_m (65 lb_m) and 52 kg_m (114 lb_m) and for LO_2 subcooler 16 kg_m (35 lb_m), 33 kg_m (73 lb_m) and 55 kg_m (122 lb_m).

F. Other Subcooler Related Weights and Weight Summary

The use of subcoolers to provide required boost pump NPSP results in three additional sources of payload penalty; propellant residuals remaining in the subcooler cold side, a pumping system to return cold side propellants into the tanks and a volume penalty for propellants not tanked due to added hardware in the tanks. By far the most severe of the above penalties is the LO_2 residual remaining in the subcooler cold side. Propellant residuals for this study were computed by ratioing residuals from Reference 6 by the subcooler weights (which are generally proportional to volume). The resulting residual propellant weights are:

	9,072 kg_f (20,000 lb_f) Thrust Veh.	18,144 kg_f (40,000 lb_f) Thrust Veh.	27,216 kg_f (60,000 lb_f) Thrust Veh.
LO_2, kg_m (lb_m)	45 (100)	98 (215)	163 (360)
LH_2, kg_m (lb_m)	2 (5)	5 (10)	8 (17)

Pumping systems to return cold side propellants back to the tanks were sized for the three vehicle sizes above. The systems include a battery, surge tank, pump, other hardware and resulting propellant boil-off. The weights ranged from 9 kg_m (20 lb_m) to 16 kg_m (36 lb_m) for the 9072 (20,000) to 27,216 (60,000) kg_f (lb_f) vehicles.

The volume penalties due to hardware in the tanks are negligible for the LH_2 tank and less than 14 kg_m (30 lb_m) for the LO_2 tanks.

Vehicle weight penalties related to the use of subcoolers are summarized in Table 2-23. The numbering system accompanying the weight items corresponds to the weight tables of Reference 17. The total penalties are seen to be strongly influenced by vehicle thrust (propellant flow rate) which affects required heat removal rate for a given delivered NPSP. Subcoolers for lower thrust vehicles are seen to have considerably lower payload penalties when stage size and propellant load are identified.

G. Weight Sensitivity To Tank Pressure

Recognizing that lower tank pressure is detrimental to the subcooler system (because it both increases the required heat removal and decreases heat removal performance), initial tank pressures were set as high as possible [137.8 kN/m^2 (20 psia)] without causing additional weight penalties such as tanking density, skin thickness, etc. Estimated end-of-mission tank pressures for 137.8 kN/m^2 (20 psia) initial pressure in both tanks are 110.3 kN/m^2 (16 psia) for the LO_2 tank and 89.6 kN/m^2 (13 psia) for the LH_2 tank. To determine system weight sensitivity to tank pressure, the subcooler sizing analysis was also performed for lower tank pressures of 75.8 kN/m^2 (11 psia) in the LO_2 tank and 68.4 kN/m^2 (10 psia) in the LH_2 tank. The results showed that subcooler size must be increased considerably to handle tank pressures that are only a few psi lower. A penalty weight summary for the lower tank pressures is shown in Table 2-23 for three vehicles for comparison. Subcooler weights, and especially LO_2 fluid residuals on the LO_2 subcooler cold side, are extremely high. The system is seen to be very sensitive to minimum tank pressure and indicates the desirability of using the higher tank pressures from Table 2-23 in this study. The table shows in excess of double the payload penalty for the low tank pressures for the three stages considered.

Increasing the final tank pressure results in a weight penalty which does not appear in the weight summary. Vapor residuals in the tanks have a higher density at higher pressure. Vapor residual weights are proportional to densities which are shown below:

	GO_2		GH_2	
	110.3 kN/m^2 (16 psia)	75.8 kN/m^2 (11 psia)	89.6 kN/m^2 13 psia)	68.9 kN/m^2 10 psia)
Density, gm/cc (lb/ft^3)	0.00486 (0.303)	0.00343 (0.214)	0.00120 (0.0748)	0.00095 (0.0591)

GO_2 residuals are seen to be higher by 42 percent and GH_2 residuals are higher by 27 percent at the higher pressures.

2.4.2.3 Acquisition System - Weight Estimates. Four capillary acquisition devices for POTV and APOTV applications are described in Layouts No. 1, 2, 3 and 4, Figures 2-22 through 2-25, respectively. The purpose of these layouts is to present brief design cuts coupled with weight breakdowns. Ideally, all of the walls of the capillary devices should be fine mesh screen with continuous wicking paths. However, screens cannot react to loads, therefore, the designs emphasize structural backup systems for supporting the screens when exposed to fluid impingement, pressure differentials, vibration and acceleration. Referring to Layout No. 1, the device shown is for a POTV oxidizer tank, and consists of a channel assembly enveloped by an ellipsoidal bottom section and a conical top section. The complete assembly is supported at the LO_2 tank outlet and spaced 2.54 cm (1 in) from the tank wall. Except for CRES fasteners and teflon gaskets, all parts are 2219 aluminum alloy.

The channel assembly consists of four branches spaced at 1.57 radians (90°) and interconnected at the center to a flanged outlet equipped with stiffener webs. Each branch has a 1.25×30.48 cm (0.5×12 in) rectangular flow path enclosed by two perimeter frames at the edges and two flat side walls. A typical cross section is shown in Section "D-D" in Layout No. 1 and Section "A-A" in Layout No. 4. The flat side walls are constructed of 325×2300 mesh screen seam welded at the edges to the perforated support sheets. The screens are also intermittently spotwelded to the support sheets in the centra. areas.

The bottom section is a shallow ellipsoidal dish equipped with an outlet hub at the center, a perimeter ring and twelve stiffener ribs spaced at 0.52 radians (30°). The ribs are attached to the perimeter ring, the hub, and to the main screen wall. Arrangements between the perimeter ring, stiffeners and hub are shown in Details "B" and "C." The typical main screen wall section shown in Detail "E" consists of two screens spot-welded to perforated sheets. A 0.05 centimeter (0.021 in) gap is maintained between the screens using buttons which are spotwelded to the screen/perforated sheet assemblies.

The top section is a shallow cone equipped with an apex ring at the center, a standpipe, a perimeter ring and twelve stiffener ribs. Similar to the bottom section, the ribs are attached to the perimeter ring, the apex ring, and to the main screen wall. The main screen wall is the same as that described for the bottom section. The standpipe is a single formed screen seam welded to the apex ring (see Detail "A" on Layout No. 3). Also to permit assembly, the top section perimeter ring is attached to the bottom section perimeter ring using a gasket and screw set. The basket weight for Layout No. 1 has been determined to be 33.5 kg_m (73.9 lb_m).

Layout No. 2 describes a second acquisition device for APOTV oxidizer tanks. Except for the smaller diameter (132 cm vs 170 cm for the Layout No. 1 configuration), the design is the same as that described for the POTV on Layout No. 1. Basket weight is

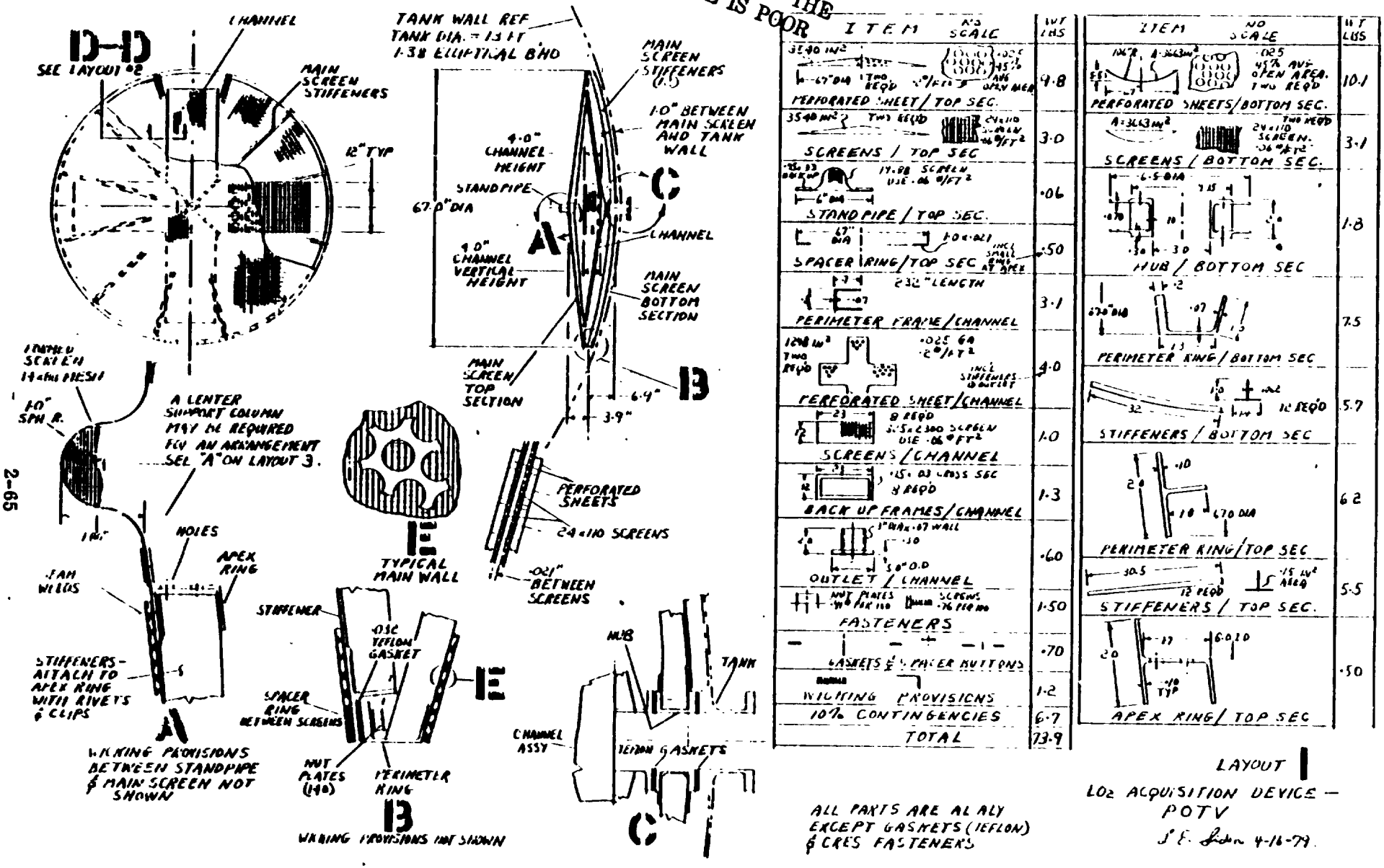

ITEM	NO	SCALE	WT LBS
PERFORATED SHEET / TOP SEC.			9.8
SCREENS / TOP SEC			3.0
STAND PIPE / TOP SEC.			.06
SPACER RING / TOP SEC			.50
PERIMETER FRAME / CHANNEL			3.1
PERFORATED SHEET / CHANNEL			4.0
SCREENS / CHANNEL			1.0
BACK UP FRAMES / CHANNEL			1.3
OUTLET / CHANNEL			.60
FASTENERS			1.50
GASKETS & SPACER BUTTONS			.70
WIRING PROVISIONS			1.2
10% CONTINGENCIES			6.7
TOTAL			73.9

ITEM	NO	SCALE	WT LBS
PERFORATED SHEETS / BOTTOM SEC.			10.1
SCREENS / BOTTOM SEC.			3.1
HUB / BOTTOM SEC			1.8
PERIMETER RING / BOTTOM SEC			7.5
STIFFENERS / BOTTOM SEC			5.7
PERIMETER RING / TOP SEC			6.2
STIFFENERS / TOP SEC.			5.5
APEX RING / TOP SEC			.50

ALL PARTS ARE AL ALY EXCEPT GASKETS (TEFLON) & CRES FASTENERS

LAYOUT

LO2 ACQUISITION DEVICE — POTV

J. E. Lehn 4-16-79

Figure 2-22. Liquid Oxygen Capillary Acquisition Device for POTV

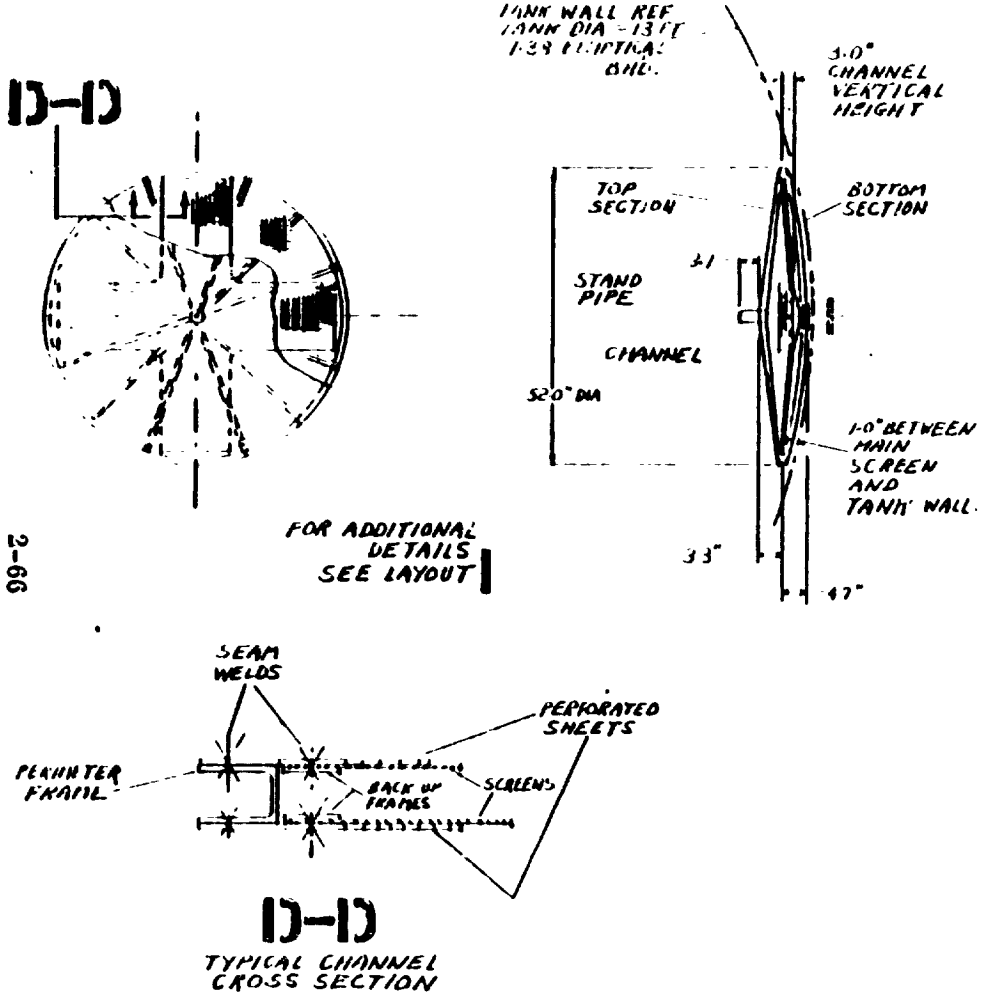

ITEM (NO SCALE)	WT LBS
SCREENS / TOP SEC	1.8
STANDPIPE / TOP SEC	.10
SPACER RING / TOP SEC	.41
PERIMETER FRAME / CHANNEL	2.5
PERFORATED SHEET / CHANNEL	3.0
SCREENS / CHANNEL	.70
BACK UP FRAMES / CHANNEL	1.1
OUTLET / CHANNEL	.60
FASTENERS	1.4
GASKETS & SPACER BUTTONS	.60
WICKING PROVISIONS	1.0
10% CONTINGENCIES	4.8
TOTAL	53.2

ITEM (NO SCALE)	WT LBS
PERFORATED SHEETS / BOTTOM SEC.	5.6
SCREENS / BOTTOM SEC.	1.7
HUB / BOTTOM SEC	1.3
PERIMETER RING / BOTTOM SEC	5.7
STIFFENERS / BOTTOM SECTION	4.4
PERIMETER RING / TOP SEC	4.7
STIFFENERS / TOP SEC	1.4
APEX RING / TOP SEC	.43
PERFORATED SHEET / TOP SEC.	6.0

EXCEPT FOR TEFLON GASKETS & CRES FASTENERS, ALL PARTS ARE AL ALY.

LAYOUT 2
LO2 ACQUISITION DEVICE — APOTV

Figure 2-23. Liquid Oxygen Capillary Acquisition Device for APOTV

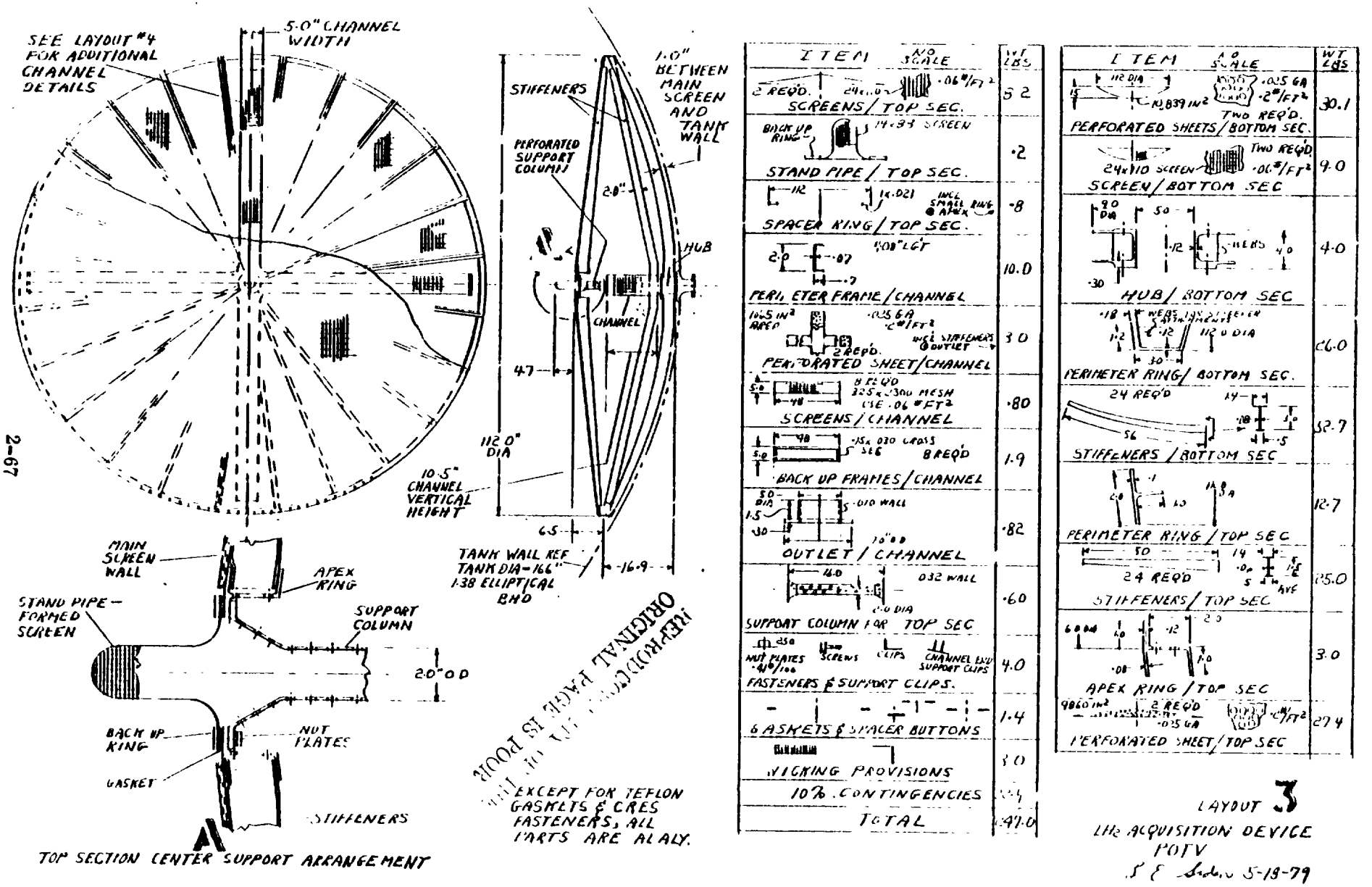

Figure 2-24. Liquid Hydrogen Capillary Acquisition Device for P OTV

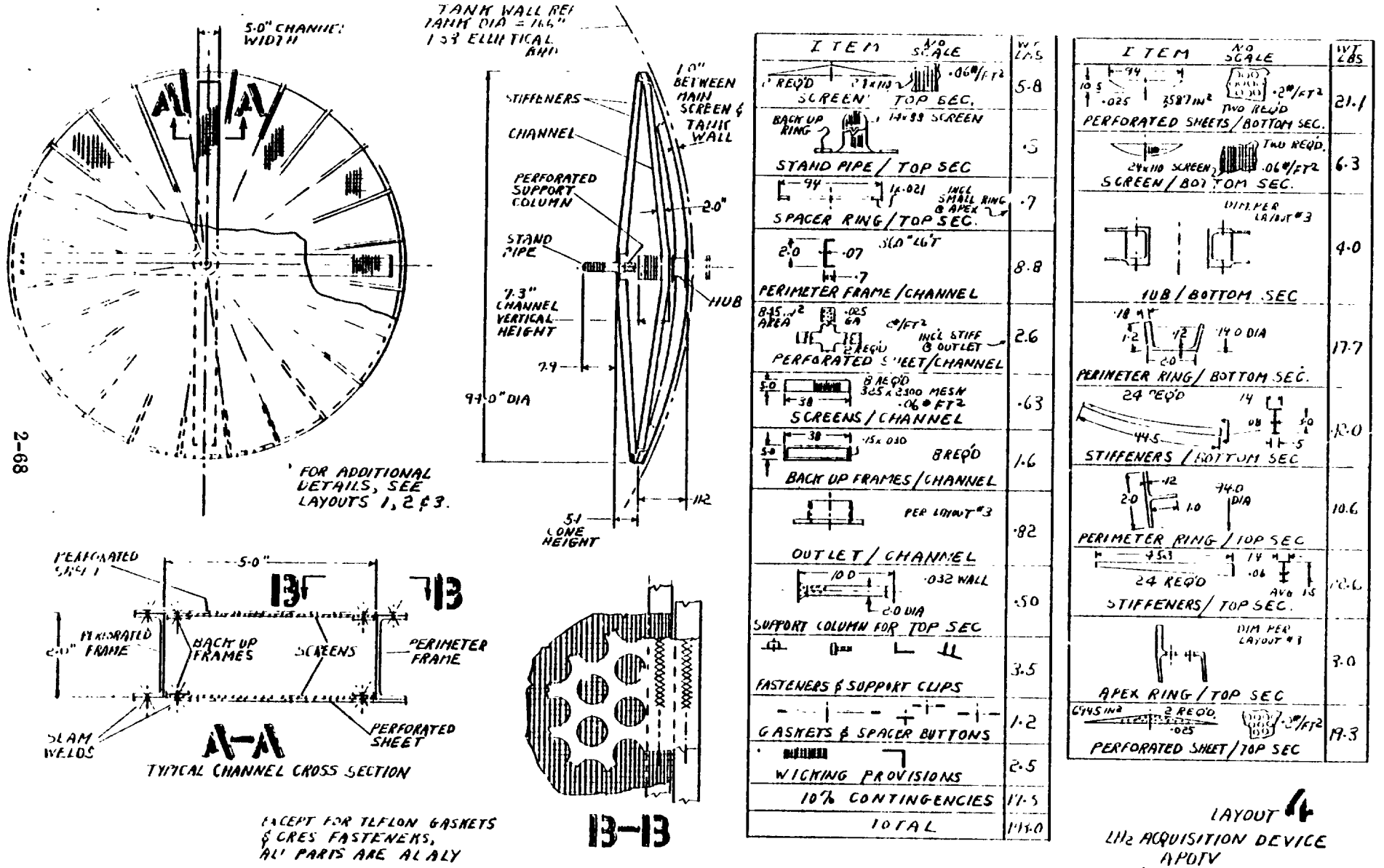

2-68

Figure 2-25. Liquid Hydrogen Capillary Acquisition Device for APOTV

24.1 kg_m (43.2 lb_m).

The acquisition device shown in Layout No. 3 is for POTV LH_2 tank applications. The configuration is basically the same as those described in Layouts No. 1 and 2 except for the large 284 cm (112 in) diameter which requires additional structure. Instead of the twelve stiffener ribs used for the previous designs, twenty-four are required for both the bottom and top sections in this case. Also the cross sections for perimeter rings, stiffeners, the hub and the apex ring have been increased. A center support column has been added and is attached to the apex ring (per Detail "A") and to the channel wall. The channel incorporates internal webs at the center for passing the column loads to the bottom section hub. Channel construction is shown in Section "A-A" of Layout No. 4 and it is the same as that described previously for the oxidizer applications. The four channel branches are long cantilever beams which will require some additional support at the ends. These supports may be fittings with the outboard ends fixed to the aft section perimeter ring and the opposite ends engaged with the channel ends through sliding connections. This arrangement permits dimensional changes along the length of the channel while providing support normal to the flat surfaces of the channel. Supports may also be required between the outboard surface of the aft section perimeter ring and the tank wall. Basket weight for the larger LH_2 basket is 112 kg_m (247 lb_m) with major items being stiffeners and perforated sheet.

Layout No. 4 describes a fourth acquisition device for use in APOTV LH_2 tanks. The device is slightly smaller (234 cm dia) than the configuration shown previously in Layout No. 3. Layout No. 4 design is the same as the previous case except that some of the structural members have been scaled down slightly. This basket weight is 87.5 kg_m (193.0 lb_m).

2.4.3 PROPELLANT ACQUISITION WITH SETTLING. An alternative to capillary acquisition devices is propellant collection with the reaction control system (RCS). This system may be used either in conjunction with a thermal subcooler (see 2.4.2.2) or a pressurization system (see 2.4.3.3). The settling system utilizes the existing RCS system on the vehicle so the only penalties involved in this system are additional propellant and storage bottle weight. For purposes of this study, the propellants are N_2O_4/MMH. A pressurization system is used in one of the concepts selected. The pressurization system provides the NPSP of 3.45 kN/m^2 (0.5 psia) and 6.89 kN/m^2 (1.0 psia) to the hydrogen and oxygen boost pumps, respectively. In all three concepts selected for this study, boost pumps will be used.

2.4.3.1 Propellant Settling Analysis. Mission profiles were established in Section 2.4.1 for single and dual stage POTV and APOTV configurations. These profiles determine, among other things, the mass of the vehicle and each of the propellants subsequent to each of the various burns that the mission requires. Before each of these burns, however, the liquid propellant (hereafter to be referred to as liquid hydrogen) must be settled in the aft end of the propellant tank to assure ignition. It is observed from experience with Centaur flight data that the liquid hydrogen will

require longer settling times than the liquid oxygen. Therefore only the hydrogen settling requirements are analyzed. The preferred thrust level and resultant duration for settling is the subject of this section.

To evaluate the amount of settling propellant, the time required to settle the liquid hydrogen must be calculated. Two documented approaches will be used to calculate the settling times (References 21 and 22). To lessen any deviation from reality which the results of either method may introduce, the settling time used to calculate the settling propellant required for any one mission will be a weighted average of the results of the two aforementioned methods.

The general features of the POTV were shown in Figure 2-15. The APOTV is the same diameter but is less than half as long. In either case the second stage of the dual stage configuration is identical to the first stage. From Figure 2-15, the liquid hydrogen tank is observed to be larger than the liquid oxygen tank. Therefore, the hydrogen will take much longer to settle. It is for this reason that when the hydrogen is considered settled, the vehicles' propellants are considered settled. The dimensions of the hydrogen tank for the APOTV and POTV are shown below.

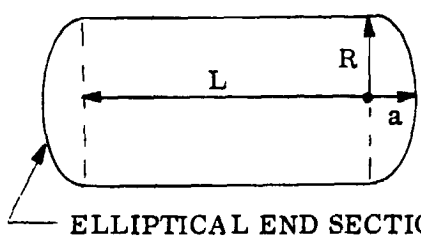

	APOTV	POTV
a	155.4 cm (61.2 in)	155.4 cm (61.2 in)
R	214.6 cm (84.5 in)	214.6 cm (84.5 in)
L	286.3 cm (112.7 in)	594.9 cm (234.2 in)
FR	1.391	2.110

Fineness ratio (FR) = (2a + L)/2R

The mission profile determines, for a given stage of a given vehicle, a sequence of main engine starts (MES). Associated with each main engine start is the percentage of the hydrogen tank filled with liquid, (fill level), as well as the overall mass of the vehicle. The fill level and the mass of the vehicle are necessary data in determining the amount of settling time required to settle propellants. This information is given in Table 2-24. Also included in Table 2-24 is the acceleration of the vehicle as a result of a resettling thrust assumed to be 18.1 kg_f (40 lb_f). The acceleration is calculated from the formula $a_T = (F/M)\ g_c$.

Knowing the reorientation acceleration applied to the vehicle, the geometry of the hydrogen tank, the fill level and the specific surface tension of hydrogen [$\sigma/\rho = 27.2$ cm^3/sec^2 ($9.6093 \cdot 10^{-4}$ ft^3/sec^2)], the reorientation times can now be calculated. It is conservatively assumed that the liquid exists in a zero-gravity configuration occupying the end of the tank opposite to which the liquid hydrogen is to be settled. Figure 2-26 clarifies this and shows how various parts of the total collection time are defined.

Table 2-24. Vehicle Fill Level, Mass, and Acceleration for Various Mission-MES

		APOTV Single Stage	APOTV Dual Stage		POTV Single Stage	POTV Dual Stage	
			1st Stage	2nd Stage		1st Stage	2nd Stage
Fill Level	MES2	0.613	0.366	0.859	0.613	0.545	0.876
	MES3	0.409	0.083	0.482	0.392	0.052	0.489
	MES4	0.171	-	0.229	0.134	-	0.230
	MES5	0.085	-	0.120	0.066	-	0.119
	MES6	0.048	-	-	0.036	-	-
Mass of Vehicle (lbm)	MES2	74,006	132,471	90,972	128,342	235,782	150,690
	MES3	58,064	14,599	61,508	100,320	16,914	101,758
	MES4	21,600	-	41,693	27,552	-	68,952
	MES5	14,513	-	33,105	18,956	-	54,588
	MES6	11,871	-	-	15,070	-	-
Acceleration of Vehicle Assuming F=40 lb_f	MES2	$1.7388 \cdot 10^{-2}$	$9.7138 \cdot 10^{-3}$	$1.4145 \cdot 10^{-2}$	$1.0026 \cdot 10^{-2}$	$5.4576 \cdot 10^{-3}$	$8.5394 \cdot 10^{-3}$
	MES3	$2.2162 \cdot 10^{-2}$	$8.3143 \cdot 10^{-2}$	$2.0921 \cdot 10^{-2}$	$1.2827 \cdot 10^{-2}$	$7.6079 \cdot 10^{-2}$	$1.2646 \cdot 10^{-2}$
	MES4	$5.9574 \cdot 10^{-2}$	-	$3.0864 \cdot 10^{-2}$	$4.6704 \cdot 10^{-2}$	-	$1.9689 \cdot 10^{-2}$
	MES5	$8.6870 \cdot 10^{-2}$	-	$3.9870 \cdot 10^{-2}$	$6.8244 \cdot 10^{-2}$	-	$2.3573 \cdot 10^{-2}$
	MES6	$1.0840 \cdot 10^{-1}$	-	-	$8.5388 \cdot 10^{-2}$	-	-

The equations used to calculate the collection times depend on the velocity of leading edge at station 3 , V_L. From this velocity a Weber number can be calculated, ($We = V_L^2 R\rho/\sigma$) whose value will determine whether or not a geyser will form. When $We \leqq 4$ no geyser will form and the total collection time can be calculated from either of the two formulas below.

$$t'_T = t_1 + t_2 + \ell^*/V_o$$

$$t''_T = t_4 + t_5$$

The term ℓ^*/V_o is the additional time required for the liquid to collect once the leading edge has reached station 3. Values of t_1, t_2, t_4, t_5 and V_o are calculated as outlined in Sumner's report (Ref. 21). Since his equations dealt with a cylindrical tank with hemispherical end sections, the equations were slightly modified to apply to the present application. The radius of a sphere with the equivalent volume of the elliptical volume was used. If $4 \leq We \leq 20$ a geyser will form but its axial progression will not proceed past a certain point. In this Weber number range, Sumner's equation for t_3 is valid and hence can be used in calculating collection times.

$$t'_T = t_1 + t_2 + t_3$$

$$t''_T = t_4 + t_5$$

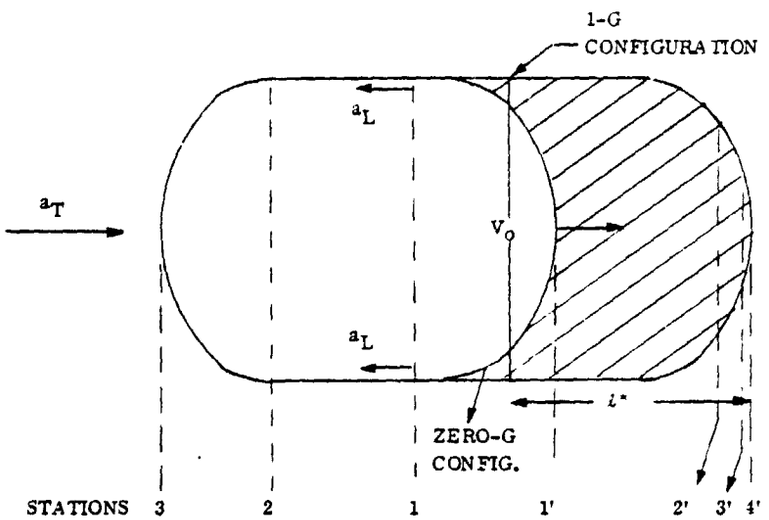

t_1 = the amount of time it takes the leading edge to proceed from Station 1 to Station 2

t_2 = the amount of time it takes the leading edge to proceed from Station 2 to Station 3

t_3 = the amount of time it takes the liquid to collect and settle once the leading edge has reached Station 3

t_4 = the amount of time it takes the vapor bubble to proceed from Station 1' to Station 4'

t_5 = the amount of time it takes liquid to clear the walls once the vapor bubble has reached Station 4'

t_ϵ = the amount of time it takes vapor bubble to proceed from Station 1' to Station 3' (distance between Stations 4' and 3' is $\epsilon = 0.005R$)

$t_{0.23}$ = the amount of time it takes vapor bubble to proceed from Station 1' to Station 2' (distance between stations 4' and 2' is 0.23R)

Figure 2-26. Relation of Settling Times to Tank Stations

If We ≧ 30, a geyser will form and proceed in the direction of the applied acceleration with a constant velocity. By conservation of momentum arguments, this affect will slow the rate at which liquid is collected in the tank. As the Weber numbers will typically be on the order of a few thousand, an alternate method of calculating t''_T will be used.

$$t'_T = t_1 + t_2 + \ell^*/V_c$$

$$t''_T = t_\epsilon + 2\, t_{0.23}$$

where

$$V_c = V_o \left[1 - (2.76)\, K \left[(\ell_i + a)/R \right]^{1/2} \right]$$

t_ϵ and $t_{0.23}$ are found using the equations contained in the work of Hollister and Satterlee (Reference 22).

Settling Times and Propulsive Requirements

The results of the calculations of collection times, t'_T and t''_T, for each burn of each vehicle configuration are presented in Table 2-25 for three different settling thrust levels.

One observes that a disparity exists between the two estimates of collection times. An averaging technique must be employed to decide upon one value. A rationale that may be used to decide upon a compromise value is as follows. Admittedly, a more conservative approach would be to use the larger of the t_T values, however that conservatism is not considered warranted. If t'_T and/or t''_T is greater than, say, 1000 sec let more weight

Table 2-25. Settling Burn Times in Seconds Determined by Two Calculation Methods

		F = 40 lb_f		F = 4 lb_f		F = 0.4 lb_f	
		t'_T	t''_T	t'_T	t''_T	t'_T	t''_T
APOTV	MES2	116	412	612	1303	3369	914
SINGLE	MES3	86	349	499	1103	1580	814
STAGE	MES4	42	187	155	592	1096	1873
	MES5	26	147	94	466	917	1475
	MES6	22	129	77	408	7[illegible]	1291
APOTV 1ST	MES2	146	516	774	1630	1510	1380
DUAL	MES3	25	146	93	462	909	1462
STAGE 2ND	MES2	188	457	881	1444	2256	1046
	MES3	92	372	488	1177	1549	903
	MES4	62	269	468	850	1479	2689
	MES5	48	225	176	712	1380	2251
POTV	MES2	281	672	1588	2125	1582	2262
SINGLE	MES3	181	511	1207	1616	2524	1452
STAGE	MES4	51	217	210	687	932	2172
	MES5	38	169	147	533	637	1686
	MES6	31	146	117	463	490	1464
POTV 1ST	MES2	381	872	2757	2635	4804	4495
DUAL	MES3	34	158	133	498	568	1576
STAGE 2ND	MES2	362	765	1728	2418	2709	4135
	MES3	197	552	2156	1744	3517	1631
	MES4	124	373	546	1180	1737	3732
	MES5	91	302	401	954	1270	1270

be given to the lesser value and let this weighting increase as the disparity between t'_T and t''_T increases. This procedure will allow reasonable settling without excessive fuel consumption. If t'_T and t''_T are less than 1000 sec, let more weight be given to the greater value and let this weighting increase as the disparity increase. This will assure settling without excessive propellant usage. The averaging procedure is symbolically depicted below.

Given $A > B$ where A and B are t'_T or t''_T depending on their magnitudes

if	A and/or B > 1000	if	A and B < 1000
	$C = \frac{(A - B)}{A} B + \frac{(B)}{A} A$		$C = \frac{(A-B)}{A} A + \frac{(B)}{A} B$
	$= B\,(2-B/A)$		$= A - B + B^2/A$

Estimates of the collection times for each burn of each vehicle have been found for three discrete thrust levels. These times are summarized in Table 2-26. It remains to calculate the amount of propellant necessary to accomplish all of the settling requirements that a mission for a given vehicle configuration demands. This is found by summing the collection times over the various burns of a mission (listed in Table 2-26) and using this information in conjunction with an appropriate ISP to calculate settling propellant requirements. Assuming an ISP of 260 sec for the propellants N_2O_4/MMH the settling propellant mass requirements are determined as a function of thrust level and presented in Figure 2-27. The settling system takes no hardware weight penalties other than propellant and storage tank mass in the latter system comparisons, assuming RCS hardware exists.

As can be seen in Figure 2-27, the amount of settling propellant required for a mission is least when the settling thrust is 0.4 lb_f. The time required, however, may be excessive at this thrust level. If a larger thrust level is chosen instead, the propellant requirements are still not large. For purposes of the system comparisons, a conservative settling thrust of 18.2 kg_f (40 lb_f) is assumed to give propellant weight requirements. This resulted in the maximum settling time being 657 seconds for MES2 of the dual stage POTV, most others were considerably shorter. Obviously lower weights can be used as the mission becomes better defined.

2.4.3.3 Helium Pressurization Mass Requirements. Pressurization, or the equivalent thermal subcooling for use with the start basket concept, will be required to provide adequate net positive suction pressure (NPSP) for feed system pump operation. Both the hydrogen and oxygen tanks will be pressurized prior to and during main engine firing. Helium pressurization is required prior to and during engine firing for the oxygen tank and prior to engine firing for the hydrogen tank. During engine firing the hydrogen tank will utilize autogeneous pressurization.

Helium requirements were computed based on a 6.89 kN/m^2 (1.0 psia) and 3.45 kN/m^2 (0.5 psia) pressurization for the oxygen and hydrogen tanks, respectively. For the

Table 2-26. Collection Times in Seconds From Weighted Average of the Times Contained in Table 2-25

$F = 40\ lb_f$	APOTV SINGLE STAGE	APOTV DUAL STAGE; 1st STAGE	APOTV DUAL STAGE; 2nd STAGE	POTV SINGLE STAGE	POTV DUAL STAGE; 1st STAGE	POTV DUAL STAGE; 2nd STAGE
MES2	329	411	346	509	657	574
MES3	284	125	303	394	131	425
MES4	154	-	221	178	-	290
MES5	126	-	187	140	-	238
MES6	111	-	-	122	-	-
Σt	1004	536	1057	1343	788	1527
$F = 4\ lb_f$						
MES2	937	1180	1224	1989	2752	2221
MES3	772	388	774	1512	401	2077
MES4	478	-	640	541	-	839
MES5	391	-	580	427	-	722
MES6	346	-	-	376	-	-
Σt	2924	1568	3218	4845	3153	5859
$F = 0.4\ lb_f$						
MES2	1580	1499	1607	2058	4784	3077
MES3	1209	1253	1280	2069	931	2506
MES4	1551	-	2145	1464	-	2666
MES5	1264	-	1914	1033	-	1270
MES6	1084	-	-	816	-	-
Σt	6688	2752	6946	7440	5715	9519

oxygen tank the helium usage was calculated using the LOXPRES computer program described in Section 2.4.1. The helium mass required to pressurize the hydrogen tank was obtained from results of the MULTBOT computer program (for a description of MULTBOT see Reference 23). Calculations based on the output from LOXPRES and on Centaur flight data were used to set up the input data for MULTBOT.

The results of the helium pressurization analysis for the four vehicles under consideration are presented in Tables 2-27 through 2-30. These results are based on a helium pressure vessel having the following physical characteristics: maximum dry weight of 35.2 kg_m (77.5 lb_m), internal volume of 0.134 m^3 (4.734 ft^3), maximum pressure between 278K (500R) and 367K (660 R) at 31026 kN/m^2 (4500 psia). For analysis purposes, initial bottle conditions of 31026 kN/m^2 (4500 psia) and 278K (500R) and final conditions of 3758 kN/m^2 (400 psia) and 167K (300R) were used. Based on these conditions the results indicate that a single helium bottle should be adequate for tank pressurization in each of the systems analyzed.

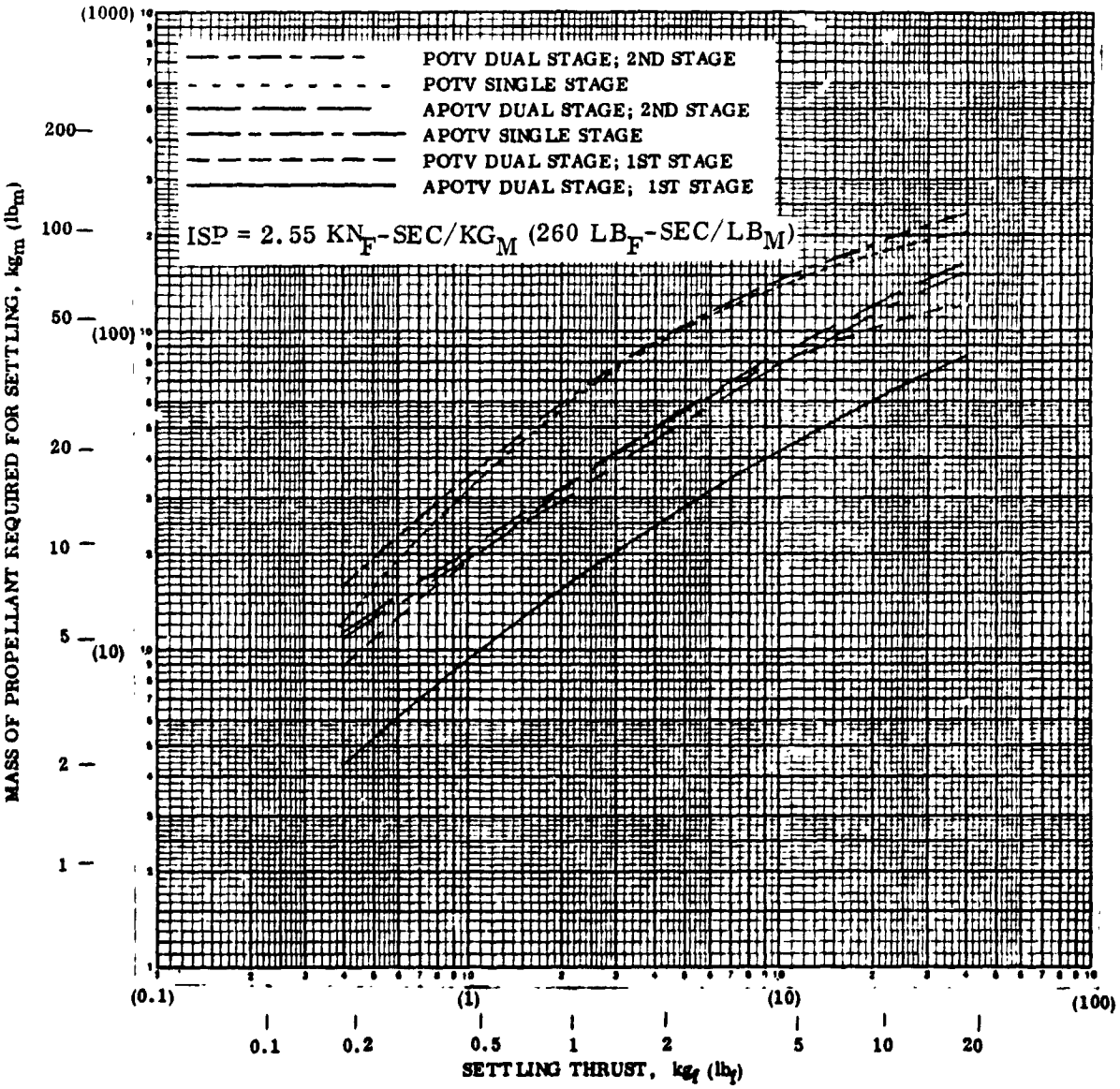

Figure 2-27. Propellant Mass Required to Settle Liquid Hydrogen for Various Thrust Levels

Table 2-27. Helium Expended for Pressurization, kg_m (lb_m), Single Stage APOTV - Delivery Only

Burn Number	He Pressurization Prior to Burn	He Pressurization During Burn	Total He Pressurization	He to LO_2 Tank	He to LH_2 Tank
1	0.045 (0.100)	0.33 (0.72)	0.372 (0.820)	0.33 (0.73)	0.041 (0.090)
2	0.026 (0.564)	0.14 (0.30)	0.392 (0.864)	0.20 (0.45)	0.188 (0.414)
3	0.361 (0.796)	0.13 (0.29)	0.493 (1.086)	0.24 (0.53)	0.252 (0.556)
4	0.484 (1.068)	0.0 (0.0)	0.484 (1.068)	0.15 (0.34)	0.330 (0.728)
5	0.529 (1.167)	0.0 (0.0)	0.529 (1.167)	0.17 (0.38)	0.357 (0.787)
6	0.535 (1.179)	0.0 (0.0)	0.535 (1.179)	0.18 (0.39)	0.358 (0.789)
Total He	2.211 (4.874)	0.59 (1.31)	2.805 (6.184)	1.28 (2.82)	1.526 (3.364)

Volume Expended:

V_i = 0.0730 m^3 (2.579 ft^3) if
P_f = 2758 kN/m^2 (400 psia) and
T_f = 167K (300R)

V_i = 0.0694 m^3 (2.452 ft^3) if
P_f = 1379 kN/m^2 (200 psia) and
T_f = 111K (200R)

Table 2-28. Helium Expended for Pressurization, kg_m (lb_m), Dual Stage APOTV - Round Trip

Burn Number	He Pressurization Prior to Burn	He Pressurization During Burn	Total He Pressurization	He to LO_2 Tank	He to LH_2 Tank
FIRST STAGE					
1	0.045 (0.100)	0.57 (1.26)	0.617 (1.360)	0.58 (1.27)	0.041 (0.090)
2	0.398 (0.877)	0.18 (0.39)	0.574 (1.267)	0.29 (0.65)	0.280 (0.617)
3	0.528 (1.163)	0.0 (0.0)	0.528 (1.163)	0.17 (0.38)	0.355 (0.783)
Total He	0.971 (2.140)	0.75 (1.65)	1.719 (3.790)	1.04 (2.30)	0.676 (1.490)
SECOND STAGE					
1	0.045 (0.100)	0.09 (0.19)	0.132 (0.290)	0.09 (0.20)	0.041 (0.090)
2	0.128 (0.282)	0.35 (0.78)	0.482 (1.062)	0.37 (0.82)	0.110 (0.242)
3	0.323 (0.712)	0.16 (0.35)	0.482 (1.062)	0.25 (0.55)	0.232 (0.512)
4	0.454 (1.000)	0.0 (0.0)	0.454 (1.000)	0.14 (0.31)	0.313 (0.690)
5	0.506 (1.116)	0.0 (0.0)	0.506 (1.116)	0.16 (0.36)	0.343 (0.756)
Total He	1.456 (3.210)	0.60 (1.32)	2.055 (4.530)	1.02 (2.24)	1.039 (2.290)

Volume Expended:

First Stage

V_i = 0.0448 m^3 (1.581 ft^3) if
P_f = 2758 kN/m^2 (400 psia) and
T_f = 167K (300R)

V_i = 0.0426 m^3 (1.503 ft^3) if
P_f = 1379 kN/m^2 (200 psia) and
T_f = 111K (200R)

Second Stage

V_i = 0.0535 m^3 (1.889 ft^3) if
P_f = 2758 kN/m^2 (400 psia) and
T_f = 167K (300R)

V_i = 0.0509 m^3 (1.796 ft^3) if
P_f = 1379 kN/m^2 (200 psia) and
T_f = 111K (200R)

Table 2-29. Helium Expended for Pressurization, kg_m (lb_m), Single Stage POTV - Delivery Only

Burn Number	He Pressurization Prior to Burn	He Pressurization During Burn	Total He Pressurization	He to LO_2 Tank	He to LH_2 Tank
1	0.063 (0.139)	0.53 (1.16)	0.589 (1.299)	0.54 (1.18)	0.054 (0.119)
2	0.367 (0.810)	0.25 (0.55)	0.617 (1.360)	0.36 (0.79)	0.259 (0.570)
3	0.560 (1.234)	0.24 (0.54)	0.805 (1.774)	0.43 (0.94)	0.378 (0.834)
4	0.754 (1.663)	0.0 (0.0)	0.754 (1.663)	0.26 (0.58)	0.491 (1.083)
5	0.811 (1.788)	0.0 (0.0)	0.811 (1.788)	0.29 (0.63)	0.525 (1.158)
6	0.939 (1.850)	0.0 (0.0)	0.840 (1.951)	0.29 (0.65)	0.545 (1.201)
Total He	3.396 (7.486)	1.02 (2.25)	4.416 (9.735)	2.16 (4.77)	2.252 (4.965)

Volume Expended:

V_i = 0.1150 m^3 (4.060 ft^3) if
P_f = 2758 kN/m^2 (400 psia) and
T_f = 167K (300R)

V_i = 0.109 m^3 (3.860 ft^3) if
P_f = 1379 kN/m^2 (200 psia) and
T_f = 111K (200R)

Table 2-30. Helium Expended for Pressurization, kg_m (lb_m), Dual Stage POTV - Round Trip

Burn Number	He Pressurization Prior to Burn	He Pressurization During Burn	Total He Pressurization	He to LO_2 Tank	He to LH_2 Tank
FIRST STAGE					
1	0.063 (0.139)	0.64 (1.41)	0.703 (1.549)	0.65 (1.43)	0.054 (0.119)
2	0.433 (0.954)	0.68 (1.50)	1.113 (2.454)	0.81 (1.79)	0.301 (0.664)
3	0.830 (1.830)	0.0 (0.0)	0.830 (1.830)	0.29 (0.64)	0.540 (1.190)
Total He	1.326 (2.923)	1.32 (2.91)	2.646 (5.833)	1.75 (3.86)	0.895 (1.973)
SECOND STAGE					
1	0.063 (0.139)	0.11 (0.24)	0.172 (0.379)	0.12 (0.26)	0.054 (0.119)
2	0.157 (0.347)	0.59 (1.31)	0.752 (1.657)	0.62 (1.36)	0.135 (0.297)
3	0.464 (1.022)	0.28 (0.61)	0.740 (1.632)	0.42 (0.93)	0.318 (0.702)
4	0.676 (1.490)	0.0 (0.0)	0.675 (1.489)	0.23 (0.51)	0.444 (0.979)
5	0.760 (1.675)	0.0 (0.0)	0.760 (1.675)	0.27 (0.59)	0.492 (1.085)
Total He	2.120 (4.673)	0.98 (2.16)	3.099 (6.832)	1.66 (3.65)	1.443 (3.182)

Volume Expended:

First Stage

V_i = 0.0689 m^3 (2.433 ft^3) if
P_f = 2758 kN/m^2 (400 psia) and
T_f = 167K (300R)

V_i = 0.0655 m^3 (2.313 ft^3) if
P_f = 1379 kN/m^2 (200 psia) and
T_f = 111K (200 R)

Second Stage

V_i = 0.0807 m^3 (2.849 ft^3) if
P_f = 2758 kN/m^2 (400 psia) and
T_f = 167K (300 R)

V_i = 0.0767 m^3 (2.709 ft^3) if
P_f = 1379 kN/m^2 (200 psia) and
T_f = 111K (200R)

2.4.4 FEED SYSTEM COMPARISONS. The ten candidates considered in the earlier study were narrowed to three for this study. The three feed systems selected from the earlier study are Systems A, B and K; see Section 2.3.5.1 for details on the various alternatives. These three candidate systems were selected because they ranked highest in the previous study; they further provide the comparison between settling and capillary devices as well as a comparison between pressurization and thermal subcooling to provide boost pump NPSP. The comparisons are made for the two APOTV and two POTV missions indicated in Tables 2-16 through 2-19. For each mission, different vehicle configurations were selected; two are single-stage and two dual-stage. For the latter the weights of feed systems for both stages have been summed together. All systems have boost pumps since the current engine development work indicates tank-mounted electrically-driven boost pumps are the preferred alternative to two-phase pumping or pressurization to provide the initial start transient NPSP. Additional subcooling of 21 to 28 kN/m^2 (3 to 4 psia) would be required if boost pumps were not used. It was determined that this would result in more than doubling the weight of subcoolers sized to provide the current NPSP plus subcooler pressure losses; therefore options D and N from the previous study were not considered here. In this preliminary study for OTVs, no further consideration has been given to propellant duct cooling or coolant handling and the preferred concepts of cooled ducts with coolant pumped back into the tank are used. Only the latter effects this weight comparison.

2.4.4.1 Hardware Weight Comparisons. In this weight comparison, those items which are equal for all three systems have been eliminated from the tables and were not considered. All other items considered here were part of the previous study, Section 2.3.5, and are addressed here and in the payload penalty section. The results of the hardware weights are presented in Tables 2-31 through 2-34 for the four missions considered.

The capillary device weights were presented in detail in Figures 2-22 through 2-25. Pressurant requirements which defined the bottle hardware were discussed in Section 2.4.3.3. Two types of bottles were considered for this study. The earth-based APOTV has hard mounted ambient-storage bottles whereas the POTV has ambient storage bottles which can be replaced during EVA on-orbit. The increase in weight for this capability is from 21 kg_m (47 lb_m) to 52 kg_m (115 lb_m) for a 0.071 m^3 (2.5 ft^3) bottle. Plumbing was typically 34 kg_m (75 lb_m) to 44 kg_m (98 lb_m) for all missions while valves, controls and other components were 31 kg_m (69 lb_m) to 47 kg_m (104 lb_m). These pressurization systems have been designed and their weight defined in detail in our OTV studies. The previous study carried a pressurization system weight 41 kg_m (90 lb_m) for other than the feed systems which is not considered in this study. Also, the helium required to pressurize the N_2O_4/MMH system was determined to be negligible in this preliminary comparison and is neglected.

The subcooler analysis of Section 2.4.2.2 provided the weights for the subcooler hardware. One component of the subcooler system is the plumbing to route the

Table 2-31. Hardware Weight Penalties for Systems Comparison, kg_m (lb_m), APOTV Single Stage

Hardware Weight Penalty Element	Feed System Concept	Settling, Pressurization, Boost Pump, Uncooled Duct, No Coolant Required A	Settling, Thermal Subcooler Before Boost Pump, Uncooled Duct, Coolant Pumped B	Capillary Device, Thermal Subcooler Before Boost Pump, Uncooled Duct, Pumped Coolant K
1. Capillary Device	LH_2	-	-	87 (193)
	LO_2	-	-	24 (53)
2. Pressurization		87 (191)	-	-
3. Subcooler	LH_2	-	13 (28)	13 (28)
	LO_2	-	16 (35)	16 (35)
4. Settling System		18 (39)	18 (39)	-
5. Coolant Pumping System	LH_2	-	9 (20)	9 (20)
	LO_2	-	10 (23)	10 (23)
TOTALS		104 (230)	66 (145)	160 (352)

Tabl3 2-32. Hardware Weight Penalties for Systems Comparison, kg_m (lb_m), APOTV Dual Stage

Hardware Weight Penalty Element	Feed System Concept	Settling, Pressurization, Boost Pump, Uncooled Duct, No Coolant Required A	Settling, Thermal Subcooler Before Boost Pump, Uncooled Duct, Coolant Pumped B	Capillary Device, Thermal Subcooler Before Boost Pump Uncooled Duct, Pumped Coolant K
1. Capillary Device	LH_2	-	-	175 (386)
	LO_2	-	-	48 (106)
2. Pressurization		186 (410)	-	-
3. Subcooler	LH_2	-	25 (56)	25 (56)
	LO_2	-	32 (70)	32 (70)
4. Settling System		28 (61)	28 (61)	-
5. Coolant Pumping System	LH_2	-	18 (40)	18 (40)
	LO_2	-	21 (46)	21 (46)
TOTALS		214 (471)	124 (273)	319 (704)

Table 2-33. Hardware Weight Penalties for Systems Comparison, kg_m (lb_m), POTV Single Stage

Hardware Weight Penalty Element	Feed System Concept	Settling, Pressurization, Boost Pump, Uncooled Duct, No Coolant Required A	Settling, Thermal Subcooler Before Boost Pump, Uncooled Duct, Coolant Pumped B	Capillary Device, Thermal Subcooler Before Boost Pump, Uncooled Duct, Pumped Coolant K
1. Capillary Device	LH_2	-	-	112 (247)
	LO_2	-	-	34 (74)
2. Pressurization		142 (313)	-	-
3. Subcooler	LH_2	-	29 (65)	29 (65)
	LO_2	-	33 (73)	33 (73)
4. Settling System		24 (52)	24 (52)	-
5. Coolant Pumping System	LH_2	-	10 (22)	10 (22)
	LO_2	-	13 (29)	13 (29)
TOTALS		166 (365)	109 (241)	231 (510)

Table 2-34. Hardware Weight Penalties for Systems Comparison, kg_m (lb_m), POTV Dual Stage

Hardware Weight Penalty Element	Feed System Concept	Settling, Pressurization, Boost Pump, Uncooled Duct, No Coolant Required A	Settling, Thermal Subcooler Before Boost Pump, Uncooled Duct, Coolant Pumped B	Capillary Device, Thermal Subcooler Before Boost Pump, Uncooled Duct, Pumped Coolant K
1. Capillary Device	LH_2	-	-	224 (494)
	LO_2	-	-	67 (148)
2. Pressurization		254 (561)	-	-
3. Subcooler	LH_2	-	81 (179)	81 (179)
	LO_2	-	88 (195)	88 (195)
4. Settling System		40 (89)	40 (89)	-
5. Coolant Pumping System	LH_2	-	20 (44)	20 (44)
	LO_2	-	29 (65)	29 (65)
TOTALS		295 (650)	259 (572)	510 (1125)

C-8

coolant fluid back to the tank. These hardware weights are also determined and are included in hardware weight summaries.

The settling system hardware weight consists only of the additional tankage hardware required to store the N_2O_4/MMH since only a delta is considered above the onboard RCS system. The total settling propellants for the selected 18 kg_f (40 lb_f) thrust are presented in Figure 2-27 for each of the stages. Considerable weight saving may be realized here if mission time lines permit longer settling periods than 650 seconds. In noting the mission timelines, some burns may better be served by maintaining control of the propellant between burns. Moreover, with all other burns, settling times of approximately 1800 seconds could well be acceptable. The tankage factor used to define N_2O_4/MMH storage weights was 0.113 kg_m (0.25 lb_m) propellant supply system weight including tankage per kg_m (lb_m) propellant for bellows equipped bottles.

System B with settling and thermal subcooling has the lowest hardware weight for all missions. System B is followed by System A using settling and pressurization with System K with capillary device and thermal subcooler the heaviest system with significant weight differences occurring for all missions. Adjustment on the above assumptions will not change this ranking. This same ranking was observed in the earlier study, however the differences were not as pronounced.

2.4.4.2 Payload Penalty Comparisons. Payload penalty comparisons are made for both hardware weights and fluids. The payload partials data from Table 2-20 is used with the data in the previous section to generate payload weight penalties for the four missions. These are presented in Tables 2-35 through 2-38. The high payload partials of the second stage are major factors on dry hardware weights. The largest driver in fluid weights is the significant residuals in the LO_2 subcooler. Considering all elements, System A with settling and pressurization has the lowest payload penalty for all missions considered. System B with settling and thermal subcooling is a nominally close second with System K using a capillary device and subcooling having the largest penalty. For the dual-stage POTV, System A is a significant amount lighter than B or K. In comparing these results with the previous study, Table 2-12, the results are different; there system B showed a slight advantage while Systems A and K were similar. It is significant that as vehicle size increases, Systems A and B shift ranking, most likely because of the trade-off between pressurization and subcooler residuals.

2.4.4.3 Relative Reliability. The relative reliability of the three concepts is determined for the four missions using the procedures developed for the Centaur vehicle (Ref. 17) with environmental factors defined in prior Interim Upper Stages Studies (Ref. 24). The operating hours t are multiplied by a factor of 0.1 to account for electromechanical parts in standby or off condition during boost and coast. The environmental factors K are respectively 50, 20 and 1 for boost, burn and coast. Reliability is then defined by the expression $R = e^{-\lambda Kt}$ where λ is the failure rate accumulated for all the system components of each concept. The results of this

Table 2-35. Payload Weight Penalties for System Comparison, kg_m (lb_m) APOTV Single Stage

Payload Weight Penalty Element	Feed System Concept	Settling, Pressurization, Boost Pump, Uncoiled Duct, No Coolant Required A	Settling, Thermal Subcooler Before Boost Pump, Uncooled Duct, Coolant Pumped B	Capillary Device, Thermal Subcooler Before Boost Pump, Uncooled Duct, Pumped Coolant K
1. Capillary Device	LH_2	-	-	88 (193)
	LO_2	-	-	24 (53)
2. Pressurization System		87 (191)	-	-
3. Subcooler	LH_2	-	13 (28)	13 (28)
	LO_2	-	16 (35)	16 (35)
4. Settling System Including N_2O_4/MMH Penalty		34 (74)	34 (74)	-
5. Pumping Sys. to Return Coolant to Tank Incl. Boiloff, Batt. and Hdwr.	LH_2	-	9 (20)	9 (20)
	LO_2	-	10 (23)	10 (23)
6. Volume Penalty Due to Hardware Added	LH_2	-	Neg.	Neg.
	LO_2	-	1 (3)	1 (3)
7. Fluid Residuals Cold Side Subcooler	LH_2	-	3 (6)	3 (6)
	LO_2	-	54 (118)	54 (118)
TOTALS		120 (265)	139 (307)	217 (479)

Table 2-36. Payload Weight Penalties for System Comparison, kg_m (lb_m) APOTV Dual Stage

Payload Weight Penalty Element	Feed System Concept	Settling, Pressurization, Boost Pump, Uncoiled Duct, No Coolant Required A	Settling, Thermal Subcooler Before Boost Pump, Uncooled Duct, Coolant Pumped B	Capillary Device, Thermal Subcooler Before Boost Pump Uncooled Duct, Pumped Coolant K
1. Capillary Device	LH_2	-	-	388 (855)
	LO_2	-	-	107 (235)
2. Pressurization System		376 (830)	-	-
3. Subcooler	LH_2	-	56 (124)	56 (124)
	LO_2	-	70 (155)	70 (155)
4. Settling System Including N_2O_4/MMH Penalty		177 (390)	177 (390)	
5. Pumping Sys. to Return Coolant to Tank Incl. Boiloff, Batt. and Hdwr.	LH_2	-	40 (88)	40 (88)
	LO_2	-	46 (101)	46 (101)
6. Volume Penalty Due to Hardware Added	LH_2	-	1 (2)	1 (2)
	LO_2	-	10 (22)	10 (22)
7. Fluid Residuals Cold Side Subcooler	LH_2	-	13 (28)	13 (28)
	LO_2	-	261 (575)	261 (575)
TOTALS		553(1220)	674(1485)	991(2185)

Table 2-37. Payload Weight Penalties for System Comparison, kg_m (lb_m), POTV Single Stage

Payload Weight Penalty Element		Feed System Concept A: Settling, Pressurization, Boost Pump, Uncooled Duct, No Coolant Required	Feed System Concept B: Settling, Thermal Subcooler Before Boost Pump, Uncooled Duct, Coolant Pumped	Feed System Concept K: Capillary Device, Thermal Subcooler Before Boost Pump Uncooled Duct, Pumped Coolant
1. Capillary Device	LH_2	-	-	112 (247)
	LO_2	-	-	34 (74)
2. Pressurization System		142 (313)	-	-
3. Subcooler	LH_2	-	29 (65)	29 (65)
	LO_2	-	33 (73)	33 (73)
4. Settling System Including N_2O_4/MMH Penalty		43 (94)	43 (94)	
5. Pumping Sys. to Return Coolant to Tank Incl. Boiloff, Batt. and Hdwr.	LH_2	-	10 (22)	10 (22)
	LO_2	-	13 (29)	13 (29)
6. Volume Penalty Due to Hardware Added	LH_2	-	Neg.	Neg.
	LO_2	-	3 (5)	3 (5)
7. Fluid Residuals Cold Side Subcooler	LH_2	-	5 (12)	5 (12)
	LO_2	-	114 (252)	114 (252)
TOTALS		185 (407)	250 (552)	353 (779)

Table 2-38. Payload Weight Penalties for System Comparison, kg_m (lb_m), POTV Dual Stage

Payload Weight Penalty Element		Feed System Concept A: Settling, Pressurization, Boost Pump, Uncooled Duct, No Coolant Required	Feed System Concept B: Settling, Thermal Subcooler Before Boost Pump, Uncooled Duct, Coolant Pumped	Feed System Concept K: Capillary Device, Thermal Subcooler Before Boost Pump, Uncooled Duct, Pumped Coolant
1. Capillary Device	LH_2	-	-	548(1209)
	LO_2	-	-	148 (326)
2. Pressurization System		562(1238)	-	-
3. Subcooler	LH_2	-	145 (320)	145 (320)
	LO_2	-	161 (356)	161 (356)
4. Settling System Including N_2O_4/MMH Penalty		276 (608)	276 (608)	-
5. Pumping Sys. to Return Coolant to Tank Incl. Boiloff, Batt. and Hdwr.	LH_2	-	44 (97)	44 (97)
	LO_2	-	60 (133)	60 (133)
6. Volume Penalty Due to Hardware Added	LH_2	-	2 (4)	2 (4)
	LO_2	-	23 (50)	23 (50)
7. Fluid Residuals Cold Side Subcooler	LH_2	-	30 (66)	30 (66)
	LO_2	-	643(1418)	643(1418)
TOTALS		837(1846)	1384(3052)	1805(3979)

analysis are presented in Table 2-39 where reliability R and mean missions between failures MMBF equal to $-1/\ell n$ R are presented. Concept A has the highest reliability for all missions considered.

Table 2-39. Comparison of Relative Reliability for Three Concepts Under Comparison

Mission	Single Stage APOTV		Dual Stage APOTV		Single Stage POTV		Dual Stage POTV	
Concept	R	MMBF	R	MMBF	R	MMBF	R	MMBF
A	0.998539	684	0.997988	497	0.998642	736	0.998195	553
B	0.998046	511	0.997311	371	0.998184	550	0.997586	414
K	0.997703	435	0.996839	316	0.997866	468	0.997163	352

2.4.4.4 Mission Profile Flexibility. Both settling systems and capillary systems impose restrictions on mission timelines. Settling systems with 18.2 kg_f (40 lb_f) thrust may require up to 657 seconds for settling prior to each burn of a mission. Capillary devices impose a restriction on design that the capillary device must refill within the shortest burn duration of the mission. Additionally, capillary device thermal conditioning requirements are proportional to coast durations and longer coast periods may require devices with increased volume. The restrictions of the settling systems are more easily met and for successive burns with short coast periods, maintaining propellant control during coast with settling motors is a possible solution.

2.4.4.5 Conclusions and Recommendations. The major consideration in propellant feed system selection is the payload penalty. Secondary considerations are hardware weight, mission flexibility, system reliability, and development status. The system (Concept A) with settling motors and pressurization has the lowest payload penalty of the three concepts considered for both single and dual stage APOTV and POTV missions. The capillary device system (Concept K) was the heaviest of the three concepts considered. Large LO_2 subcooler residuals were a major weight consideration with the two concepts requiring thermal subcoolers. Mission flexibility was not significantly restrictive for any system considered. Concept A had the highest system reliability, a satisfactory value, and requires no new technology. Concepts B and K both require thermal subcooler development and system K requires start basket development. Concept B with propellant settling and a thermal subcooler has lower hardware weights than the other two systems, however that comparison does not consider fluids expended and fluid residuals. Concept A is the recommended system and requires minimal development of new technology. The study assumed the existence of electrically driven tank-mounted boost pumps for all three concepts which may require development. Verification with flight experiments for settling will provide confirmation of analysis in this area.

3

REFERENCES

1. Bock, E. H., "Centaur/Shuttle Integration Study," General Dynamics Convair Division Report GDCA-BNZ 73-006-8, NAS3-16786, NASA-CR-134488, December 1973.

2. Blatt, M. H., and Walter, M. D., "Centaur Propellant Acquisition System Study," General Dynamics Convair Division Report CASD-NAS-75-023, NAS3-17802, NASA-CR-134811, June 1975.

3. Heald, D. A., et al, "Centaur Interim Upper Stage (IUS) System Study," Volume II, Technical, CASD/AFS-75-006, Contract F04701-75-C-0035, Final Report CDRL A008, 31 July 1975.

4. Clarke, W. D., "Baseline Space Tug - Configuration Definition," MSFC 68 M00039-2, 28 June 1974.

5. Bressler, R. G. and Wyatt, P. W., "Surface Wetting Through Capillary Grooves," Transactions of the ASME Journal of Heat Transfer, February 1970.

6. Blatt, M. H., Pleasant, R. L., and Erickson, R. C., "Centaur Propellant Thermal Conditioning System," General Dynamics Convair Division Report CASD-NAS-76-026, NAS3-19693, NASA CR135032, July 1976.

7. Mitchell, R. C., et al, "Study of Zero-Gravity, Vapor/Liquid Separators," General Dynamics Convair Division Report GDC-DDB65-009, NAS8-20146, January 1966.

8. Fox, E. A. and Gex, V. E., AIChE, 2, 1956, 539.

9. Fossett, H. and Prosser, I. E., Proceedings of the Institute of Mechanical Engineers (London), Vol. 160, 224, 1944.

10. Uhl, V. W., and Gray, J. B., Mixing Theory and Practice, Academic Press, New York, p. 245.

11. Poth, L. J. and VanHook, J. R., et al, "A Study of Cryogenic Propellant Stratification Reduction Techniques," General Dynamics Fort Worth Division Report FZA-419-1, NAS8-20330, 15 September 1967.

12. Lovrich, T. M., et al, "Development of Thermal Stratification and Destratification Scaling Concepts," MDC G4753, NAS8-23747, July 1973.

13. Aydelott, J. C., "Axial Jet Mixing of Ethanol in Cylindrical Containers During Weightlessness," TP-1487, NASA Lewis Research Center, July 1979.

14. Stark, J. A. and Blatt, M. H., "Cryogenic Zero-Gravity Prototype Vent System," General Dynamics Convair Division Report GDC-DDB67-006, Contract NAS8-20146, October 1967.

15. Sterbentz, W. H., "Liquid Propellant Thermal Conditioning System," Final Report, NAS3-7942, Lockheed Missiles and Space Report LMSC K-07-68-2, 15 August 1968.

16. Erickson, R. C., "Space LOX Vent System," General Dynamics Convair Division Report CASD-NAS75-021, NAS8-26972, April 1975.

17. Blatt, M. H. and Risberg, J. A., "Study of Liquid and Vapor Flow into a Centaur Capillary Device", GDC-NAS-79-001, NASA CR-159657, NAS3-20092, September 1979.

18. Rager, J. M., "Centaur Simplification for Interim Upper Stage (IUS)," CASD-ERR-75-016, 15 December 1975.

19. Merino, F., Risberg, J. A. and Pleasant, R. L., "Orbital Propellant Transfer," GDC-ERR-79-057, December 1979.

20. Heald, D. A., et al, "Orbital Propellant Handling and Storage Systems Definition Study-Final Report," GDC-ASP-79-002, Contract NAS9-15640, August 1979.

21. Sumner, I. E., "Liquid Propellant Reorientation in a Low-Gravity Environment," TM-78969 NASA Lewis Research Center, July 1978.

22. Hollister, M. P. and H. M. Satterlee, "Low-Gravity Liquid Reorientation," at Symposium on Fluid Mechanics and Heat Transfer Under Low Gravity Held at Palo Alto, CA, 24 June 1965.

23. Krause, R. P., "Computer Program Operational Instructions for Calculating Helium Monitor Constants," General Dynamics/Convair Report 696-0/R78/008, 28 April 1978.

24. "Centaur Interim Upper Stage (IUS) System Study," Vol. I Technical, Book II, Section 7, General Dynamics/Convair Division Report CASD/AFS75-004, Contract F04701-75-C-0035, 15 May 1975.